EU GRADUATE SCHOOL OF NATURAL AND APPLIED SCIENCE

# EGE UNIVERSITY

## MASTER OF SCIENCE THESIS

# MECHANICAL PROPERTIES OF FIBER REINFORCED LIME STABILIZED CLAY BEFORE AND AFTER FREEZE-THAW EFFECT


**Aslı BOZ**

**Supervisor : Assoc. Prof. Dr. Alper SEZER**

**Civil Engineering Department**


**Presentation Date : 29.12.2017**


**Bornova-İZMİR**
**2017**

EGE UNIVERSITY

GRADUATE SCHOOL OF NATURAL AND APPLIED SCIENCES

(MASTER OF SCIENCE THESIS)

# MECHANICAL PROPERTIES OF FIBER REINFORCED LIME STABILIZED CLAY BEFORE AND AFTER FREEZE-THAW EFFECT

**Aslı BOZ**

**Supervisor: Assoc. Prof. Dr. Alper SEZER**

**Civil Engineering Department**

**Presentation Date: 29.12.2017**

**Bornova-İZMİR**

**2017**

Aslı Boz tarafından Yüksek Lisans tezi olarak sunulan "Mechanical properties of fiber reinforced lime stabilized clay before and after freeze-thaw effect" başlıklı bu çalışma EÜ Lisansüstü Eğitim ve Öğretim Yönetmeliği ile EÜ Fen Bilimleri Enstitüsü Eğitim ve Öğretim Yönergesi'nin ilgili hükümleri uyarınca tarafımızdan değerlendirilerek savunmaya değer bulunmuş ve 29.12.2017 tarihinde yapılan tez savunma sınavında aday oybirliği/~~oyçokluğu~~ ile başarılı bulunmuştur.

| **<u>Jüri Üyeleri</u>:** | | **<u>İmza</u>** |
|---|---|---|
| **Jüri Başkanı** | **: Prof. Dr. Selim ALTUN** | ................................ |
| **Raportör Üye** | **: Doç. Dr. Alper SEZER** | ................................ |
| **Üye** | **: Y. Doç. Dr. H. Fırat PULAT** | ................................ |

**EGE ÜNİVERSİTESİ FEN BİLİMLERİ ENSTİTÜSÜ**

**ETİK KURALLARA UYGUNLUK BEYANI**

EÜ Lisansüstü Eğitim ve Öğretim Yönetmeliğinin ilgili hükümleri uyarınca Yüksek Lisans Tezi / Doktora Tezi olarak sunduğum **"Mechanical Properties of Fiber Reinforced Lime Stabilized Clay Before and After Freeze-Thaw Effect"** başlıklı bu tezin kendi çalışmam olduğunu, sunduğum tüm sonuç, doküman, bilgi ve belgeleri bizzat ve bu tez çalışması kapsamında elde ettiğimi, bu tez çalışmasıyla elde edilmeyen bütün bilgi ve yorumlara atıf yaptığımı ve bunları kaynaklar listesinde usulüne uygun olarak verdiğimi, tez çalışması ve yazımı sırasında patent ve telif haklarını ihlal edici bir davranışımın olmadığını, bu tezin herhangi bir bölümünü bu üniversite veya diğer bir üniversitede başka bir tez çalışması içinde sunmadığımı, bu tezin planlanmasından yazımına kadar bütün safhalarda bilimsel etik kurallarına uygun olarak davrandığımı ve aksinin ortaya çıkması durumunda her türlü yasal sonucu kabul edeceğimi beyan ederim.

29 / 12 / 2017

Aslı

ASLI BOZ

# ÖZET

## FİBER İLE DONATILANDIRILMIŞ KİREÇ STABİLİZE KİLİN DONMA ÇÖZÜNME ETKİSİ ÖNCESİ VE SONRASI MEKANİK ÖZELLİKLERİ

BOZ, Aslı

Yüksek Lisans Tezi, İnşaat Mühendisliği Anabilim Dalı
Tez Danışmanı: Doç. Dr. Alper SEZER
Aralık 2017, 92 sayfa

Kireç hidrolik bir bağlayıcı olup, özellikle plastisitesi yüksek zeminlerin stabilizasyonunda kullanılmaktadır. Öte yandan boy/çap oranları yüksek olan fiber, zeminlerin donatılandırılmasında kullanılmakta, bu malzemenin kullanımı, ortamdaki çekme gerilmelerini karşılayan bir yapı oluşumuna yardım etmektedir. Bu çalışmada, değişik tipte fiber malzemelerin kireç ile stabilize edilen veya edilmeyen kil zeminin mekanik özelliklerine etkisi deneysel bir çerçevede incelenmiştir. Çalışmada bazalt ve polipropilen fiber ile stabilize edilen kil örneklerin bir standart Proktor, donma-çözünme, serbest basınç deneyleri ve ultrasonik dalga hızı deneylerine tabi tutularak sıkışma ve mekanik özellikleri belirlenmiştir. Bir kısım örnek fiber/kireç kombinasyonu ile stabilize edilerek benzer deneyler de bu örneklerin üzerinde de yapılmıştır. Bununla birlikte, seçilen örnekler üzerinde Taramalı Elektron Mikroskopisi (SEM) ve Enerji Dağılımlı Spektroskopi (EDS) görüntülemesi kullanılarak stabilize ortamın mikroyapısal özellikleri incelenmiştir. Beklendiği üzere, kireç içeren ve içermeyen örneklerin mekanik özellikleri hem bazalt hem de polipropilen fiberin kullanım ile gelişim göstermiştir. Genellikle polipropilen fiber ile güçlendirilen kireç stabilize kil örneklerin dayanımı, bazalt fiber ile stabilize edilen benzer örneklerin dayanımından fazla olsa da 90 günlük küre tabi tutulan örneklerden ağırlıkça % 0.75 oranında 19 mm uzunluğunda bazalt fiber içeren %9 kireç içeriğine sahip örnek en büyük dayanımı vermiştir. Donma-çözünme etkisi gerek dayanım deneylerinin sonuçlarından gerekse tahribatsız bir deney olan ultrasonik hız deneyi ölçümlerinden gözlenmiştir, dayanımlar ve ultra ses hızları düşmektedir. Örneklerin donma çözünme etkisinden sonra kütle kayıpları da kaydedilmiş, kütle kaybı ultrasonik ses hızı ve serbest basınç dayanımı arasındaki ilişkiler de ortaya konulmuştur. Son olarak değişik sayısal yöntemler ile stabilize zeminlerin dayanımı modellenmeye çalışmıştır.

**Anahtar sözcükler:** Bazalt fiber, polipropilen fiber, kireç stabilizasyonu, serbest basınç dayanımı, donma-çözülme, ultrases hızı, modelleme.

# ABSTRACT

## MECHANICAL PROPERTIES OF FIBER REINFORCED LIME STABILIZED CLAY BEFORE AND AFTER FREEZE-THAW EFFECT

BOZ, Aslı

MSc in Civil Engineering
Supervisor: Assoc. Prof. Dr. Alper SEZER
December 2017, 92 pages

Lime is known to be a hydraulic binder, particularly used in stabilization of soils of relatively high plasticity. On the other hand, fiber materials of high aspect ratio is used for reinforcement of soils, which help to constitute a structure counteracting the tensile stresses occuring in stabilized medium. In this study, the effect of inclusion of different types of fiber materials on clay/lime stabilized clay is investigated within an experimental framework. Lime stabilized clay samples reinforced using basalt or polypropylene fibers were subjected to standard Proctor, freeze-thaw, unconfined compressive strength and ultrasonic pulse velocity tests in order to determine their compaction and mechanical properties. A similar program excluding ultrasonic wave velocity tests were carried out on fiber reinforced specimens free of lime. Furthermore, selected specimens were subjected to Scanning Electron Microscopy (SEM) and Energy Dispersive X-Ray Spectroscopy (EDS) analyses to determine the microstructural aspects of stabilized medium. As expected, strength of clay/lime stabilized clay was improved by inclusion of both types of fibers. Although strengths of lime stabilized soils reinforced with polypropyene fiber was greater than those reinforced with basalt fiber in general, greatest strength was observed in 90-day cured basalt fiber reinforced specimen of fiber length, fiber content and lime content of 19 mm, 0.75% and 9%, respectively. Freeze-thaw effect was observed from the results of either strength or ultrasonic pulse velocity tests, these values are decreased due to freeze-thaw action. Losses in mass of specimens were determined along with measurements of ultrasonic pulse velocity and unconfined compressive strength by evaluation of the interrelationships among these parameters. Lastly, attempts using several numerical methods were made to model the strength of stabilized soils.

**Keywords:** Basalt fiber, polypropylene fiber, lime stabilization, unconfined compressive strength, freeze-thaw, ultrasonic pulse velocity, modelling.

# ACKNOWLEDGEMENT

First and foremost, I would like to express my deepest gratitude and sincere thanks to my supervisor Assoc. Prof. Dr. Alper SEZER for his continuous support, encouragement, care and invaluable guidance throughout the preparation of this thesis. It would not have been possible to complete this thesis without his contributions.

I owe special thanks to the members of my thesis committe: Prof. Dr. Selim ALTUN and Assist. Prof. Dr. Hasan Fırat PULAT for their attendance at my thesis defence seminar and their insightful comments to my thesis.

Last but not the least, I sincerely thank to my all family particularly my parents Tülay BOZ and Ramadan BOZ who always believe in me and made me overcome all difficulties with their endless support, encouragement, care and love throughout my life. As the experimental part of study was going on, I lost my grandmother Nazife ACU who made a great effort with my grandfather Ekrem ACU to make me the person who I am today since I was born. I am highly thankful to them for everything they did for me. This thesis is dedicated to my beloved family and especially my precious grandmother.

# TABLE OF CONTENTS

## TABLE OF CONTENTS (continued)

# TABLE OF CONTENTS (continued)

# LIST OF FIGURES

## LIST OF FIGURES (continued)

## LIST OF FIGURES (continued)

## LIST OF FIGURES (continued)

## LIST OF FIGURES (continued)

# LIST OF TABLES

# SYMBOLS AND ABBREVIATIONS

| Symbols | Explanation |
|---|---|
| % | Percentage |
| °C | Celcius |
| Al | Aluminium |
| $Al_2O_3$ | Aluminium oxide |
| Ca | Calcium |
| $Ca^{2+}$ | Calcium cation |
| CaO | Calcium oxide |
| $CaOH_2$ | Calcium hydroxide |
| $CO_2$ | Carbon dioxide |
| $Fe_2O_3$ | Iron (III) oxide |
| $H_2O$ | Hydrogen oxide (water) |
| MgO | Magnesium oxide |
| $Na_2O$ | Sodium oxide |
| O | Oxygen |
| $OH^-$ | Hydroxide ion |
| $P_2O_5$ | Phosphorus pentoxide |
| Si | Silicium |

## SYMBOLS AND ABBREVIATIONS (continued)

| | |
|---|---|
| $SiO_2$ | Silicon dioxide |
| $SO_3$ | Sulfur trioxide |
| $\Delta\alpha$ | Increment vector |

Abbreviations

| | |
|---|---|
| ASTM | American Society of Testing and Materials |
| BF | Basalt Fiber |
| Bnat | Bentonite |
| CBR | California Bearing Ratio |
| CID | Isotropic Consolidated-Drained |
| CIU | Isotropic Consolidated-Undrained |
| CP | Curing Period |
| EDS | Energy Dispersive Spectroscopy |
| FC | Fiber Content |
| F-T | Freeze-Thaw |
| g | Gram |
| $g/cm^3$ | Gram/Cubic Centimeter |
| J | Matrix |
| kJ | Kilojoule |

## SYMBOLS AND ABBREVIATIONS (continued)

| | |
|---|---|
| Knat | Kaolinite |
| kPa | Kilopascal |
| L | Path Length |
| m | Meter |
| m/sec | Meter/Second |
| MDD | Maximum Dry Density |
| ML | Mass Loss |
| mm | Milimeter |
| nycy | Number of Freeze-Thaw Cycles |
| n_UCS | Normalized Unconfined Compressive Strength |
| n_UPV | Normalized Ultrasonic Pulse Velocity |
| MPa | Megapascal |
| PF | Polypropylene Fiber |
| PML | Mass Loss in Percent |
| $R^2$ | Coefficient of Determination |
| RA | Residual Average |
| $r_i$ | Residual |
| S | Sum of the Squares of the Residuals |

## SYMBOLS AND ABBREVIATIONS (continued)

| | |
|---|---|
| SE | Standard Error |
| SEM | Scanning Electron Microscopy |
| TS EN | Turkish Standardization Institute |
| t | Ton and Travel Time |
| UCS ($q_u$) | Unconfined Compressive Strength |
| UPV | Ultrasonic Pulse Velocity |
| w | Water Content |
| W | Weight |
| V | Pulse Velocity |
| µm | Micrometer |

# 1. INTRODUCTION

In this chapter, objective and significance of my thesis entitled “Mechanical Properties of Fiber Reinforced Lime Stabilized Clay Before and After Freeze-Thaw Action” are defined. The scope of this thesis is also explained.

## 1.1. Objective of Study

Due to their low bearing capacity and high compressibility, clay is not a proper foundation soil. Deep foundation option should be considered or, if financially feasible, clay soil should be improved before construction of superstructures. Chemical stabilizers such as lime, cement, fly ash can be used for soil improvement. These binders, providing hydration reactions and void-filling effects, can increase the strength of soils. The use of fiber reinforcement along with chemical stabilisers causes development in ductility of soils and reduces the stiffness (Olgun, 2013). In the literature, several studies concerning the effects of lime stabilized clay soils stabilized with polypropylene fiber were encountered. However, the effects of basalt fiber and a comparison concerning the mechanical and freeze-thaw properties of lime stabilized clay reinforced with polypropylene and basalt fibers were not investigated. Therefore, this comparative experimental study was carried out to determine the effect of different fiber types on strength of clay before and after freeze-thaw action. A considerable amount of lime stabilized polypropylene or basalt fiber reinforced clay specimens were tested and compared in accordance with this objective.

## 1.2. Significance of Study

To date, various improvement techniques have been utilized to provide developments in engineering properties of clays. Soil reinforcement by use of fiber which was patented by Freed (1988) is one of the most preferred and beneficial ground improvement methods, since use of fiber may provide additional strength due to changes in stress transfer mechanism of soil matrix. It should be underlined that, use of fiber materials are reasonable in terms of financial considerations, they are also reproducible and adaptable materials (Al Adili et al., 2012). Fiber reinforcements are beneficial to prevent the formation of the tensile cracks; enhance hydraulic conductivity and liquefaction strength; decrease the thermal conductivity, the soil brittleness and weight of building materials; and restrain the swelling tendency of expansive soils. Pavement layers, retaining walls, earthquake engineering, railway embankments, protection of slopes and soil-foundation engineering are some fields which those reinforcements can be appropriate to use (Hejazi et al., 2012). Of all the fibers commercially available, basalt fiber is a more environmental-friendly material, of which the contribution to mechanical properties to stabilized clay needs further investigation, along with a performance comparison with polypropylene fiber.

### 1.3. Scope

In order to investigate individual effects of fiber type (basalt and polypropylene), content (0, 0.25, 0.5, 0.75, 1%) and dimension (6, 12 and 19 mm), lime content (0 and 9%), curing period (1, 7, 28 and 90 days) on mechanical performance of a clay soil, a series of unconfined compressive strength tests were carried out on specimens including basalt or polypropylene fiber compacted under standard Proctor effort (i.e. 35% by weight of soil). Additionally, specimens including 3 and 6% lime and 12 mm basalt fiber were prepared and strength tests were carried out after 1, 7, 28 and 90-day curing. Thereafter, Scanning Electron Microscopy (SEM) and Energy Dispersive Spectroscopy (EDS) imaging were conducted on shear bands of tested soil specimens to obtain morphological structure and elemental composition of specimens. The specimens, which were prepared to compare influences of freeze-thaw action on lime stabilized basalt or polypropylene fiber reinforced clay, including 0%, 0.5% and 1% 12 mm basalt or polypropylene fiber were stabilized with 0% or 3% lime and compacted under standard Proctor effort (i.e. 45% by weight of soil). All specimens were cured for 28 days in a moist room (relative humidity above 95±2%) at an average temperature of 20°C. After curing, specimens were subjected to 0, 1, 3, 7 and 10 cycles of freeze-thaw action in accordance with ASTM D560. A series of unconfined compression and ultrasonic pulse velocity tests were conducted on specimens. Consequently, test results were modelled.

# 2. LITERATURE REVIEW

In this chapter, mechanism of lime stabilization, the effect of lime stabilization and fiber presence on engineering properties of clay and lastly the effect of freeze-thaw action on treated clay are discussed in the light of information obtained from past studies.

## 2.1. Mechanism of Lime Stabilization

Lime is an effective material for stabilization of new materials and reclamation of clay soil, clay contaminated aggregate bases and even calcareous bases which have little or no appreciable clay (Little, 1999). First use of lime as a stabilizer for soil in modern construction practice was in 1924 on short stretches of highway strengthened through the inclusion of hyrated lime (McCaustland, 1925; Bell, 1996).

When limestone or dolomite is burned at a certain temperature (magnesium carbonate is 500°C and calcium carbonate is over 900°C), limestone and dolomite fragmentise and carbon dioxide arises. Calcium oxide or calcium-magnesium oxide (quicklime) remains. If quicklime reacts with water, hydration reaction causes occurance of hydrated lime (Atay, 2011). Lime can absorb 30% water (by weight) throughout extinguishing. Table 2.1 shows chemical and physical properties of lime which can be utilized for stabilization purposes based on TS EN 459-2 (Kavak et al., 2008).

Table 2.1. Chemical and physical properties of lime for stabilization (Kavak et al., 2008)

| **Property (TS EN 459-2)** | **Quicklime** | **Hyrated Lime** |
|---|---|---|
| $CO_2$ (Loss of Ignition) (%) | ≤ 7 % | ≤ 7 % |
| Total (CaO+MgO) (%) | ≥ 80 % | ≥ 80 % |
| $SO_3$ (%) | ≤ 2 % | ≤ 2 % |
| MgO (%) | ≤ 10 % | ≤ 10 % |
| $SiO_2+Al_2O_3+Fe_2O_3+SO_3$ (%) | ≤ 5 % | ≤ 5 % |
| Parts (mm) | ≤ 2 | - |
| Amount remaining on sieve by weight (%) | | 0.09 mm ≤ 7%<br>0.2 mm ≤ 2% |

All fine-grained soils can be converted to have better workability and lower plasticity by the addition of lime. Indeed, strength properties of lime stabilized soil depends on the type of soil, type and percentage of lime used and curing conditions.

Many factors such as pH level of the soil, amount of organic matter, drainage conditions and water content influence the soil-lime reaction. In non-acidic soils (pH> 7), reaction between the soil and lime is more efficient (Lambe, 1962;Türköz, 2006). Lime may react with all types of clay minerals. In kaolinitic clay soils, the nature of the exchangeable cation does not create much difference, however it may affect remarkably in clay soils including montmorillonite. Actually, expansive clays tend to react readily with lime and a substantial decrease in plasticity is immediately observed (Bell and Coulthard, 1990; Bell 1996).

When lime is added to any type of soil–water system forming quick lime (CaO), “soil drying” increases the soil workability as a consequence of dewatering due to highly exothermic hydration reaction of quick lime in the form of hydrated lime, $Ca(OH)_2$ (Di Sante et al., 2014). The hydration reaction causes high concentrations of $Ca^{2+}_{(aq)}$ and $OH^{-}_{(aq)}$ ions in the pore water of the soil. This dissocation of ions causes some reactions which vary with soil composition, mineralogy, and pore water chemistry. For the existing cations at negative charge sites on the clay mineral lattice, cation exchange of calcium ($Ca^{2+}$) ions leads to modification in reactions. Flocculation of mineral particles is observed and the plasticity characteristics of soil changes as a result of cation exchange (Boardman et al., 2001). A part of this reaction is shown in Figure 2.1. (Little, 1987; Mallela et al., 2004). Pozzolanic reactions which occur among lime, water, soil silica, and alumina and lead to several cementing-type products. The cementing materials which the same hydrates formed along the hydration of Portland cement, are calcium–silicate–hydrates and calcium–aluminate–hydrates (Terrel et al., 1979; Mallela et al., 2004). Solidification which occurs as a result of pozzolanic reactions, causes long-term physico-chemical changes (Sherwood, 1993; Boardman et al., 2001).The pozzolanic reactions are clarified in the following equations: (Mallela et al., 2004; Jawad et al., 2014):

$$Ca(OH)_2 \rightarrow Ca^{2+} + 2(OH)^- \quad (1)$$

$$Ca(OH)_2 + SiO_2 \rightarrow CaO\text{-}SiO_2\text{-}H_2O \quad (2)$$

$$Ca(OH)_2 + Al_2O_3 \rightarrow CaO\text{-}Al_2O_3\text{-}H_2O \quad (3)$$

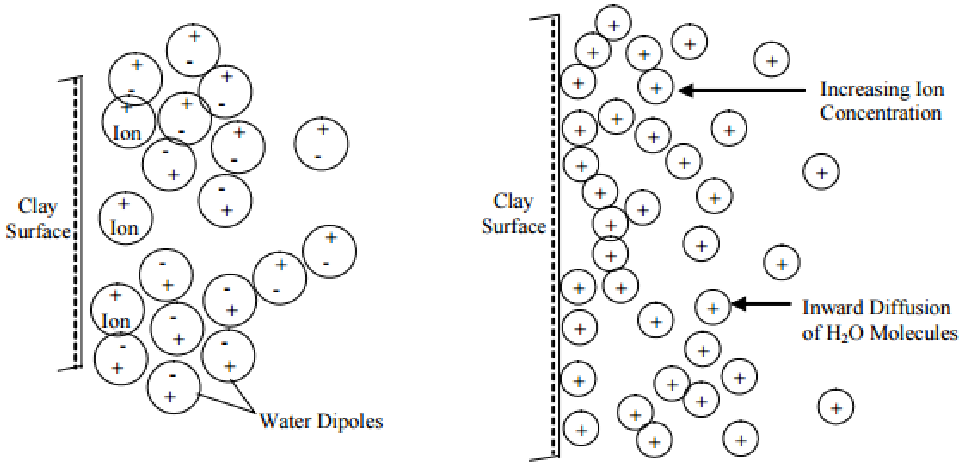


Figure 2.1. Diffused water layer around a clay particle (Little, 1987; Mallela et al., 2004)

## 2.2. Effect of Lime Stabilization on Engineering Properties of Clay

Lime stabilization is a very common method used to chemically convert unstable soils into structurally sound construction foundations and also significant in road construction to modify subgrade soils, subbase materials and base materials. More rigid portland cement concrete and more flexible asphalt pavements are can be constructed by use of improved engineering characteristics of lime-amended materials (Little et al., 2000).

Lime stabilization affects montmorillonitic clay more quickly in comparison with kaolinitic clays. Montmorillonitic clays gain strength earlier. On the other hand, as the curing period increase, additional strength gains by kaolinitic clays are higher than those gains by montmorillonitic clays. If lime is added to fine quartz, the most remarkable increment in strength is obtained. Optimum gains in strength are around 4% for montmorillonite, between 4%-6% for kaolinite and between 4%-8% for quartz. Greatest strength gains are obtained when the mix water content is just above the optimum water content. Increasing curing period causes that the strength continues to improve, but mostly significant increments are obtained within the first 7 days. Besides, temperature of curing affects strength significantly. Above 30°C the strength can increase drastically (Bell, 1996). For stabilization of phyllite clay, 3% lime content increases capacity amble of the soil (Garzón et al., 2016). According to Ingles and Metcalf (1972), the amount of lime to be added for stabilization is approximately 3% for well-graded clay-gravel, 5% for sandy clay, 2~4% for silty clay, 3~8% for plastic clay and 3~10% for high plastic clay. Lime stabilization is not recommended for fine cracked rocks, sands and organic soils (Kızılçelik, 2010).

It was found by Kızılçelik (2010) that unconfined compressive strengths (UCS) of quicklime and hydrated lime stabilized high plasticity clay increase and deformations decrease proportionally with increasing curing period. Even though unconfined compression strength values of quicklime stabilized specimens in the natural water content are slightly lower than those of hydrated lime stabilized high plasticity clay after 1 and 7-day curing, after 28-day curing the use of quicklime gives better results. This suggests that the use of quicklime, instead of hydrated lime, for lime stabilization is appropriate. Furthermore, in California Bearing Ratio (CBR) tests 5% lime stabilized clay shows an increase up to quintuple in compared to untreated clay. Tonoz et al. (2004) investigated the stabilization of smectite rich Ankara clay using quicklime and it was observed that at the end of 28 days, unconfined compressive strength values of specimens increases about 84%. Nevertheless, when curing period is less than 28 days, UCS values of lime stabilized specimens are greater in comparison with those of untreated specimens. This means that pozzolanic reaction is slower compared to flocculation in Ankara clay, which obtains optimum stabilization at %4 lime content and 28-day curing if swelling is considered. According to Kassim and Chern (2004), clay with high intensity of kaolinite and with alkaline origin show more remarkable increment in UCS in comparison with clay with acidic origin. Mostly, lime content between 3% and 6% improves UCS remarkably from 2.5 to 11 times more than unamended clay soils. In Figure 2.2. , UCS values of various amount of lime stabilized clay soils are shown.

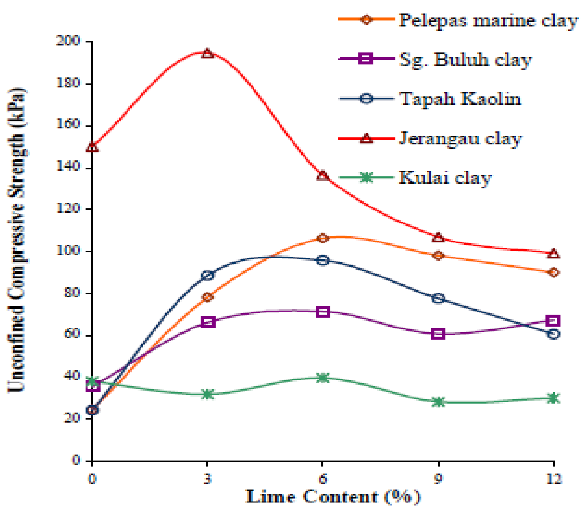


Figure 2.2. UCS values at 14 days with various lime content (Kassim and Chern, 2004)

Di Sante et al. (2015) reported that when the compaction of clayey soil stabilized with quicklime or hydrated lime delay for 48 hours, a remarkable reduction of dry unit weight and an increment of compressibility at high effective stresses occur. The use of quick lime, instead of hydrated lime, can decrease the effect of a delayed compaction both with regards to compressibility and hydraulic conductivity. Quicklime which is a material with high reactivity and calcium content, do not need a prompt wetting to guarantee great hydraulic conductivity. Besides, 3, 5 and 7% lime content for phyllite-lime mixture provide good compaction features and quite low water-permeability coefficient values (Garzón et al., 2016).

Al-Rawas et al. (2005) experimentally found that the addition of 6% lime to an expansive soil from Oman comprising montmorillonite (43%), palygorskite (23%), illite (23%) and kaolinite (16%) decreases the swell percent and swell pressure to zero. Inclusion of 5% lime in a clay of high plasticity, the amount of swelling is reduced by 83% (Kızılçelik, 2010). The addition of quicklime could be successfully used to control the swelling potential of high plasticity clay. More than 3% lime content is effective and the effect is relatively higher at higher energy levels (modified Proctor effort) (Türköz, 2006). Furthermore, it substantially changes the grain size distributions of the soils. As lime and curing period increase, the clay fractions diminishes, in contrast the coarse-grain fractions improve. Increasing lime content causes that concentrations of calcium and magnesium ions in pore water improve, controversially those of sodium and potassium ions diminish. Additionally, the inclusion of lime also reduces the potential expansiveness of the soils. Increasing lime content and curing period also reduce swell percent, swell pressure measurements and primary consolidation whereas those increase prompt settlement (Basma and Tuncer, 1991).

The study by Broderick and Daniel (1991) demonstrated that lime stabilized kaolinite is more invulnerable to attack by organic chemicals, in comparison with unamended kaolinite. Moreover, lime increases the resistance of illitic soil to attack, yet improvement of kaolinite is greater. Moreover, Castro-Fresno et al. (2011) made investigation on lime stabilization of bentonite sludge from tunnel boring and it was found that the addition of 3% lime improves its mechanical properties by 80% compared to the initial sludge mechanical properties.

To sum up, inclusion of lime decreases the swelling potential, liquid limit, plasticity index and maximum dry density of soil and improve its optimum water content, shrinkage limit, resilient properties, durability, workability, compressibility and strength (Croft, 1967; Little et al., 2000; Al-Rawas et al., 2005; Jawad et al. 2014). Increased resistance to fracture, fatigue, permanent deformation and the hazardous influences of moisture are achieved. The most significant improvements in these properties are reasonably visible in highly plastic soils, such as heavy clay (Little et al., 2000).

## 2.3. Effect of Fiber Presence on Engineering Properties of Clay

The use of randomly distributed fiber is more advantageous in comparison with conventional geosynthetics such as geotextile, geogrid strips to reinforce the soil due to limiting potential planes of weakness which can improve parallel to oriented reinforcement (Tang et al., 2007). The potential cracking induced by differential settlement can be reduced and then landfill covers can be stabilized by the use of discrete fiber. Unlike continuous horizontal reinforcement, fiber reinforcement does not require any anchoring (Plé et al., 2009). In literature, natural fibers such as coir, sisal, jute, Barley-straw, baggase, basalt and synthetic fibers such as polypropylene, polyester, polyethylene, nylon, carpet waste, steel have been used to improve the engineering properties of clay or clayey soil (Gao et al. 2015; Hejazi et al. 2012; Mirzababaei et al., 2013; Dang et al., 2016). In this part, it is focused on the effect of polypropylene and basalt fiber presence on engineering properties of clay due to utilizing these materials for this thesis.

Polypropylene material is hydrophobic and chemically ineffective. This material does not absorb or react with soil moisture or leachates (Miller and Rifai, 2004). Many researchers utilized polypropylene fiber as a soil reinforcement agent. The mechanical properties such as unconfined compressive and splitting tensile strength, CBR, internal friction angle, cohesion, ductility and flexural toughness of kaolinite clay are increased by inclusion of randomly distributed fiber (Maher and Ho, 1994; Öztürk, 2007). The increment in strength and toughness depends on fiber length and content, and water content of the soil composite as well. Increasing fiber content improves the compressive & tensile strength and toughness & brittleness index of clay (Maher and Ho, 1994; Plé and Lê, 2012). Besides, increase in fiber length improves the contribution to energy absorption or ductility whereas decreasing the contribution of fiber existence on peak compressive strength (Maher and Ho, 1994).

Jiang et al. (2010) investigated the engineering properties of short discrete polypropylene fiber reinforced clayey soil using four different fiber lengths (10, 15, 20 and 25 mm) with four different percentages of fiber content (0.1, 0.2, 0.3 and 0.4%). Based on test results increasing fiber length and content firstly increase UCS values and then reduce them rapidly. With the addition of 0.3 fiber content maximum UCS values are reached for all fiber length and using 15 mm fiber length gives the maximum UCS values for all fiber content. The unconfined compression test results on 0.25, 0.5, 0.75, 1 and 1.25% in length of 6.19 mm polypropylene fiber reinforced low plasticity clays showed that greatest strength values are produced by 0.75% fiber content (Senol et al., 2014). However, it is emphasized that UCS of expansive clay is improved increasingly by the addition of 0.5, 0.75 and 1% in length of 12 mm polypropylene fiber by Soğancı (2015). When fiber content is enhanced, the peak axial stress increases and the loss of post-peak strength diminishes. For instance, the addition of 1% fiber increases the UCS from 202 Mpa to 285 Mpa (Soğancı, 2015). In contrast to many researchers, Yilmaz (2015) found that the use of only polypropylene fiber reinforcement reduces UCS of clay soil.

The pure kaolinite clay specimens exhibit brittle failure with visible crack formations, however polypropylene fiber reinforced specimens exhibit ductile failure with multiple crack formations (Öztürk, 2007). Fiber addition can increase the soil tensile failure ductility remarkably and under direct tensile test 0.6% fiber reinforcement which can reduce potential cracks for silty clay specimens, changes the ductility in range of 62% (Li et al., 2014; Plé and Lê, 2012). The use of fiber provides high load retention after occurence of first crack and prevents the brittle (catastrophic) failure. For instance, after formation of first crack, 75 % and 50% of strength of fiber reinforced mudstone (a low plasticity silty clay) and Oxford clay (a medium-plasticity to high-plasticity clay) retained. The addition of fibers also increases remarkably the flexural load-carrying capacity of the soils (Onyejekwe and Ghataora, 2014).

Throughout direct shear tests, polypropylene fiber reinforced clay specimens exhibit dilative behaviour, however untreated specimens exhibit contractive behaviour. This means that tensile strength of fiber addition is mobilized (Öztürk, 2007). The use of fiber can improve the soil tensile strength substantially. Increasing fiber content from 0% to 0.2% causes an increase in tensile strength by 67%. Moreover, as dry density increases, the tensile strength of fiber reinforced soil increases whereas decreasing water content reduces tensile strength.

The interfacial mechanical interaction among fiber surface and soil matrix which can be enhanced better by use of W-shaped polypropylene fiber: compared to straight polypropylene fiber, use of W-shaped PF influences fiber pull-out resistance which markedly increases the tensile strength of fiber reinforced soil (Li et al., 2014; Tang et al., 2016). In addition to strength properties under tensional stresses, inclusion of fiber at a level of 0.6% in silty clay causes improvement in strength up to 100%. The use of polypropylene fiber also improves the initial Young modulus of clay and silty clay soils (Plé and Lê, 2012; Plé et al., 2009).

The research of Freilich et al. (2010) on effective shear strength of fiber reinforced clays using isotropic consolidated-undrained (CIU) and isotropic consolidated-drained (CID) triaxial tests revealed that the use of fiber changes the stress-strain behaviour of clay throughout shearing and pore pressure generation behavior. The addition of fiber increases the effective shear strength and based on CID triaxial tests the strength of fiber-soil structure is less for long term-fully drained conditions. This suggests that time and drainage may reduce the effective strength of fiber-soil structure remarkably. It is also understood that CIU testing provides a higher estimation of effective shearing strength on the influence of fiber in clay soil specimens in comparison with CID. Besides, the peak shear strength of clay soil is increased by the use of polypropylene fiber, however in some cases the post-peak strength loss is decreased by the inclusion of fiber (Nataraj and McManis, 1997). The research of Casagrande et al. (2006) showed that the peak shear strength of bentonite is increased by the addition of randomly distributed fiber, however the increment in strength deteriorates after greater amount of displacements. It is also experienced that fiber reinforcement does not affect residual strength significantly. Increasing fiber content and length also causes an increment in the peak shear strength. According to Nataraj and McManis (1997) friction angle of clay soil is increased by the use of polypropylene fiber. The investigation of Plé et al. (2009) indicated that fiber content enhances apparent undrained friction angle between the range of 6.3° and 15.3°. The use of fiber in length of 6 mm produces highest undrained friction angle. According to Jiang et al. (2010) as fiber length and content is increased, the initial increase in cohesion and internal friction angle is followed by a decrease of a high rate. With the inclusion of 0.3% fiber content, cohesion and internal friction angles reach to their maximum for all fiber lengths, where use of 15 mm fiber length gives maximum cohesion and internal friction angles for all fiber contents. In addition to that, as fiber content and length increase, shrinkage limit of fiber reinforced clay soil increases substantially. This suggests that fiber reinforced specimens have much less volumetric changes due to decreasing desiccation, and the extent of crack formation substantially (Abdi et al., 2008). Polypropylene fiber reinforcement also reduces linear shrinkage value substantially. The inclusion of 1% fiber reduces linear shrinkage from 4.29% to 1.43%. The volumetric shrinkage strains of expansive clays are also decreased by fiber reinforcement (Puppala and Musenda, 2000).

The hydraulic conductivity of kaolinite clay  and silty clay is improved by the use of polypropylene fiber (Maher and Ho 1994; Plé and Lê, 2012). Particularly, higher fiber contents are more effective but still low enough to be considered for some landfill practices (Maher and Ho, 1994). It is found that increasing fiber content and length increases hydraulic conductivity slightly similar to Maher and Ho (1994) by Abdi et al. (2008).

According to Miller and Rifai (2004), optimum polypropylene fiber reinforcement content for clay soil is 0.3%, neglecting hydraulic conductivity by Nataraj and McManis (1997) 0.2%, for Oxford clay and for Mercia mudstone (Onyejekwe and Ghataora, 2014)  is among 0.4 and 0.5% which is found in order to obtain highest crack reduction and highest dry density, while sustaining a feasible level hydraulic conductivity. The crack reduction for this range of fiber content is roughly 50% in comparison with untreated soil specimens. 0.8% fiber content provides the highest crack reduction (at a degree of 90%). Despite the crack reduction can further be enhanced with increasing fiber content, specimen hydraulic conductivity improves substantially and soil specimens become unworkable.

Polypropylene fiber reinforcement reduces consolidation settlements and swelling of soil consisting of 75% kaolinite and 25% montmorillonite significantly and swell pressure of expansive clays (Abdi et al., 2008; Puppala and Musenda, 2000). Increasing fiber content reduce the swell percent. The addition of 1% fiber reduces the one dimensional swell significantly. For instance, as the fiber content reaches to 1% (w/w) one dimensional swell is reduced from 11.6% to a 5.3% (Soğancı, 2015). Furthermore, free swell potential of the soils is also improved by fiber reinforcement (Puppala and Musenda, 2000).

Öztürk (2007) studied engineering properties of kaolinite clay reinforced with polypropylene fibers and it was found that the inclusion of 1% fiber increases internal friction angle by 10° for standard and modified compaction. This amount of fiber presence in clay also causes an improvement in cohesion by 75% and 13%, for standard and modified Proctor energies, respectively. Unconfined compressive strength approximately increased by 82% and 118%, for densification with standard and spring tampers, respectively. Corresponding increases in CBR was experienced between 21.50 and 60.13. In addition to that, soil strength parameters are slightly greater for modified compaction in comparison with those for standard compaction. The specimens with spring tamper compaction have greater UCS values due to the kneading influence caused by piston, that lead to curved shape fiber distribution in soil matrix.

Cai et al. (2006) investigated the effect of polypropylene fiber and lime admixure on engineering properties of clayey soil. Test results showed that fiber content, lime content and curing period affect the engineering characteristics of fiber-lime amended soil remarkably. Increasing lime content causes an initial increase followed by a slight decrease in UCS, cohesion and angle of internal friction of the clayey soil whereas causes a bare reduction in swelling and shrinkage potential. Additionally, increasing fiber content increases the strength and shrinkage potential whereas that reduces the swelling potential. Furthermore, increasing curing period increases UCS and shear strength parameters of amended soil remarkably. Figure 2.3 demonstrates the influences of various fiber and lime content within soil specimens on UCS after 28 day-curing. Figure 2.4 shows four specimens including various fiber content and 8% lime inclusion after compression failures. As is seen in Figure 2.4, increasing fiber content reduces cracks of higher dimension gradually.

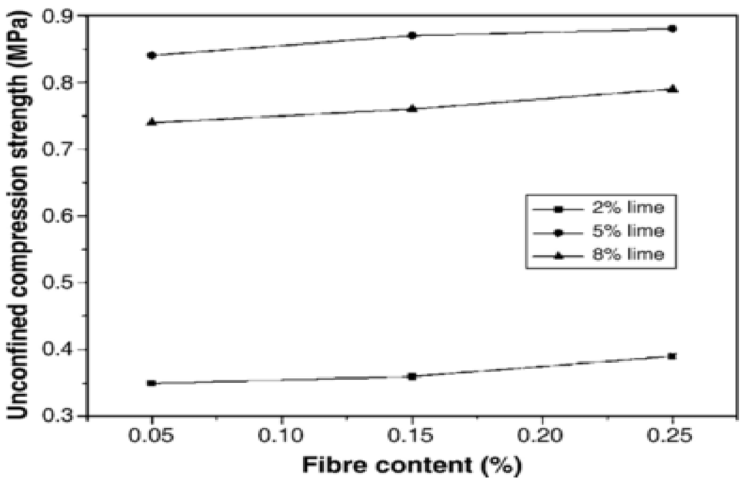


Figure 2.3. The influences of various fiber and lime content within soil specimens on UCS after 28 day-curing (Cai et al., 2006)

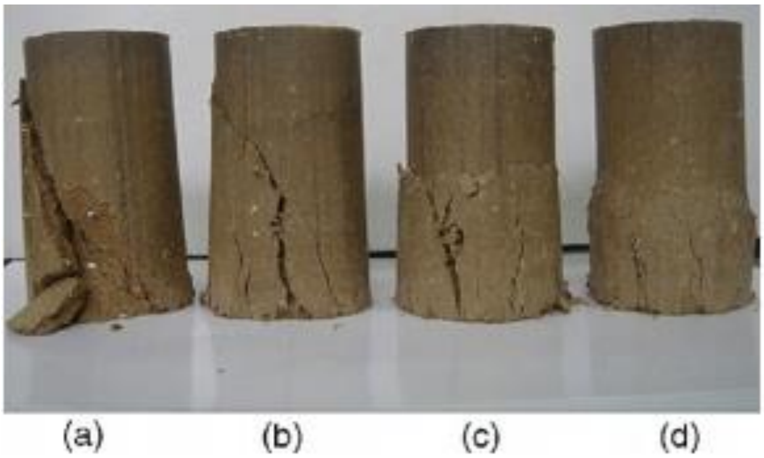


Figure 2.4. Various failure characteristics of 8% lime stabilized soil specimens inclusing the fiber content of: a) 0%; b) 0.05%; c) 0.15%; d) 0.25% (Cai et al., 2006)

First attempts for basalt fiber production go back to 1923 (U.S. Patent 1,462,446) and it was developed more during World War II (Seydibeyoğlu, 2017). Basalt is chemically ineffective, highly corrosion-resistant and lowly thermal-conductive (Dhand et al., 2015). High strength, good modulus, improved strain to failure and high-temperature resistance are some structural characteristics of basalt fiber which are obtained from basalt rocks and can be evaluated as green friendly, nonhazardous bio-based fibers (Seydibeyoğlu, 2017; Fiore et al., 2015). According to Deák and Czigány (2009) $SiO_2$ and $Al_2O_3$ content which is components of basalt fibers demonstrate correlation with tensile characteristics of fibers and the performance of short basalt fibers is weaker in terms of mechanical characteristics. In literature, basalt fiber has been commonly investigated to improve the engineering characteristics of various concrete (Dias and Thaumaturgo, 2005; Sim et al., 2005; Li and Xu, 2009; Di Ludovico et al., 2010; Morova, 2013; Kabay 2014; Kizilkanat et al., 2015; Lipatov et al., 2015), cement mortar (Jiang et al., 2010), polypropylene matrice (Greco et al., 2014), plastic (Lopresto et al., 2011) polymer (Czigány et al., 2005; Pearson et al., 2013; Banibayat and Patnaik, 2014; Gholkar and Jadhav, 2014; Pandian et al., 2014; Dhand et al., 2015; Elgabbas et al., 2015; Alaimo et al., 2016; Shi et al., 2017; Wang et al., 2014, 2015, 2017) and composites (Scalici et al., 2016). There is a very limited number of studies on the use of basalt fiber reinforcement for soil in the literature. Gao et al. (2015) conducted an experimental study on UCS of basalt fiber (BF) reinforced clay soil. The experimental results indicated that basalt fiber can significantly improve the UCS of clay soil. Peak strength is observed by incorporation of 12 mm fiber length and the optimum fiber content is 0.25%. Moreover, basalt fiber reinforced soil shows poststrong property in comparison with unamended soil, a more stable behaviour is observed due to improvements in strength. Figure 2.5 shows failure form of basalt fiber reinforced soil specimen. Cracks occur slowly and can be predicted. Figure 2.6 shows fiber-soil column and net relation. In Figure 2.6a, the fiber behaves as a center line and the surrounding soil particles are closely around the fiber at a certain radius. In Figure 2.6b, the discrete distribution of fibers in the soil transforms the soil to a three-dimensional fiber-soil net in which fibers behave as a skeleton. According to Ndepete and Sert (2016) basalt fiber enhances undrained shear strength. More than 2% basalt fiber content do not provide additional gain in strength and 24 mm fiber length gives greater undrained shear strength values as compared to 6 mm and 12 mm.


Figure 2.5. Failure form of basalt fiber amended soil specimen (Gao et al., 2015)

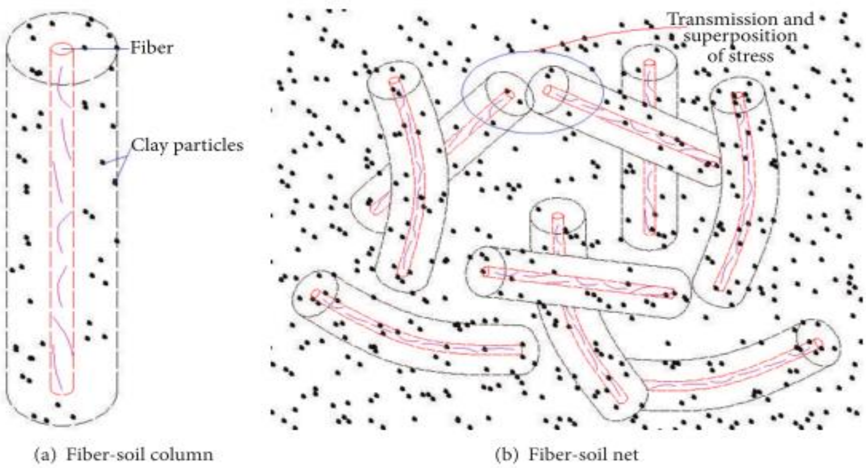


Figure 2.6. Model of a) fiber-soil column and b) fiber-soil net (Gao et al., 2015)

## 2.4. Effect of Freeze-Thaw Action on Treated Clay

In cold regions, soils are exposed to freeze-thaw action which influences engineering characteristics of soils such as volume, strength, compressibility, densification, unfrozen water content, bearing capacity, and microstructure. This phenomenon should be considered in selection of relevant soil parameters for stability and deformation analysis of slopes, embankments and cuts, particularly those underlain by permafrost (Ghazavi and Roustaie, 2010; Qi et al., 2006). After freeze-thaw action, crack propagation and stability failures are likely to occur due to the fact that exposure of large voids within fine grained soils to low temperatures results in formation of glaciers and subsequent freezing of water within smaller voids. When water freezes, this causes an increase in its volume at a level of 9% which leads to crack formation in the soil (Yıldız et al., 2004; Altun et al., 2009). According to Lu et al. (2016) the surface crack pattern slowly changes from an irregularly rectilineal pattern to a polygonal or quasihexagonal one and water loss which is closely relevant with the specimen thickness, is substantial for the process of cracking in clay. For freeze-thaw, the surface crack ratio is well correlated with the fractal dimension logarithmically.

Zhang et al. (2016) reported that the freeze-thaw action can change the granulometric composition of mineral particles and soil structure substantially and improve particle bonding to achieve an overall aggregate stability in the soil. Nonetheless, the investigation of Qi et al. (2006) demostrated that freeze-thaw cycles improve the structure in reconstituted normally consolidated clays, however, leads to degradation of structure in clays. According to Oztas and Fayetorbay (2003) exposure to freeze-thaw reduces the aggregate stability which depends on the initial aggregate size and stability, soil moisture content at freezing, the number of freeze-thaw cycles and the freezing temperature for clay soil. The influence of freeze-thaw is less dangerous to clay structure in comparison with that of silt in terms of aggregate stability (Kværnø and Øygarden, 2006).

Exposure to freeze-thaw cycling changes physical and mechanical properties of clay. Increasing number of freeze-thaw cycles increase the height of the specimen whereas that reduces water content until seventh cycle (including the seventh cycle). When more than seven cycles are applied to specimen, the height and water content do not change. The freeze-thaw action affects the resilient modulus and the failure strength significantly whereas that does not influence the shape of the stress–strain behavior curves. Mostly, application of 3 to 7 freeze-thaw cycles causes lowest resilient modulus and failure strength under confining pressure ($\sigma_3$) 200, 400, 600 and 800 kPa as is seen in Figure 2.7a and Figure 2.7b (Wang et al., 2007). Moreover, exposure to surcharge load reduces the freeze-thaw resistance of clay soil specimens (Zaimoğlu et al., 2012, 2013). Freeze-thaw tests also revealed the fact that, increasing overburden pressure reduces void ratio and permeability (Hirose and Ito, 2017).

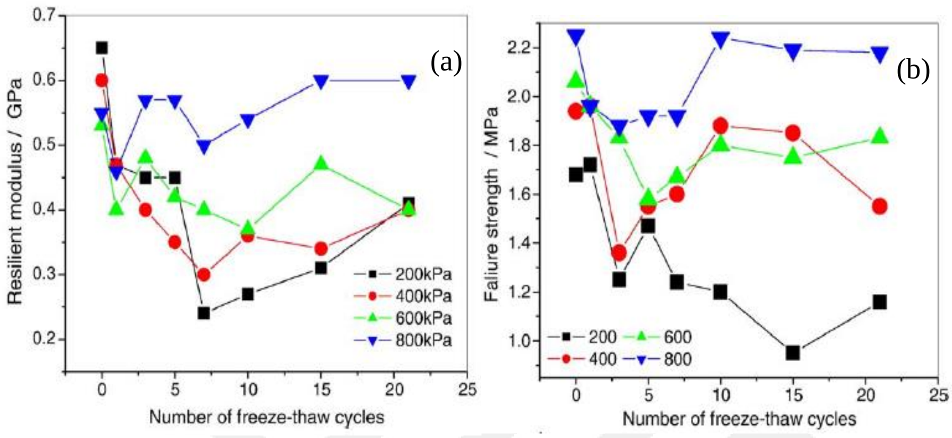


Figure 2.7. a) Resilient modulus and b) failure strength of specimens with number of applied freeze-thaw cycles (Wang et al., 2007)

Increasing number of freeze-thaw cycles causes an increment in the normalized accumulative strain of the saturated clay and the angle of internal friction whereas reduces the cohesion and UCS of clay soil (Wang et al., 2007; Zaimoğlu et al., 2012, 2013; Lin et al., 2017). The decrement of cohesion in clay soil depends on increasing distance between soil particles due to forming ice lenses after freeze-thaw action (Roustaei et al., 2015). In addition to that, an unsaturated clay is exposed to freeze-thaw action non-uniform volumetric shrinkage, or freeze-necking phenomenon appears (Wang et al., 2017).

Many researchers have studied on the improvement of engineering properties of clay soil with various additives due to the harmful effects of freezing-thawing. Cement is an additive used for improvement of soils, although cement was not used as an improvement agent in this thesis, in order to clarify the effects of freeze-thaw cycles on stabilized medium, it would be useful to briefly explain the effects of cement showing similar behavior to lime against freezing and thawing. Liu et al. (2010) found that the freezing-thawing durability of clay soil is improved by cement amendment. The use of this material partially prevents loss of UCS against to freeze-thaw effect. However, the investigation of Shibi and Kamei (2014) showed that first or second freeze-thaw cycle reduces UCS and durability of cement stabilized clay soil sharply. According to Mardani-Aghabaglou et al. (2015) increasing cement content causes an higher strength loss of clay soil specimens and binding characteristics of cement treated soil and microcracks affect freeze-thaw resistance due to frost action. The inclusion of both recycled bassanite and coal ash increases freeze–thaw durability of cement-stabilized clay soils. After five freeze-thaw cycles, the use of these materials increases durability index from 50% to 85% (Shibi and Kamei, 2014). The study of Kamei et al. (2012) also showed that the addition of only recycled bassanite improves the durability of very soft clay soil at an acceptable level with regards to strength, volume change and mechanical characteristics against the influences of freeze–thaw action. Additionally, experimental study on the dynamic properties of cement- and lime-modified clay soils subjected to freeze–thaw cycles of Liu et al. (2010) demonstrated that increasing number of freeze-thaw cycles reduces the critical dynamic stress. The strength of both modified and unmodified specimens are decreased due to freeze-thaw action, however, the durability of stabilized clay soil is improved by cement- and lime-modified blends. Furthermore, the performance of cement-modified clay is better compared to the performance of lime-modified clay despite the fact that mechanical characteristics of clay soils are increased by both modifications.

The pozzolanic reaction is not stopped by the influence of freeze-thaw. Yet, the reaction delays in the lime stabilized clay soil. This suggests that lime stabilization is convenient for clay soils in cold seasons. After 28-day curing, lime stabilization increases the strength of high (e.g. Aksaray clay) and low (e.g. Doğanhisar clay) plasticity clays roughly 15 and 3 times, respectively. 3 freeze-thaw cycles reduces the strength of both lime stabilized these clays 10-15% (Yıldız and Soğancı, 2012). Moreover, after 28-day curing 10 freeze-thaw cycles reduce UCS values of lime stabilized bentonite (high plasticity) specimens to a degree of 40%, however UCS values of these are still greater as compared unamended specimens. For lime stabilized kaolinite of low plasticity, a slight decrease is observed in strength for a short period. In Figure 2.8a and Figure 2.8b, the variation of UCS values of pure bentonite, 5% lime stabilized bentonite, pure kaolinite and 3% lime stabilized kaolinite under various freeze-thaw conditions are shown, respectively. It is clear that strength development of kaolinite is not as steep as that of bentonite due to the kinetics of the lime amendment reactions that are affected by the different mineralogical and crystallographic nature of soils (Al-Mukhtar et al. 2014; Hotineanu et al. 2015).

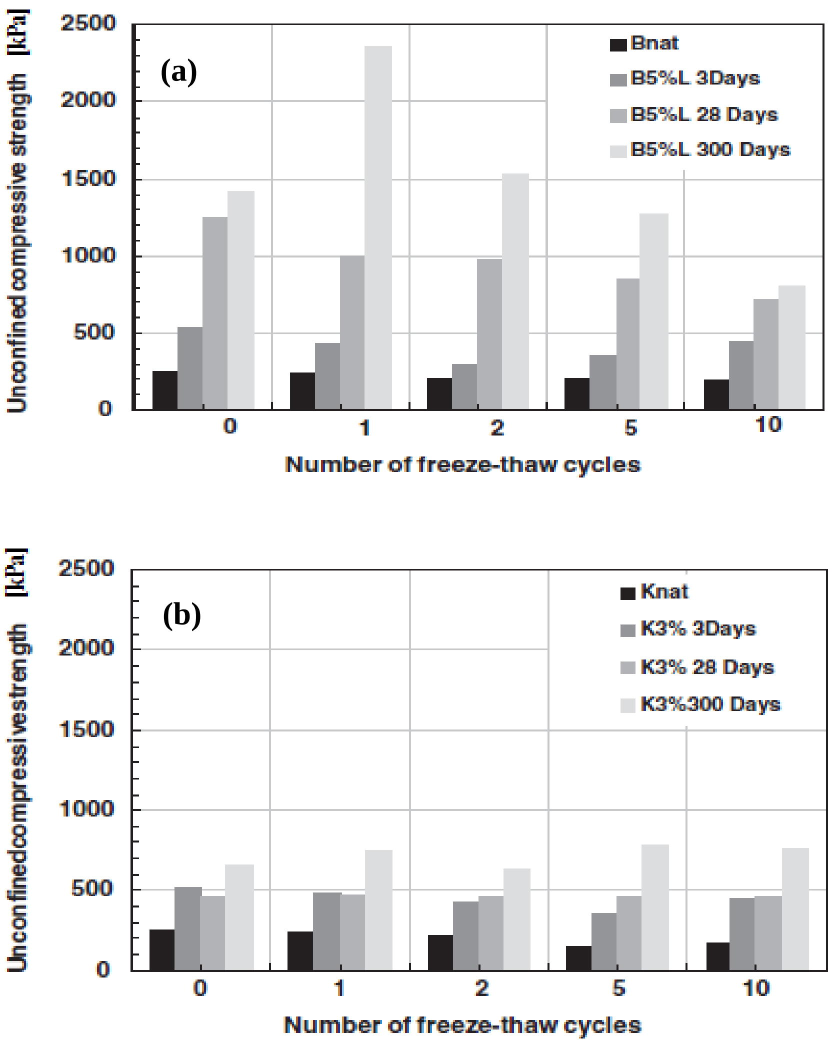


Figure 2.8. a) UCS values of pure bentonite (Bnat) and 5% lime stabilized bentonite under freeze-thaw condition b) UCS values of pure kaolinite (Knat) and 3% lime stabilized kaolinite under freeze-thaw condition (Hotineanu et al., 2015)

Greater changes in volume are obtained in lime-stabilized bentonite soil, when compared with kaolinite. Increasing number of freeze-thaw cycles cause an increment in the volume of untreated and 28-day treated specimens. Freeze-thaw conditions lead to greater pore diameters which is significant for volume alteration (Hotineanu et al., 2015). The investigation of Han and Cheng (2015) showed that freeze-thaw action enhances the number of large size pores in lime stabilized subgrade clay soil. The particle fractal dimension of lime-stabilised clay soil that is between 1.89 and 1.93, is reduced by the increasing number of freeze-thaw cycles. Superior bonding force between lime and clay soil, less free lime and restricted damage due to freeze-thaw conditions result in minimum fractal dimension of 4-6% lime stabilized clay soil. First freeze-thaw cycle leads to maximal decrease in fractal dimension. This suggests that the microstructure of clay soil is influenced greatest by first freeze-thaw cycle.

Shear strength parameters of clay soils are influenced by freeze-thaw action. Freeze-thaw cycles reduce the cohesion and improves the friction angle slightly. 5 freeze-thaw cycles cause loss of cohesion about 37% and 75%, respectively for lime stabilized 300-day cured kaolinite and bentonite specimens (Hotineanu et al., 2015). In addition to that the hydraulic conductivity of clay soil is improved 1000 times by 6% lime inclusion whereas it is improved 10-20 times after 3 freeze-thaw cycles (Yıldız and Soğancı, 2012).

Increasing number of freeze-thaw cycles reduces the UCS of polypropylene fiber reinforced and unreinforced clay soil specimens 20 to 25% (Ghazavi and Roustaie, 2010). Reduction in strength is less visible for polypropylene fiber reinforced specimens as compared with unreinforced ones. (Roustaei et al., 2015). The addition of 3% polypropylene fiber improves UCS of clayey soil by 160% whereas this increases in UCS of clay soil is rolled back by 60% after exposure to freeze-thaw conditions (Ghazavi and Roustaie, 2010). According to Roustaei et al. (2015), exposure to 9 freeze-thaw cycles reduce UCS of unreinforced clay specimens at percentages ranging among 14-43% whereas this reduces UCS of polypropylene fiber reinforced clay specimens approximately 1-32%. Furthermore, increasing number of freeze-thaw cycles from 5 to 7 increases the height of clay soil specimens. Beyond these cycles, the heights of specimens are insignificantly changed. The use of 3% polypropylene fiber reduces height of clay specimens up to 70% (Ghazavi and Roustaie, 2010).

According to Roustaei et al. (2015) increasing polypropylene fiber content in clay soil does not reduce the effects of freeze-thaw conditions. Since polypropylene fibers behave as a tensile element in clay soil matrix over the course of the frost heave of freezing cycle and the cohesion is only binder factor among polypropylene fibers and soil particles which decreases under cycles and thus, reduces the tensile influence of fibers. Therefore, 0.5% polypropylene fiber content is optimum fiber content in order to reduce the influences of freeze-thaw action. Moreover, freeze-thaw action reduces resilient modulus of clay soil and polypropylene fiber inclusion does not affect controlling decrement of resilient modulus significantly for clay soil under freeze-thaw condition. First cycles affect the decrement magnitude of resilient modulus more visibly. After 7 freeze-thaw cycles resilient modulus reachs a accurate value and does not change despite exposure to more freeze-thaw cycles.

In addition to that freeze-thaw action does not influence the friction angle of polipropylene fiber reinforced clay soil remarkably.

The investigation of Orakoglu et al. (2016) showed that increasing basalt fiber content reduces the thermal conductivity of fiber reinforced clay soil and increasing freeze-thaw cycles results in a decrement of thermal conductivity of basalt fiber reinforced soil. Moreover, frost heave on clay soil is mitigated by basalt fiber. 0.5% basalt fiber content can reduce frost heave even after 15 freeze-thaw cycles (Orakoglu et al., 2017).

Increasing basalt fiber content, confining pressure and dynamic shear strain improve the dynamic axial stress of fiber reinforced clay soil. However, freeze-thaw action reduces the dynamic axial stress. Increasing basalt fiber content, confining pressure and initial water content also improve dynamic shear modulus of fiber reinforced clay soil whereas increasing freeze-thaw cycles cause a decrease (Orakoglu et al., 2017).

In the light of the studies depicted above, it is understood that the literature includes insufficient information for characterization of basalt fiber reinforced lime lime stabilized clay, and a comparative study concerning the mechanical properties as well as the freeze-thaw behavior of lime stabilized clay reinforced with basalt and polypropylene fibers is not encountered in literature. Therefore, this study primarily focuses on benefits of the use of basalt or polypropylene fibers in evaluation of mechanical properties of lime stabilized clay, by adopting a systematic experimental approach.

# 3. MATERIALS AND METHODS

In this chapter, properties of the materials which were used in this thesis and preparation of specimens for laboratory testing are explained.

## 3.1. Materials

The materials used in this thesis are kaolin clay, quicklime, basalt fiber (BF) and polypropylene fiber (PF). The properties of these materials are explained in detail below.

### 3.1.1. Properties of Kaolin Clay

Kaolin which is soft white clay, also called china clay and named after the hill in China (Kao-ling) from that it was mined for centuries. Kaolin mainly composes of the mineral kaolinite (in Figure 3.1) that, beneath the electron microscope, is seen to compose of approximately hexagonal, platy crystals ranging in size from about 0.1 to 10 μm or even greater and mostly includes varying quantities of other minerals such as muscovite, quartz, feldspar, and anatase (Encyclopedia Britannica, 2017).

Figure 3.1. An image of kaolinite (Minerals Education Coalition, 2017)

If the water content ranging among 20 to 35% is added to kaolin, the kaolin behaves plastically due to increasing water content. Mixing kaolin with more percentages of water causes forming slurry or kaolin-water suspension. The size of kaolinite particles and chemicals existing in kaolin clay control the amount of water required in order to reach a predefined definition of water content, namely the Atterberg limits (Encyclopedia Britannica, 2017).

Before preparation of specimens, engineering properties of kaolin clay were determined. ASTM D4318-10 and ASTM D854-14 were used for determination of Atterberg limits and specific gravity. The liquid limit, plastic limit and plasticity index of clay were determined as 56, 30 and 26%, respectively. Shrinkage limit of clay was determined as 20% in accordance with ASTM D4943-08. Clay was classified as high plasticity clay (CH) based on Unified Soil Classification System. The specific gravity of clay was equal to 2.62. Besides, in order to find the compaction characteristics of clay, standard Proctor tests were conducted in accordance with ASTM D698-07. Based on the results, the optimum water content and the maximum dry-unit weight of clay were calculated as 30% and 1300 kg/m$^3$, respectively. Figure 3.2 shows the grain size distribution curve of clay. Furthermore, chemical properties of clay provided by the manufacturer are given in Table 3.1.

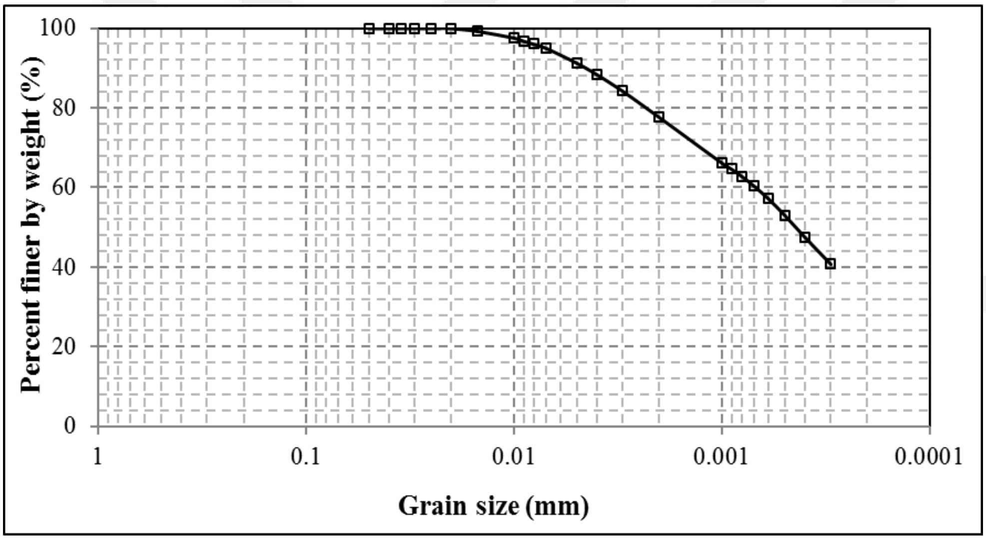


Figure 3.2. Grain size distribution of kaolin clay

Table 3.1. Chemical components of kaolin clay (%)

| **Component** | **%** |
|---|---|
| $Na_2O$ | 0.11 |
| MgO | 0.28 |
| $Al_2O_3$ | 54.13 |
| $SiO_2$ | 43.62 |
| $P_2O_5$ | 0.11 |
| $SO_3$ | 0.09 |
| $Fe_2O_3$ | 0.53 |

### 3.1.2. Properties of Polypropylene Fiber

Polypropylene is a half-crystalline polymer and its crystalline constitution, the relative quantity of amorphous and crystalline stages, crystal modification, size and perfection of crystallites and dimensions of spherulites determine the characteristics of polypropylene. The performance of polypropylene products is affected by tie molecules all (Pukánszky, 1995).

In this thesis, 100% pure, natural, white polypropylene fiber (PF) in lengths of 6, 12 and 19 mm was used. Melting and ignition points are 162°C and 593°C, respectively. This material is acid, salt, alkali and ultraviolet-resistant. Besides, it is known that oxidation and corrosion resistances of PF are high, and PF does not retain moisture. The other technical properties of this material are shown at Table 3.2. In Figure 3.3 the image of crumbled polypropylene fiber is also shown.

Table 3.2. Technical properties of PF

| **Properties** | **Polypropylene Fiber** |
|---|---|
| Diameter (μm) | 18-20 |
| Tensile Strength (MPa) | 600-750 |
| Modulus of Elasticity (MPa) | 3000-3500 |
| Density ($gr/cm^3$) | 0.91 |

Figure 3.3. Image of crumbled PF

### 3.1.3. Properties of Basalt Fiber

Basalt is a dark-coloured extrusive igneous (volcanic) rock which has low silica content and comparatively rich iron and magnesium content (Encyclopedia Britannica, 2017). Basalt fiber is made from this rock which is shown in Figure 3.4.

Figure 3.4. Basalt (Sepp, 2017)

In this thesis, basalt fiber (BF) in lengths of 6, 12 and 19 mm was used. This eco-friendly material provides high friction, frost, heat, moisture and chemical resistance. Besides, BF is salty sea water and ultraviolet radiation resistant. The other technical properties of BF are shown at

Table *3.3*. The image of crumbled basalt fiber is also shown in Figure 3.5.

Table 3.3. Technical properties of BF

| **Properties** | **Basalt Fiber** |
|---|---|
| Diameter (μm) | 14±2 |
| Tensile Strength (MPa) | 110 |
| Modulus of Elasticity (MPa) | 70000 |
| Density (g/cm$^3$) | 1.9 |

Figure 3.5. Image of crumbled BF

### 3.1.4. Properties of Quicklime

Quicklime was used in order to improve the strength of clay in this thesis. Quicklime (caustic lime) is a colorless, cubic crystalline or white amorphous substance and basic anhyride (The Columbia Encyclopedia, 2017).

## 3.2. Preparation of Specimens for Laboratory Testing

### 3.2.1. Preparation of Unconfined Compression Test Specimens

Regarding to the properties of the materials given in this chapter, an experimental framework was set up to compare the influence of inclusion of BF and PF on clay-lime mixtures. Initially standard Proctor tests were carried out to find the optimum moisture content and maximum dry unit weight of specimens containing 0, 3, 6 and 9% lime. Additionally, 6, 12 and 19 mm PF and BF were added in the mixture at rates of 0.25, 0.5, 0.75 and 1% (for each specimen) by dry weight. The prepared mixtures were placed in a mould as 3 layers and 25 strokes were applied to each layer for compaction. Before compaction, inner surfaces of moulds were lubricated to avoid side friction during extraction. The same process (3-layer compaction) was repeated at least 5 times with increasing water content by 1.5-3.0%. The water content and dry density of each specimen was calculated from the obtained values. As a result, the maximum dry unit weight and optimum water content were shown in Table 3.4.

Table 3.4. The maximum dry unit weight (g/cm$^3$) and optimum water content (%) of the designed mixtures (MDD/w)

| Fiber type | Control | BF | | | PF | | |
|---|---|---|---|---|---|---|---|
| Lime content | 0% | 3% | 6% | 9% | 3% | 6% | 9% |
| F6-0.25 | 1.30/37.98 | 1.29/38.01 | 1.28/37.40 | 1.27/38.10 | 1.29/38.77 | 1.28/37.89 | 1.27/38.60 |
| F6-0.50 | 1.28/37.82 | 1.26/37.98 | 1.24/37.26 | 1.23/38.05 | 1.26/37.15 | 1.24/37.43 | 1.23/38.73 |
| F6-0.75 | 1.30/36.24 | 1.29/36.73 | 1.28/34.25 | 1.27/37.33 | 1.29/36.99 | 1.28/34.06 | 1.27/37.98 |
| F6-1.00 | 1.27/36.03 | 1.26/36.81 | 1.24/35.96 | 1.23/37.13 | 1.26/36.78 | 1.24/35.74 | 1.23/37.57 |
| F12-0.25 | 1.30/37.89 | 1.28/37.90 | 1.27/36.41 | 1.26/37.97 | 1.28/37.85 | 1.27/36.20 | 1.27/37.83 |
| F12-0.50 | 1.28/37.86 | 1.27/37.88 | 1.26/35.86 | 1.25/37.30 | 1.27/37.41 | 1.26/35.55 | 1.25/37.64 |
| F12-0.75 | 1.30/37.09 | 1.29/37.12 | 1.28/35.47 | 1.27/36.84 | 1.29/36.83 | 1.28/35.27 | 1.27/37.11 |
| F12-1.00 | 1.27/36.80 | 1.26/36.95 | 1.24/35.99 | 1.23/36.73 | 1.26/36.79 | 1.24/35.70 | 1.23/36.98 |
| F19-0.25 | 1.29/37.84 | 1.28/37.86 | 1.27/35.51 | 1.26/37.62 | 1.28/37.93 | 1.27/35.60 | 1.26/37.90 |
| F19-0.50 | 1.29/37.62 | 1.28/37.70 | 1.27/35.47 | 1.26/37.54 | 1.28/37.77 | 1.27/35.45 | 1.26/37.88 |
| F19-0.75 | 1.30/37.40 | 1.29/37.44 | 1.28/35.21 | 1.27/37.28 | 1.29/37.56 | 1.28/35.34 | 1.27/37.65 |
| F19-1.00 | 1.30/36.91 | 1.29/36.99 | 1.28/35.10 | 1.27/37.13 | 1.29/37.21 | 1.28/35.25 | 1.27/37.60 |

In Table 3.4, F indicates the fiber. The number after F shows the length of fibers. The last numbers 0.25, 0.50, 0.75 and 1 indicate the percentage of fibers. Analyzing Table 3.4, decreasing lime content caused an increase in dry unit weight of specimens. In addition to that, maximum dry unit weights and optimum water contents of pure clay, 3, 6 and 9% lime stabilized clay were 1.31g/cm$^3$ /35.95%, 1.30g/cm$^3$ /36.70%, 1.29g/cm$^3$ /33.94% and 1.28g/cm$^3$ /36.71%, respectively. It is clear that optimum water content of mixtures ranged between 34 and 38%. Fiber type or content did not remarkably influence on the optimum moisture content of these mixtures.

The length and diameter of cylindrical unconfined compression test specimens which were compacted under standard Proctor effort and are shown in Figure 3.6 were 100 and 50 mm, respectively. All specimens (which were not subjected to freeze-thaw action and evaluated in terms of effect of freeze-thaw conditions) were prepared at 35% water content, wrapped with the stretch film and stored in a plastic container as shown in Figure 3.7 to prevent moisture loss in a moist room (relative humidity above 95±2%) at an average temperature of 20°C until strength testing. The unconfined compressive strength was determined in accordance with ASTM D2166. In Figure 3.8, the components of unconfined compression test (the device and the computer) are shown.

Figure 3.6. Unconfined compression test specimens

Figure 3.7. Specimens in a plastic container


Figure 3.8. Components of unconfined compression test: a) unconfined compression test device and b) the computer which has test result transferred from the device

### 3.2.2. Application of Freeze-Thaw Action

The comparison of influences of freeze-thaw action on lime stabilized basalt and polypropylene fiber reinforced clay was examined in this thesis. The specimens including 0, 0.5 and 1% 12 mm basalt and polypropylene fiber were stabilized with 0% and 3% lime, compacted under standard Proctor effort (i.e. 45% by weight of soil) and wrapped with the stretch film. All specimens were prepared in length and diameter of 100 mm and 50 mm, respectively and cured for 28 days in a moist room (relative humidity above 95±2%) at an average temperature of 20°C. After curing, specimens were subjected to 0, 1, 3, 7 and 10 cycles of freeze-thaw tests following the ASTM D560 test method using a deep freezer. For freezing phase, specimens were placed in the deep freezer at -23°C for 24 hours. Subsequently, for thawing phase specimens were removed from the deep freeze and subjected to thawing using air conditioner in the room at 21°C for 23 hours. Thus, freeze-thaw cycles were completed. Before unconfined compression tests, the full height and width of the specimens were expose to impact with a wire brush in accordance with ASTM D560. In Figure 3.9, the specimen including 1% basalt fiber is shown after exposure to 10 freeze-thaw cycles.

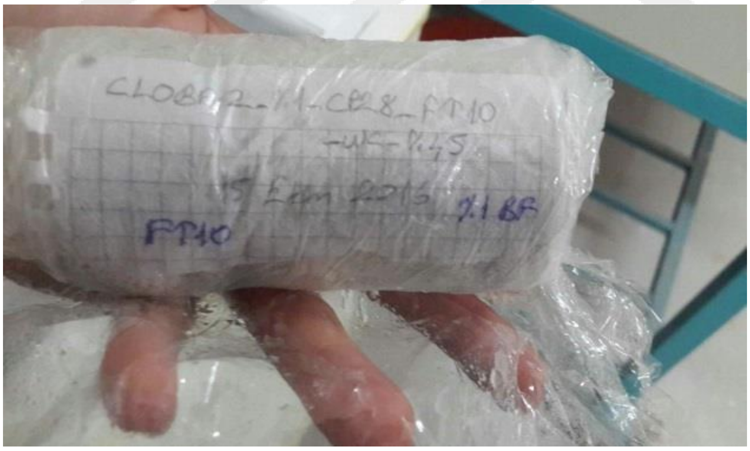

Figure 3.9. The specimen including 1% basalt fiber subjected to 10 freeze-thaw cycles

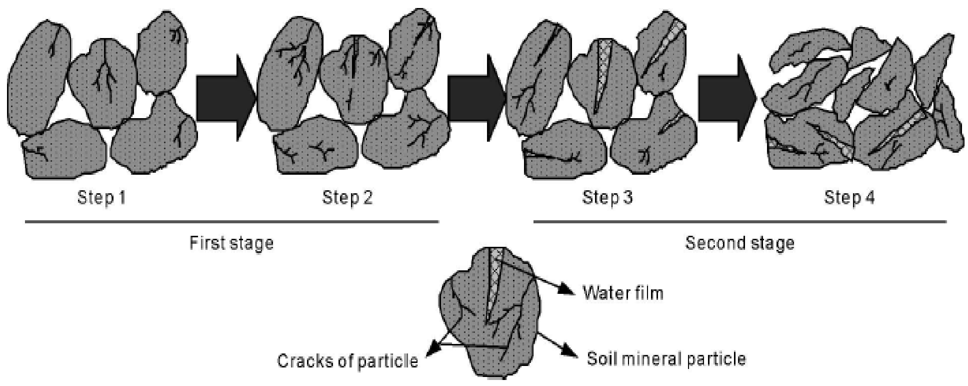


Figure 3.10. Schematic diagram of the frost weathering process of soil mineral particles (Zhang et al., 2016)

Figure 3.10 illustrates the schematic diagram of the frost weathering (fragmentation) process of soil mineral particles which are completed in four steps and divided two stages by Poltev (1967). In the first step, cracks occur on the surface of mineral particles driven by the temperature due to transforming water from liquid to solid phase. In second step, the microcracks of particles are transformed into macrocracks due to the fact that pore water transforms glacier form and causes an increment in volume (approximately 9%). In the third step, an increment in the thickness of water film in the crack of soil particles occurs. In the fourth step, further fragmentation of primary minerals occurs due to increasing the thickness of water film (Zhang et al., 2016).

# 4. RESULTS AND DISCUSSION

In this chapter, unconfined compressive strength values and secant modulus of specimens including basalt and polypropylene fiber whether subjected to freeze-thaw action or not are elucidated. The data and images obtained from Scanning Electron Microscopy (SEM) and Energy Dispersive Spectroscopy (EDS) are evaluated. Moreover, Ultrasonic Pulse Velocity (UPV) of specimens subjected to freeze-thaw cycles is determined and data obtained from tests is used for evaluation of mechanical properties.

## 4.1. Mechanical Properties

In order to compare the individual contributions of PF and BF, unconfined compression strength tests were carried out using strain-controlled application of the axial load. Initially, the tests were performed on stabilized specimens containing 0, 3, 6 and 9% of lime to investigate the strength of clay without fiber inclusion after 1, 7, 28 and 90-day curing. The results were given in Figure 4.1. Analyzing Figure 4.1, an obvious increase was observed in strength of clay with the addition of lime until 6% lime content. This can be explained by the reactions among lime and clay minerals providing an increase in the strength of the soil. As is known, the first reactions due to stabilization of lime are hydration and flocculation. After these reactions, cementation and carbonation, both which are long term reactions occur. Cementation enhances strength increase. In this phase, the calcium-aluminum-silicate-hydrate minerals in clay react with the calcium ions in the lime to form silicate gel (Hausmann, 1990). Silicate gel fills the gaps in the clay and is responsible for keeping the particles together. As the curing period increases, the time allowed for these reactions may be sufficiently large, thus UCS of specimens increases more. However, more than 6% lime content does not increase the strength up as 6% lime content does.

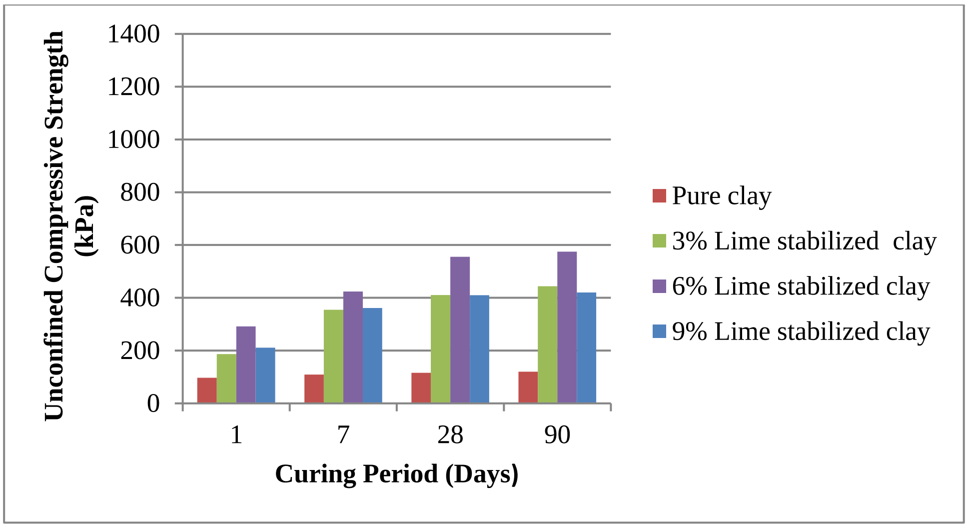


Figure 4.1. Unconfined compression test results of specimens without fibers

The main contributors that lead the role of fiber in composites are: the inherent mechanical quality of the fiber, the physico-chemical interaction between the fiber and resin component (interface interactions), the volume fraction of fiber within the composite, the position, orientation and fiber-layout in the composite, and recyclability (Dhand et al., 2015). The mechanical effects of fibers are discussed in detail.

### 4.1.1. Unconfined Compressive Strength of Specimens Free of Lime

Figure 4.3 shows results of unconfined compression tests on 0.25, 0.50, 0.75, 1% BF and PF reinforced clay. 6, 12, 19 mm fiber lengths and 1, 7, 28, 90 days curing period were used in preparation and curing of specimens before strength testing. As can be seen in Figure 4.3, the addition of PF and BF slightly increased the strength of specimens without lime inclusion. Bonding among fiber and soil matrix is the main source of strength increase. Generally, 1% fiber content and 12 mm fiber length were more effective on strength for PF reinforced specimens. For BF reinforced specimens, 1% fiber content and 6 mm fiber length gave maximum strength, however the effective fiber length changed according to curing period and fiber content. As is known, pure clay specimens can sometimes gain very little strength with aging, but this is not at the level to be considered. In Figure 4.3, this situation can be seen clearly. Since specimens did not contain lime which gives the strength to specimens by chemical reactions, strength gain was independent of curing period. However, aging may be effective on the strength increase, along with the uniformity of the fiber distribution in the specimen. Figure 4.4 shows axial stress-strain of specimens including 12 mm BF and PF in length of 0.25, 0.50, 0.75, 1% fiber content after 28-day curing. In Figure 4.4, clay and lime are indicated by C and L, respectively. The percentage of lime is shown by the number after L. The length of fibers is shown by the number after BF and PF. The percentage of fibers is indicated by the last numbers. To illustrate, the mixture including clay, 0% lime, 1% and 12 mm in length of BF was designed as CL0PF12-1. It is clearly observed that PF improved the strength but without lime inclusion, the influence of PF inclusion on strength was limited. However, both BF and PF reinforced specimens exhibit more ductile behaviour in comparison with unreinforced specimens. Figure 4.5 shows application of unconfined compression test to the specimen containing basalt fiber.

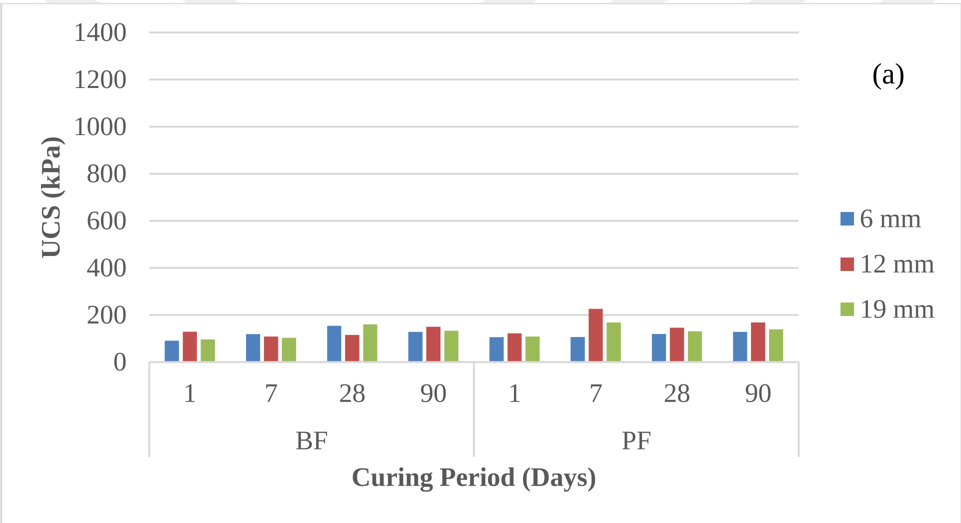


Figure 4.2. Unconfined compression test results of 1, 7, 28 and 90-day cured specimens containing a) 0.25%, b) 0.50%, c) 0.75% and d)1% BF and PF in different fiber lengths (to be continued)

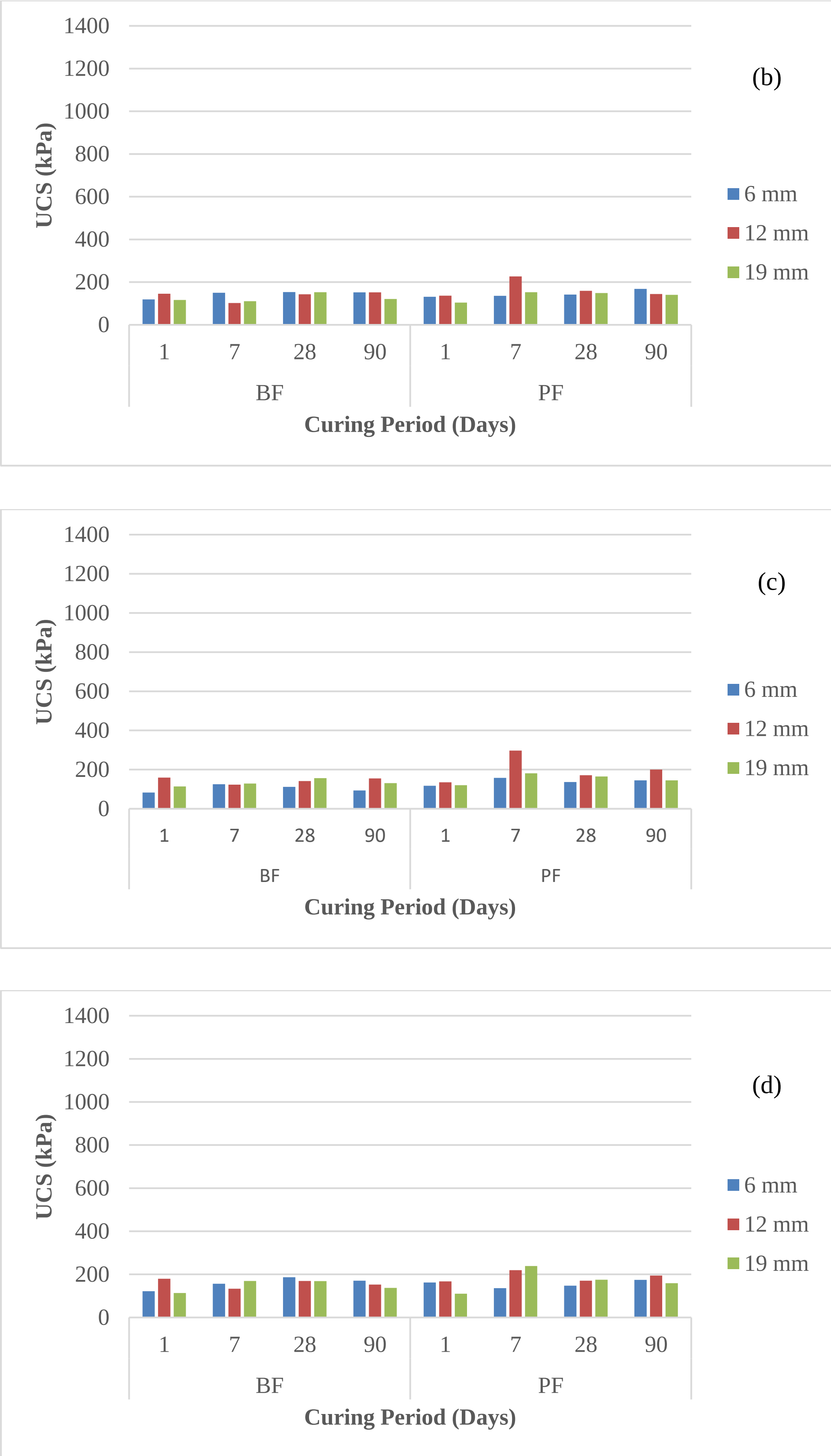


Figure 4.3. Unconfined compression test results of 1, 7, 28 and 90-day cured specimens containing a) 0.25%, b) 0.50%, c) 0.75% and d)1% BF and PF in different fiber lengths

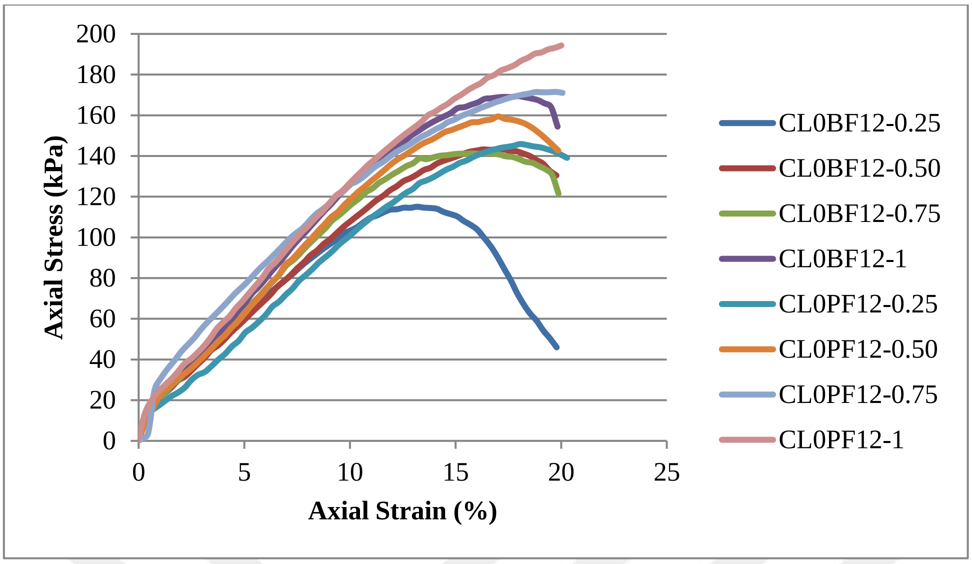


Figure 4.4. Axial stress-strain curves for specimens containing different amounts of BF and PF after 28-day curing

Figure 4.5. Application of unconfined compression test to the specimen containing basalt fiber (BF)

### 4.1.2. Unconfined Compressive Strength of Lime Stabilized Specimens

Figure 4.7 shows UCS values of 9% lime stabilized 0.25, 0.50, 0.75, 1% BF and PF reinforced clay. 6, 12, 19 mm fiber length and 1, 7, 28, 90 days curing period were used in preparation and curing of specimens before strength testing. Based on Figure 4.7, it can be concluded that increasing curing time mostly caused a linear increase in strength of 9% lime stabilized specimens. Comparing strength values, 0.75% fiber content and 12 mm fiber length after 1, 7, 28-day curing seem to be more effective to gain strength for PF reinforced specimens. After 90-day curing period, 19 mm fiber length was also effective. Analyzing UCS values of BF reinforced specimens, 0.75% fiber content and 6 mm fiber length after 1, 7, 28-day curing were more effective with respect to strength. After 90-day curing, fiber length of 12 and 19 mm were also effective. Figure 4.8 shows the axial stress-strain of 9% lime stabilized specimens including 12 mm BF and PF in length of 0.25, 0.50, 0.75, 1% fiber content after 28-day curing. In Figure 4.8, clay and lime are indicated by C and L, respectively. The percentage of lime is shown by the number after L. The length of fibers is shown by the number after BF and PF. The percentage of fibers is indicated by the last numbers. To illustrate, the mixture including clay, 9% lime, 1% and 12 mm in length of BF was designed as CL9BF12-1. As is seen, BF and PF improved the strength, and the strength increase was more evident with inclusion of lime. The use of lime also caused less axial deformation. Hence, specimens including lime exhibited more brittle behaviour. In Figure 4.9, a fractured lime stabilized specimen containing PF after unconfined compression test is shown. Furthermore, Figure 4.10 shows UCS values of 3, 6 and 9% lime stabilized, 12 mm BF reinforced clay with 0.25, 0.50, 0.75, 1% fiber content after 1, 7, 28 and 90-day curing. It was observed that increasing curing period and lime content enhance the strength of specimens for 3% and 6% lime stabilized specimens. Maximum strength for 3% lime stabilized specimens was obtained by 1% fiber content after 90-day curing. For 6% lime stabilized specimens, 0.75% fiber content provided the maximum strength after 90-day curing. 9% lime addition was not as effective as 6% lime addition to increase the strength of soil. For 9% lime stabilized specimens, maximum strength was obtained by 0.5% fiber content after 90-day curing.

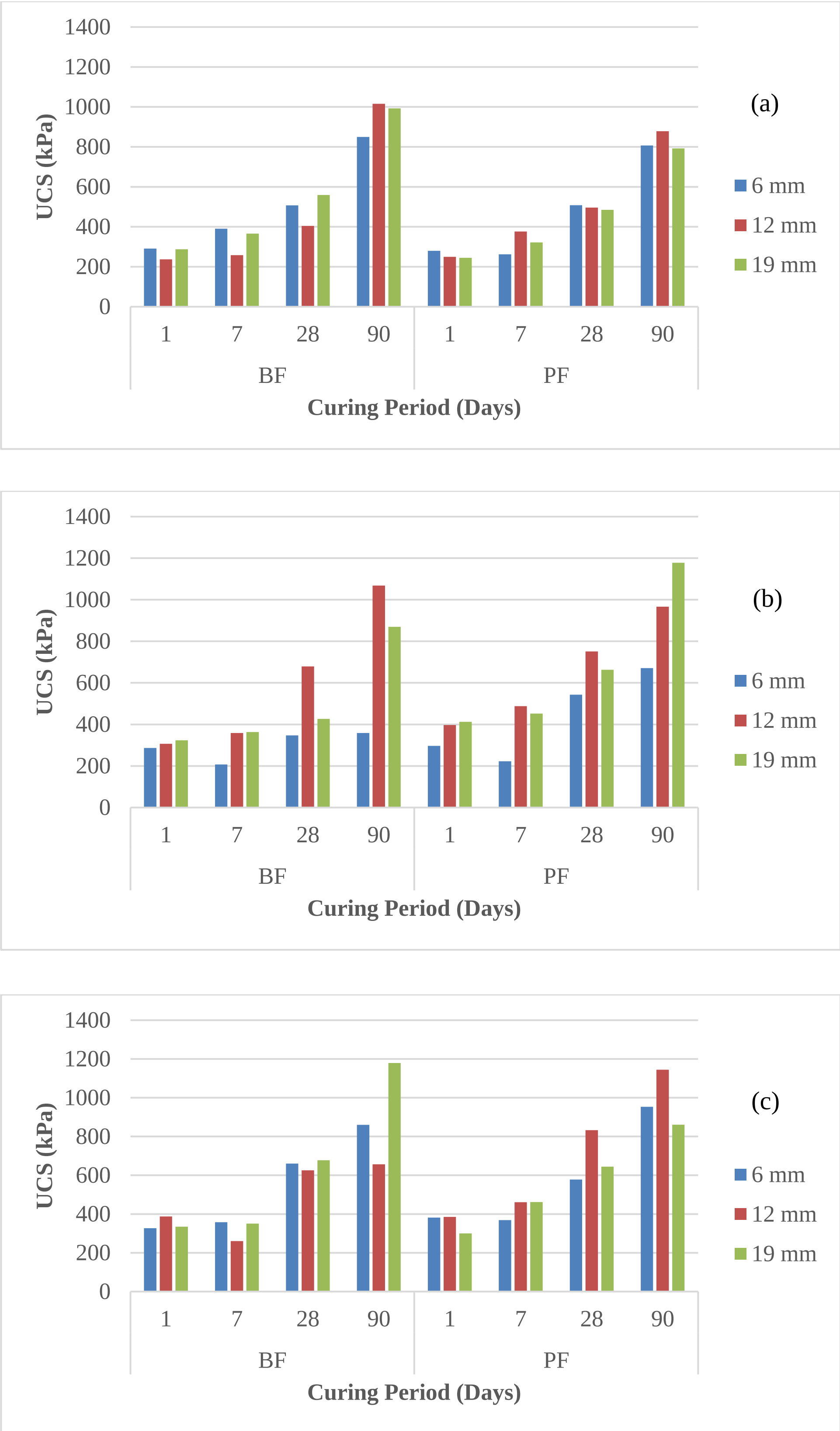


Figure 4.6. Unconfined compression test results of 1, 7, 28 and 90-day cured 9% lime stabilized specimens containing a) 0.25%, b) 0.50%, c) 0.75% and d)1% BF and PF in different fiber lengths (to be continued)

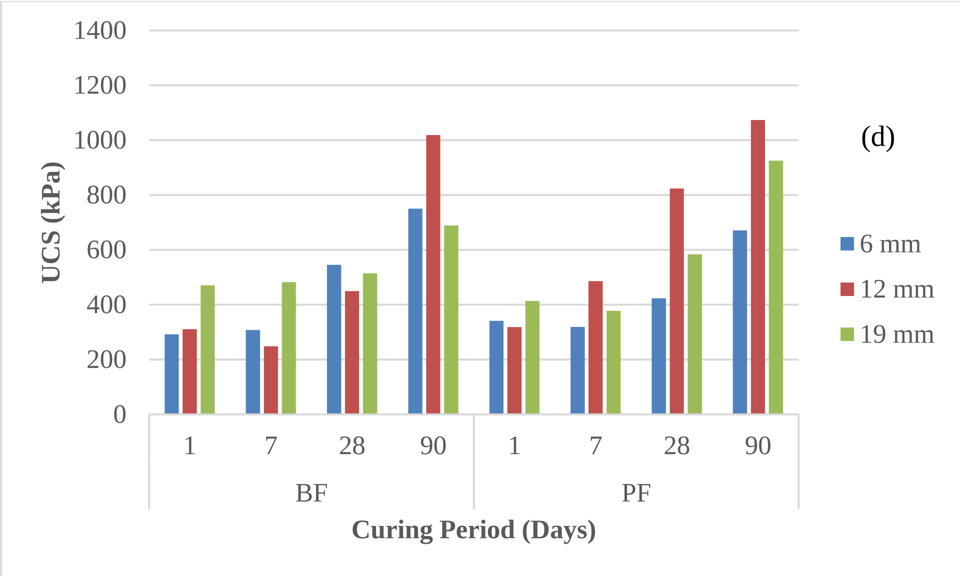


Figure 4.7. Unconfined compression test results of 1, 7, 28 and 90-day cured 9% lime stabilized specimens containing a) 0.25%, b) 0.50%, c) 0.75% and d)1% BF and PF in different fiber lengths

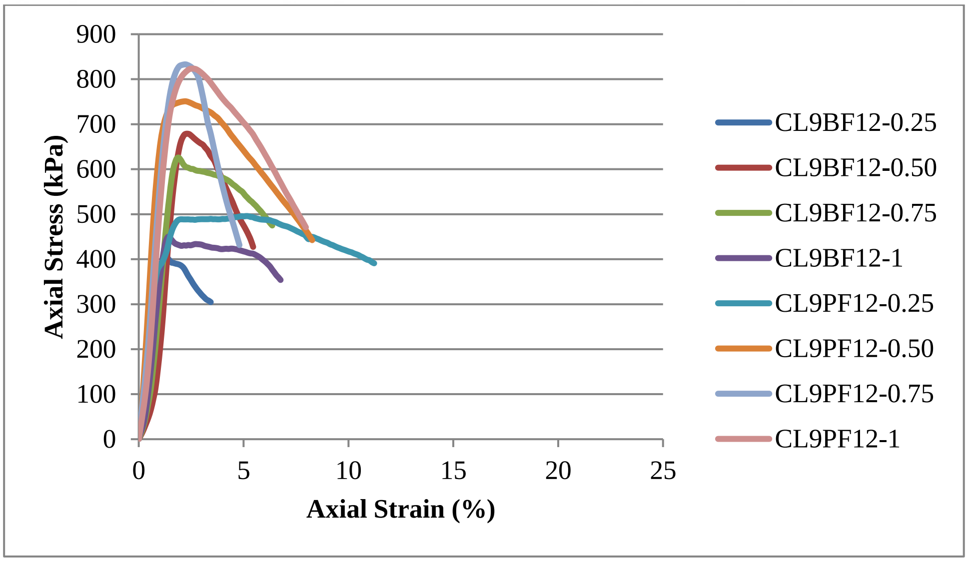


Figure 4.8. Axial stress-strain curves for 9% lime stabilized specimens containing different amounts of BF and PF after 28-day curing

Figure 4.9. A fractured lime stabilized specimen containing polypropylene fiber (PF) after unconfined compression test

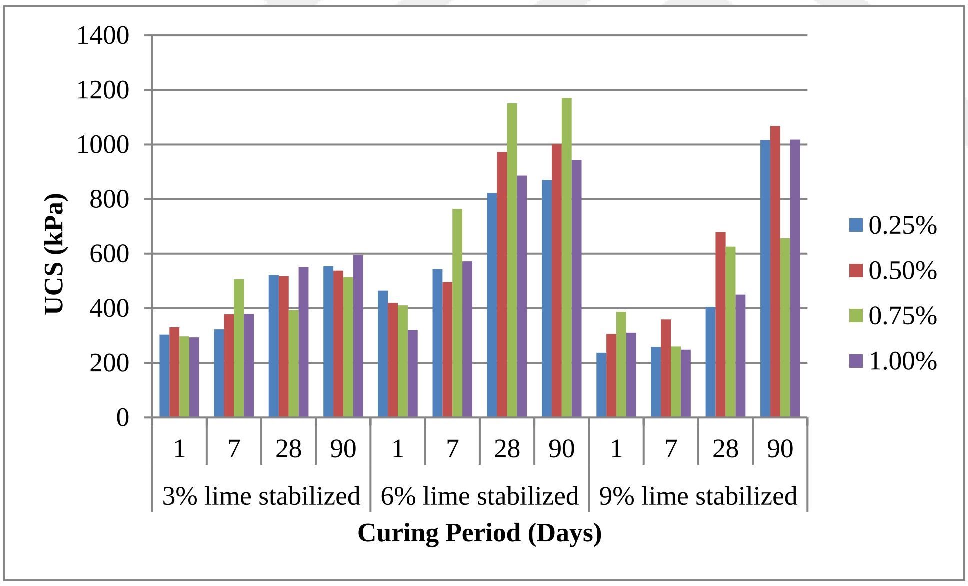


Figure 4.10. Unconfined compression test results of 3, 6 and 9% lime stabilized specimens containing 12 mm BF

### 4.1.3. Evaluation of Secant Modulus by Reinforcement and Lime Stabilization

The slope of the chord connecting the origin of the stress-strain curve to the point where the axial stress is equal to 50% of failure stress (namely, the UCS) is defined as the secant modulus of elasticity ($E_{50}$) (Yilmaz and Karatas, 2011). According to previous investigations, in most cases, $E_{50}$ varies with UCS ($q_u$) linearly. On the other hand, a generalized mathematical expression to identify the linear relationship between $E_{50}$ and the UCS is not identified yet. Different components of soils/sediments (such as organic content and heavy metals) and types of binders used as well as their content (lime, fly ash, cement and their quantity) basically are the reason behind the diversity of the equations proposed in the literature (Wang et al., 2013). $E_{50}$-$q_u$ relationship, for the PF-clay mixtures including 0.25, 0.5, 0.75 and 1% fiber contents after 1,7, 28 and 90 days was drawn in Figure 4.11a. In Figure 4.11b, same relationships were prepared for PF-lime-clay mixtures including varying (0.25, 0.5, 0.75 and 1%) fiber contents and curing period (1, 7, 28 and 90 days). As can be seen in figures, the addition of lime improved the secant modulus ($E_{50}$) due to the fact that the addition of lime not only increase the strength but also provides the specimen more stiffness which leads to brittle fracture. This means that the specimens fractured with less axial deformation and further strength. However, the use of lime reduced the correlation ($R^2$) between $E_{50}$ and the UCS ($q_u$) values. For BF-clay mixtures in Figure 4.12a and for BF-lime-clay mixture in Figure 4.12b, $E_{50}$-$q_u$ relationships were plotted. Arguably, the use of lime increased $E_{50}$, but decreased the correlation among $E_{50}$ and $q_u$ values as in specimens including PF. It can be said that the decrease of correlation is clearer for specimens including PF. Highest $E_{50}$ value was obtained by the use of 12 mm BF-lime-clay mixture with 0.5% fiber content after 90-day curing.

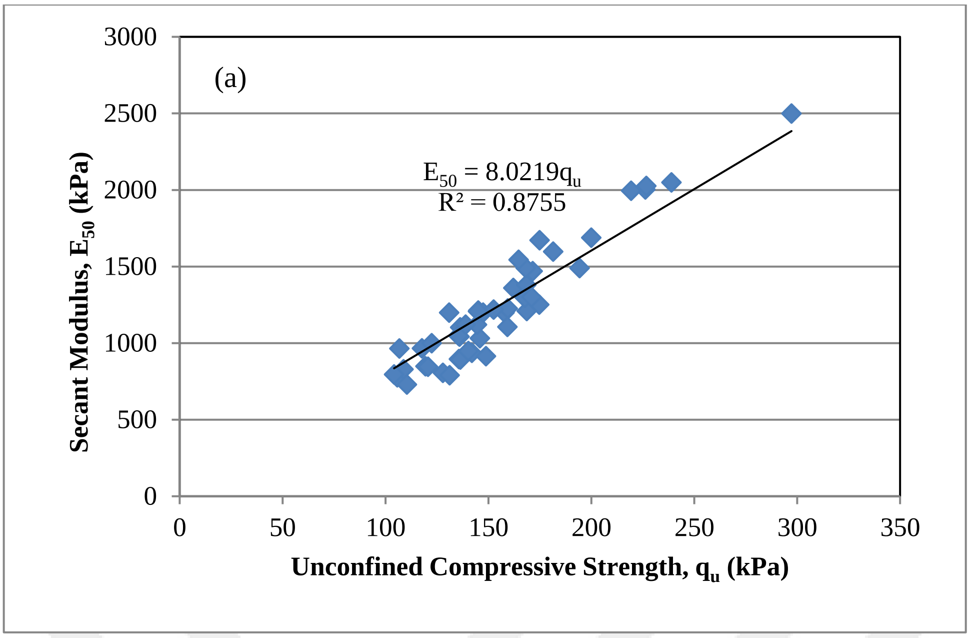


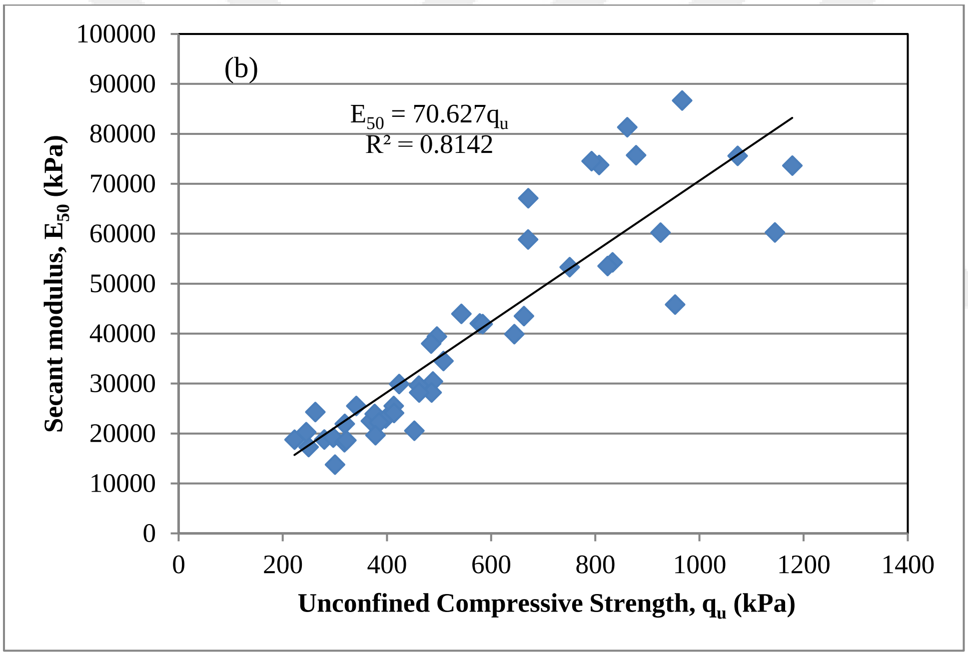


Figure 4.11. a) $E_{50}$ values for PF-clay mixtures with reference to $q_u$ b) $E_{50}$ values for PF-(9%) lime-clay mixtures with reference to $q_u$

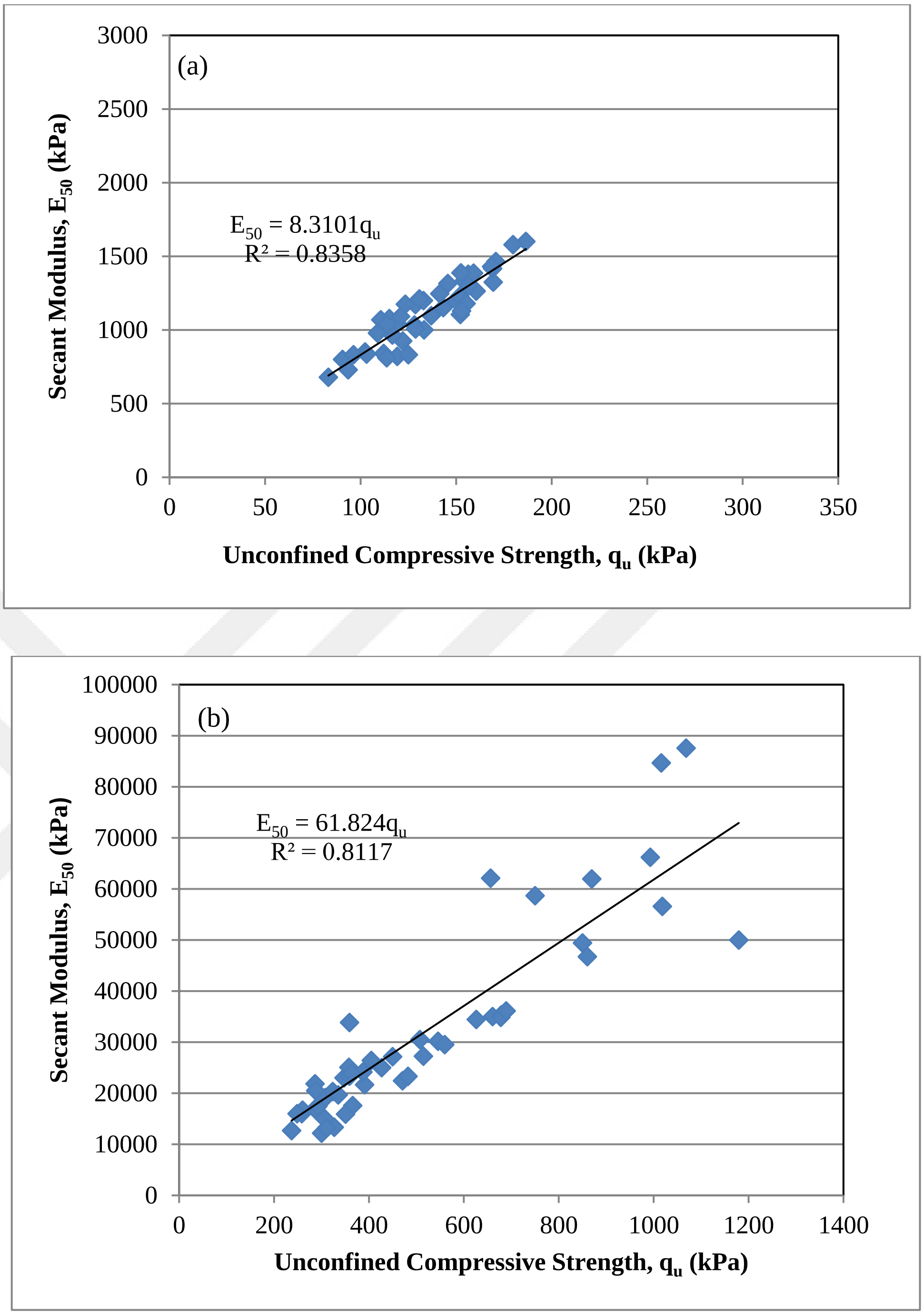


Figure 4.12. a) $E_{50}$ values for BF-clay mixtures with reference to $q_u$ b) $E_{50}$ values for BF-(9%) lime-clay mixtures with reference to $q_u$

## 4.2. Application of Scanning Electron Microscopy and Energy Dispersive Spectroscopy on Selected Specimens

Scanning Electron Microscopy (SEM) is used to monitor the micro- and nano- structural properties of solid materials. An electron gun which generates the electron beams, constitutes a major SEM. The beam is guided and focused by electromagnetic optics (Mehta, 2012). A specific specimen zone is magnified using a high energy focused beam of electrons by Scanning Electron Microscopy (SEM). The specimen is subjected to vacuum in order to ensure that the beam is focused, and the specimen is not in touch suspended particles in the environment. The beam of electrons interacts with the specimen, this results in formation of secondary electrons. The specimen releases these electrons (direct scattering or emitted from the specimen) that are detected to supply an image based off the topography of the surface. The Secondary Electron Detector and the Backscattered Electron Detector are prevalently used. Electrons, interacting with detectors, enables constitution of image by use of the energy of the detected electrons with their intensity (number density) and location of emission (Mehta, 2012; Polymer Solutions Group, 2017).

After 90-day curing, selected specimens that were reinforced with BF/PF, were applied UCS tests. After strength testing, pieces of fractured specimens from shear band were subjected to Scanning Electron Microscopy (SEM)/Energy Dispersive Spectroscopy (EDS). Firstly, the specimens were placed on the brass plate and they were glued with a double sided adhesive carbon tapes to provide conductivity in non-conductive materials as is shown in Figure 4.13. Then, specimens were subjected to vacuum for gold plating until the vacuum was $4*10^{-1}$ bar (it was waited for 45-60 minutes). When the vacuum reached the desired value, gold plating was done as is shown in Figure 4.14. The gold-plated specimens were placed on the SEM device and analyzed as is shown in Figure 4.15. The morphological structures of the products can be observed clearly in the fractured surface investigations on the SEM device. It is possible to observe weaker products more intensely due to the fact that the broken surface is a weak section of the specimen (Tosun, 2007).

Figure 4.13. Specimens on the brass plate with a double sided adhesive carbon tapes

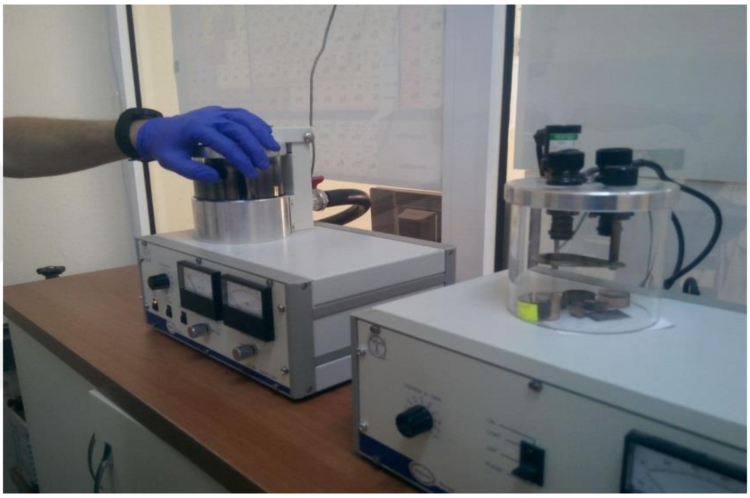

Figure 4.14. Image of gold plating process


Figure 4.15. Image of a) placing and b) analyzing gold-plated specimens in SEM device

In Figure 4.16a, the SEM image of the pure polypropylene fiber clay soil can be seen. It is evident that polypropylene fiber is pulled out of the clay soil due to the insufficient interfacial adhesion of the fiber and soil during compression. The fiber surface was not damaged during pull-out. Hence, during pull-out, a clearance was observed between fiber and soil. Fiber-soil columns were consisted and behaved as a skeleton. A three-dimensional fiber-soil net is consisted of the discrete distribution of fibers in the soil. Figure 4.16b shows an image of basalt fiber reinforced clay. Basalt fiber seems to be surrounded by the clay particles. Higher interfacial adhesion enabled better bonding strength. Clay particles formed a clustered structure on and around the basalt fiber in presence of water. Fiber-soil columns were consisted and on the fragmentized clay particles, apparent shearing traces were existed. Besides, clay particles were still on the surface of fiber. The SEM image of PF/clay/lime mixture is given in Figure 4.16c. The presence of lime caused a more rigid structure. On the other hand, a gap was observed where the polypropylene fiber was displaced which is the evidence of well bonding. PF reinforcement seems to be functional, fiber reinforced the surrounding improved soil while a pull-out behaviour was experienced. Furthermore, an abrasion trace was not observed. In Figure 4.16d, the SEM image of basalt fiber reinforced lime stabilized clay soil and the basalt fiber surface is given. The structure seems to be more stiff and compact. The fiber surface is covered by lime and clay particles. The interaction between the fiber surface and the soil matrix is clear. When lime is added to dried clayey soil, clay particles behave hydrophobicly. Hence, when water is mixed with lime-soil matrix, soil particles do not tend to form oversized aggregates. This phenomenon was referred to as sandification (Liu, 2003; Cai et al., 2006). When the fiber reinforced soil is exposed to external force, soil particles transfer the stress to vicinity of fiber-soil column. The part of external stress transforms to the internal force. In this way, it prevents the ascending of the overall strain of soil specimen. In this manner, interaction among fiber-soil-lime and by-products is effective in binding, which controls displacement and deformation of soil particles while providing improvement in strength of clay. When the basalt fiber content is excessive, lots of fiber filaments cluster in the soil specimen by electrostatic interaction. Therefore, it forms the weak area of stress readily stress transfer mechanism is disrupted. For PF, subsidiary stresses due to the use of short fiber cause soil particles surrounding fibers slide over. Selection of longer fiber causes reduction in tension, bending and torsional strength of fiber.

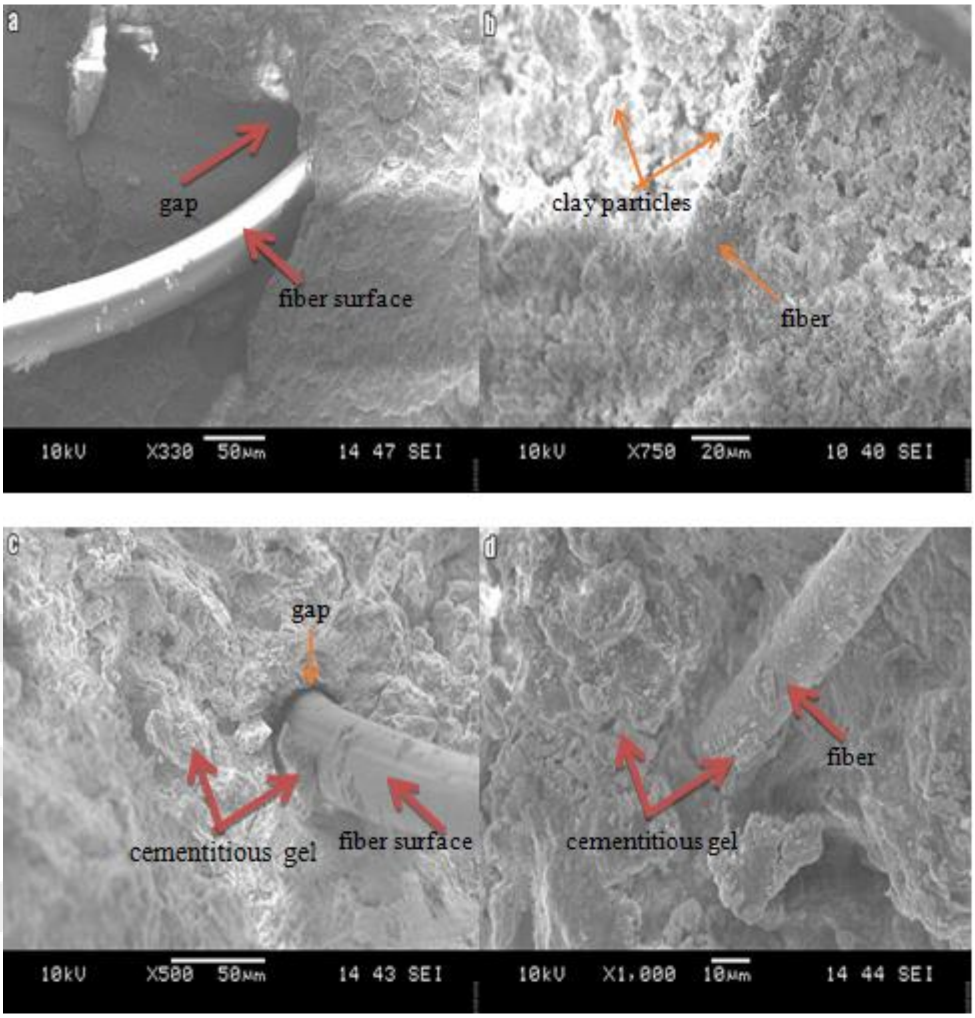


Figure 4.16. SEM images of a) PF reinforced soil with a magnification of 330 times b) BF reinforced soil with a magnification of 750 times c) 9% lime stabilized PF reinforced soil with a magnification of 500 times d) 9% lime stabilized BF reinforced soil with a magnification of 1000 times

When lime is added to kaolin clay, calcium ions react with clay minerals to form silicate gel. Void-filling effect also leads to the formation of a more stable interface reinforcing the bond between the fiber and the composite material (Hausmann, 1990). In Figure 4.16c and Figure 4.16d presence of cementitious products on fiber is apparent and it indicates the activity of reinforcement system. This demonstrates that fiber was mobilized during testing and bonding.

The characteristic X-rays of various elements into an energy spectrum is separated using an energy dispersive detector and analyzing the energy spectrum to determine the plenty of specific elements is provided by EDS (Energy Dispersive Spectroscopy). EDS is able to give basic compositional information by finding chemical composition of materials down to a spot size of a few microns and creating element composition maps over a much wider raster area. A SEM device generally includes EDS systems which contains a sensitive X-ray detector, a liquid nitrogen dewar for cooling, and software to collect and analyze energy spectra (Nazarov and Noh, 2011). EDS spot analyses was carried out to identify the chemical composition of specimens. Figure 4.17 illustrates the results of EDS analyses obtained from PF reinforced soil, BF reinforced soil, 9% lime stabilized PF reinforced soil and 9% lime stabilized BF reinforced soil. In Figure 4.17a and Figure 4.17b results from EDS showed that specimens were composed of Al, Si, O and Ca in which Al and Si are the main element. Since, kaolin clay primarily composes of $Al_2O_3$ and $SiO_2$. In Figure 4.17c and Figure 4.17d EDS analyses confirm the presence of lime, kaolin and water. It is evident that the matrix contained a high concentration of Al and Si. Besides, Ca and O were present. The amount of calcium increased due to the presence of lime. These results demonstrate the possible presence of calcium hydroxide crystals (CH).

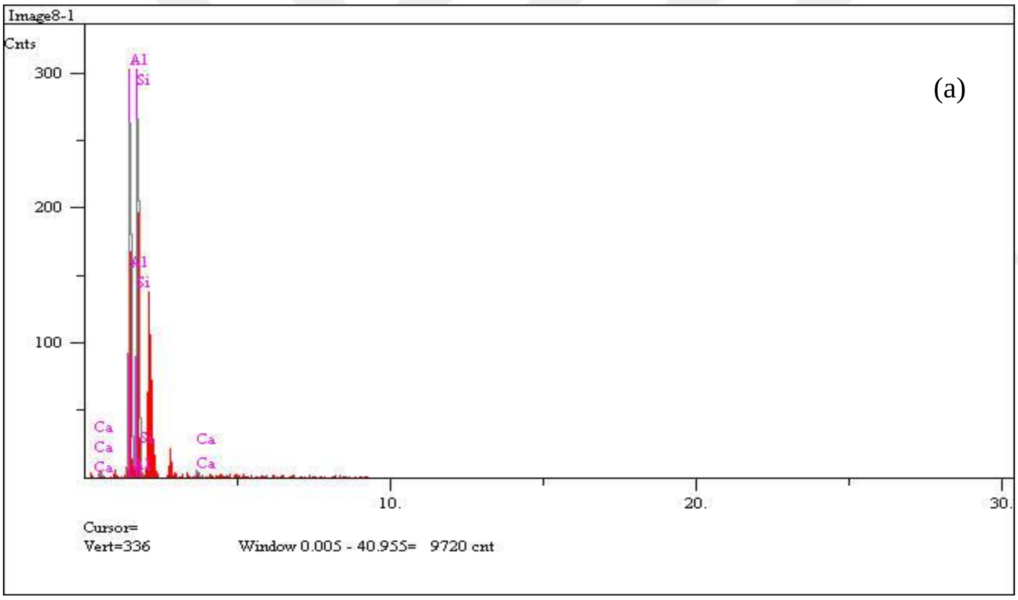


Figure 4.17. EDS analysis of a) PF reinforced soil b) BF reinforced soil c) 9% lime stabilized PF reinforced soil d) 9% lime stabilized BF reinforced soil (to be continued)

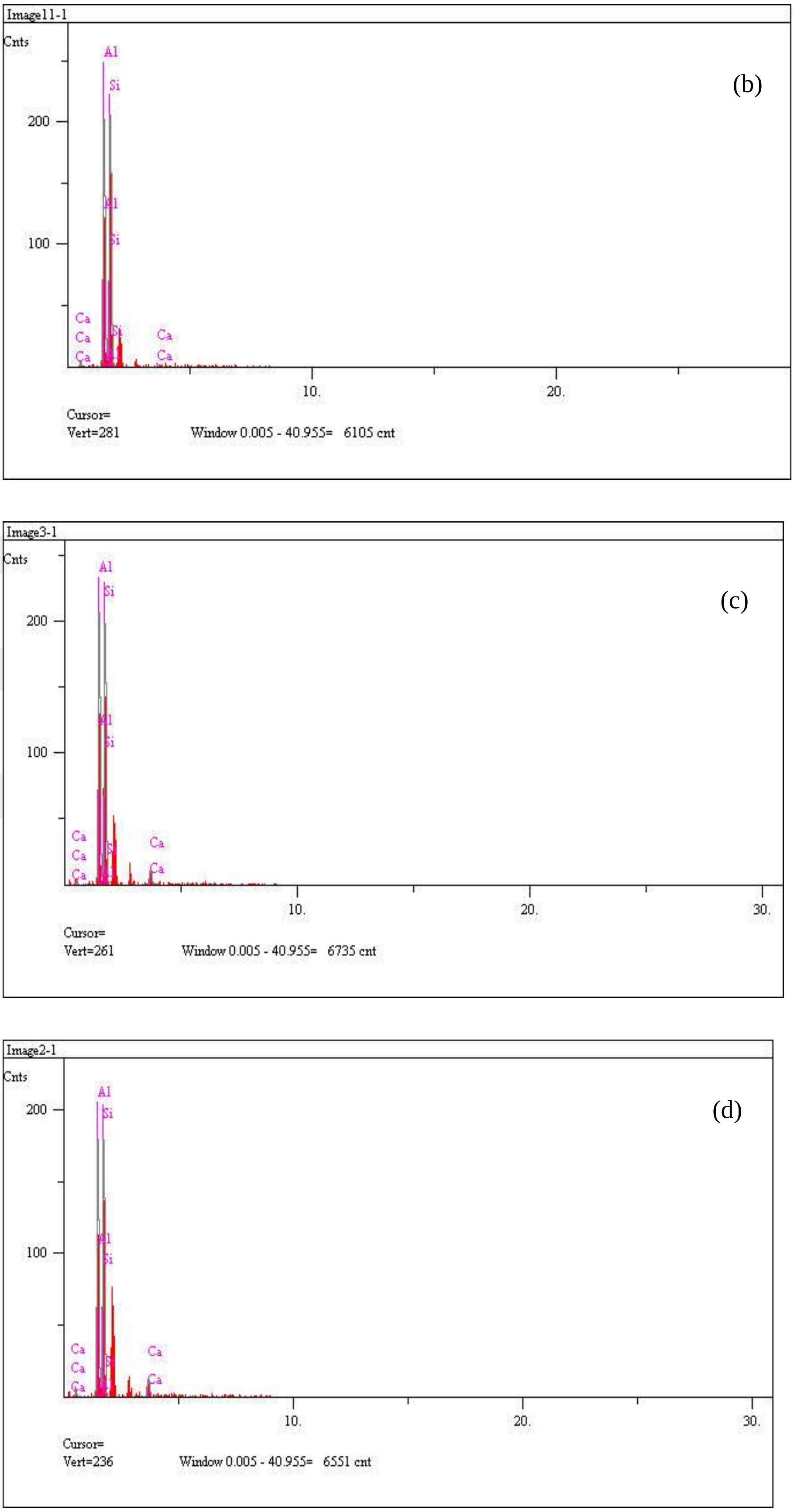


Figure 4.17. EDS analysis of a) PF reinforced soil b) BF reinforced soil c) 9% lime stabilized PF reinforced soil d) 9% lime stabilized BF reinforced soil

### 4.3. Evaluation of Effects of Freeze-Thaw Action on Lime Stabilized and/or Fiber Reinforced Clay

As is known, freeze-thaw (which was also shown as F-T in this thesis) conditions affect clay soil adversely. In the soil cracks occur and the soil loses part of its mass due to outflow of water under freeze-thaw action. In order to determine the influence of treatment (lime, BF and PF) on the durability behaviour of the specimens, prepared specimens were weighted before and after freeze-thaw cycles. Difference between two weights showed the mass loss due to freeze-thaw conditions. The results were shown in Figure 4.18. In figures below, freeze-thaw is indicated by F-T and the number after T shows the number of freeze-thaw cycles. Figure 4.18a and b show test results of specimens free of lime and 3% lime stabilized specimens, respectively. 12 mm polypropylene fiber (PF) and basalt fiber (BF) were used to reinforce the specimens. Fiber types and rates are shown below the diagrams. Analyzing Figure 4.18, as the number of freeze-thaw cycles increased, the mass loss increased. The addition of lime, BF and PF decreased the mass loss. Mostly, 0.5% fiber content decreased the mass loss more except the specimen containing 0.5% BF free of lime and effective fiber type varied according to amount of fiber and number of cycles. Moreover, lime stabilized specimens caused less mass loss due to the fact that lime reacted with water, thus more stiff structures occurred which limited outflow of water. For all specimens, mass loss was under 10%. It was proved that the strength of soil closed to the surface is not remarkably influenced by mass losses about 10-15% in the literature (Chamberlain et al., 1990; Hassini, 1992; Zaimoglu, 2010).

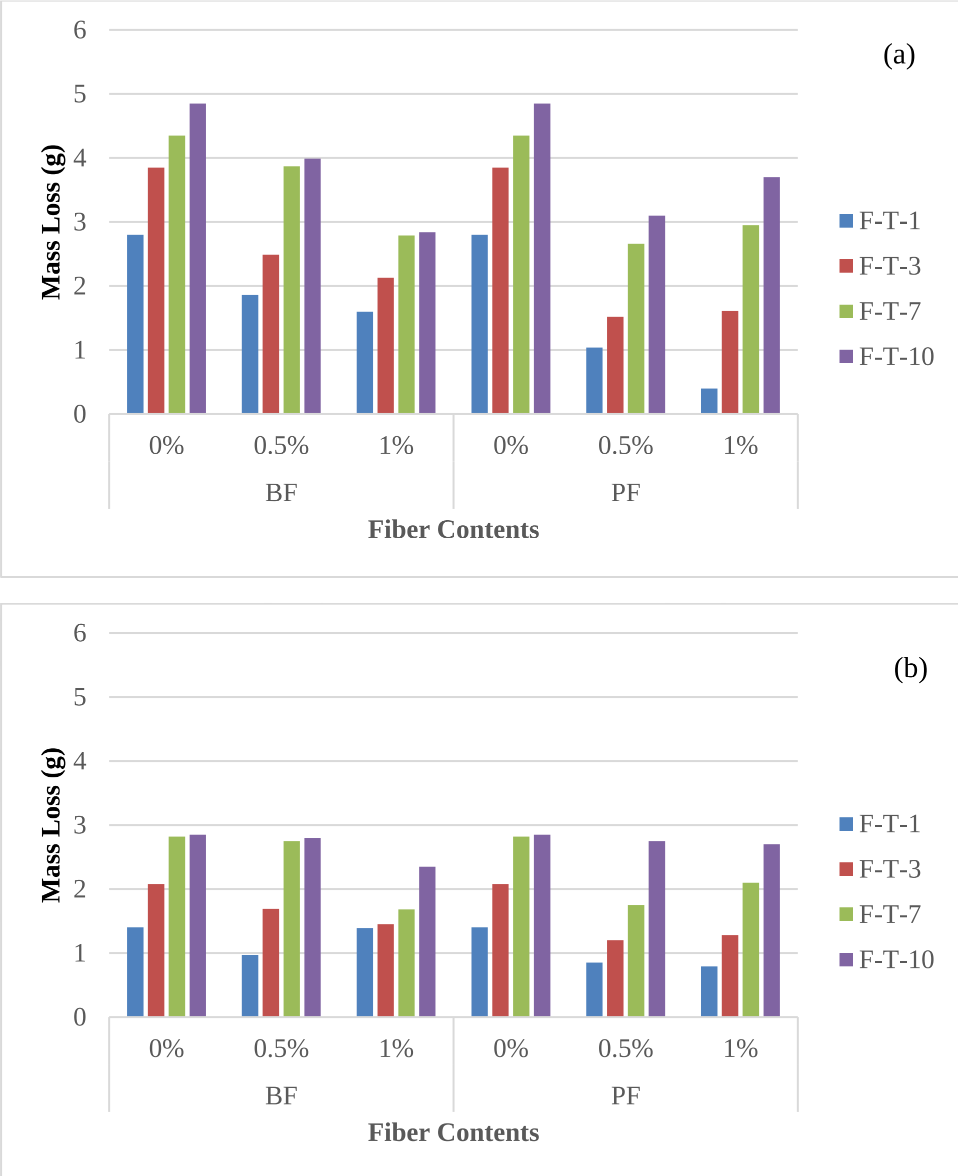


Figure 4.18. Mass loss of a) specimens free of lime and b) 3% lime stabilized specimens subjected to freeze-thaw cycles

### 4.3.1. Unconfined Compressive Strength of Specimens Exposed to Freeze-Thaw Action

Unconfined compression strength tests were conducted using strain-controlled application of the axial load to investigate effects of freeze-thaw conditions on 0 and 3% lime stabilized 0, 0.5 and 1% basalt and polypropylene fiber (in length of 12 mm) reinforced 28-day cured clay specimens after 0, 1, 3, 7 and 10 freeze-thaw cycles. The test results were given in Figure 4.19. As is seen, freeze-thaw cycles reduced the strength of all specimens. Lime stabilized specimens had more strength in comparison with specimens without lime. For lime stabilized specimens, first cycle decreased the strength sharply. The strength of specimens without lime was quite low and after the cycles, the clay soil specimens had pratically no resistance. Since the specimens were prepared with more water (i.e. 45% by weight of soil) rather than the optimum water content and this situation caused that freezing-thawing affected specimens significantly. Generally, PF increased the strength more than BF and 1% fiber content was more effective to enhance the strength againist freeze-thaw cycles. It was concluded that as fiber content increases, UCS values of specimens increase and PF reduces the detrimental effects of F-T cycles due to the fact that PF is more elastic material in comparison with BF. Owing to its elasticity, PF is more invulnerable againist freeze-thaw action. In Figure 4.20, sample fracture patterns of specimens including basalt fiber and polypropylene fiber subjected to freeze-thaw action during unconfined compression tests are shown.

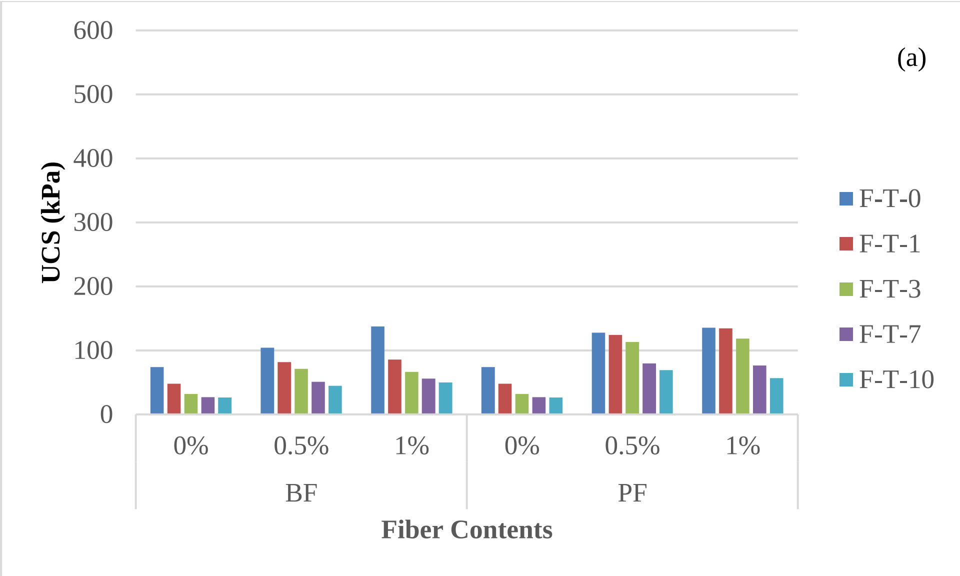


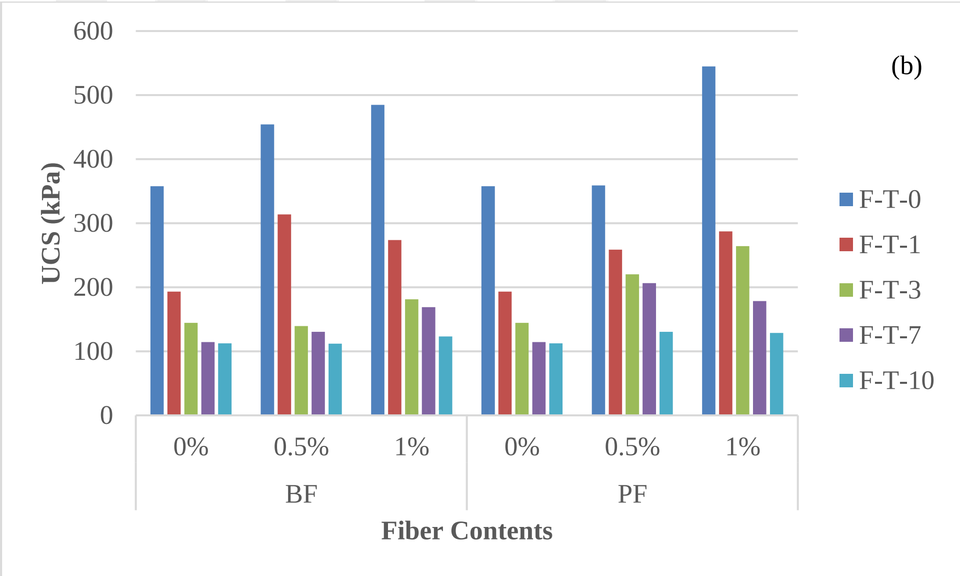


Figure 4.19. Unconfined compressive strength of a) specimens free of lime and b) 3% lime stabilized specimens subjected to 0,1, 3, 7 and 10 freeze-thaw cycles

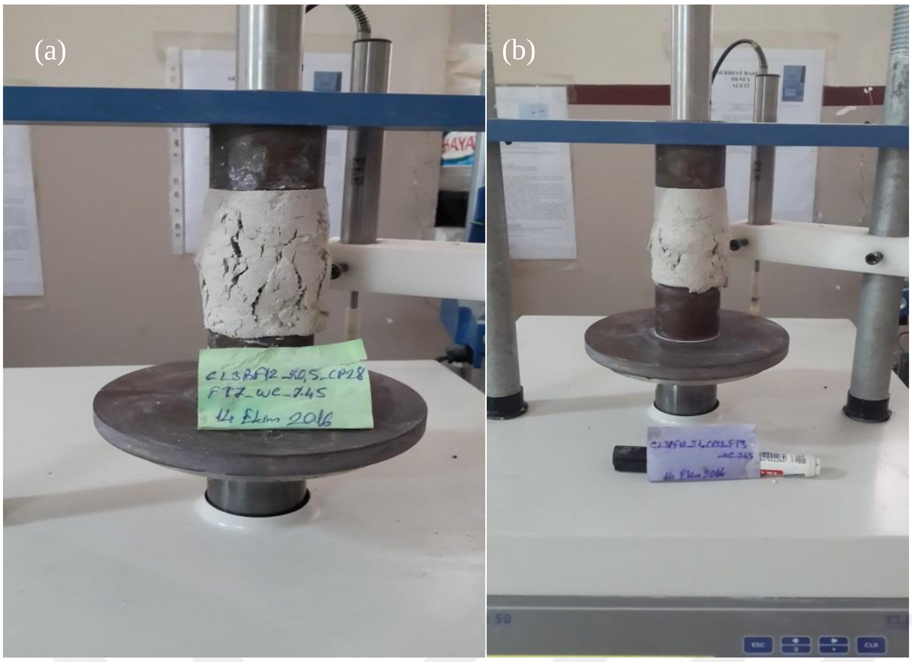


Figure 4.20. Image of fracture patterns of specimens including a) basalt fiber b) polypropylene fiber after freeze-thaw cycles during unconfined compression tests

Variation of UCS ($q_u$) of PF and BF reinforced specimens without lime inclusion and PF and BF reinforced 3% lime stabilized specimens with mass loss (ML) under 1, 3, 7 and 10 freeze-thaw cycles were drawn in Figure 4.21. Acceptable correlations among ML and UCS were obtained. The coefficient of determination values ($R^2$) were more than 0.8 and particularly the correlation for lime stabilized specimens was better.

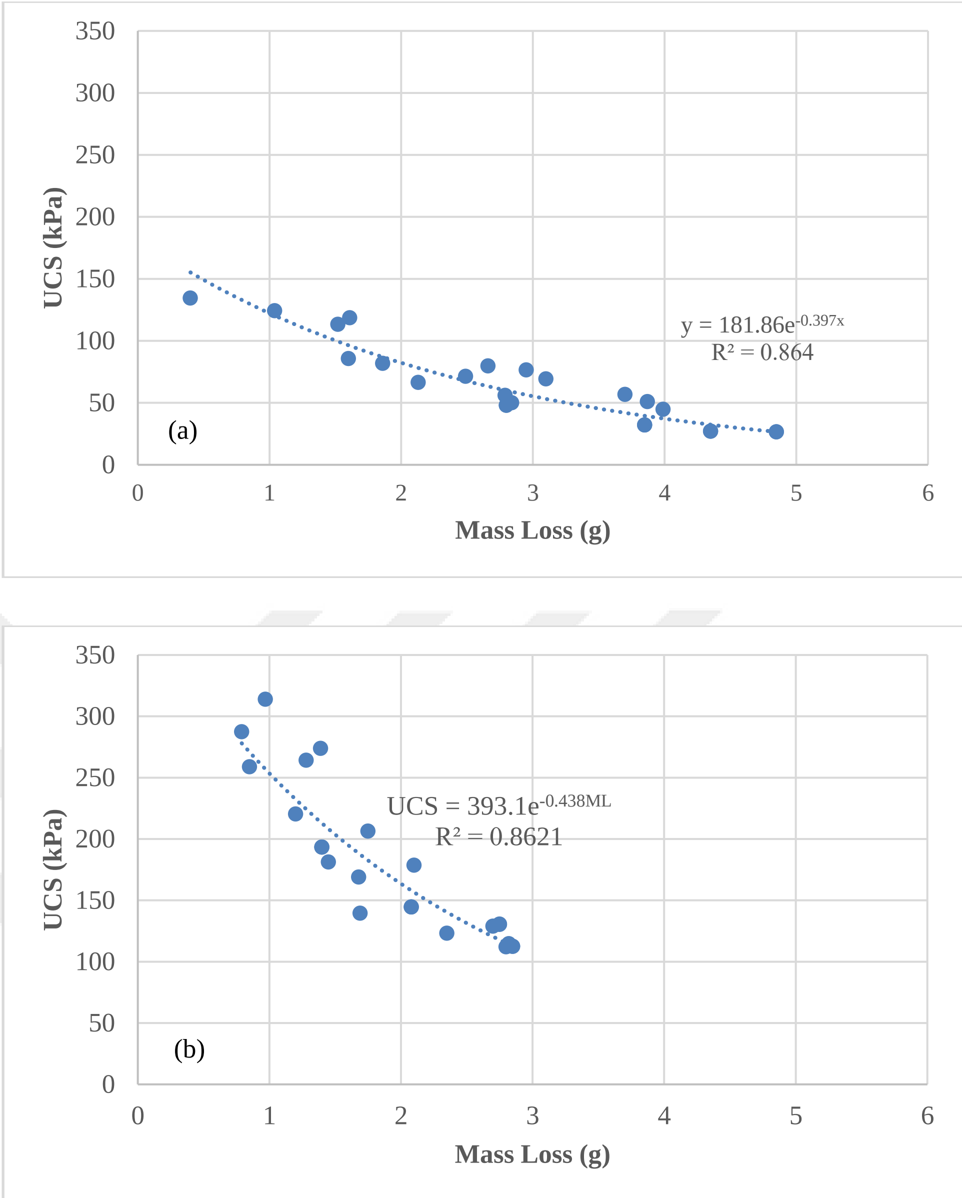


Figure 4.21. Variation of strength of PF and BF reinforced specimens with mass loss under 1, 3, 7 and 10 freeze-thaw cycles a) without lime b) stabilized with 3% lime

## 4.4. Ultrasonic Pulse Velocity

Measurement of the velocity of compression stress waves is a non-destructive test method termed ultrasonic pulse velocity method (UPV). The density and elastic characteristics of materials are effective on the velocity of these waves traveling in a solid material. The quality of materials which depends on elastic stiffness can be indicated by measuring UPV (Kewalramani and Gupta, 2006). In this method, the waves ranging in frequency from 20 kHz to 1 GHz throughout the specimen are sent and travel time is measured to determine the wave velocity and related dynamic characteristics (Su, 2012).

The ultrasonic test system for testing soil specimens was developed by Stephenson (1978) to determine their design parameters in civil work and determining Young's modulus, shear modulus, Poisson's ratio and damping was achieved. The velocity was influenced by the specimen size and increasing void ratio was tended to decrease by wave velocities for a given band of saturation. Mostly, the degree of saturation enhanced wave velocities for a constant void ratio. In addition to that wave velocities was enhanced by increasing confining pressure (Su, 2012).

Yesiller et al. (2001) indicated that in porous materials, wave propagation takes place through the quickest path in the material that is related with the stiffness of the material directly. Hence, the velocity of wave propagation depends on modulus of a material directly. In addition to that large air voids in a material do not convey pulses. Thus, the pulse path has the voids, the time taken by the pulse which circumvents the void by the fastest route is showed by the UPV device (Pundit, 1990; Panzera et al., 2011). An alternative path is offered by the addition of fibers to soil specimens and fibers influence more effectively in terms of wave travelling. However if optimum fiber content (number) is reached, additional fibers generates obstacles and reduce the wave velocity to level below those for specimens without fibers (Cristelo et al., 2015).

The investigation of Yesiller et al. (2001) showed that increasing amount of stabilizing agent and curing period enhances the wave velocity of stabilized soils. Furthermore, lime stabilized specimens has lower velocities as compared with cement stabilized specimens. Among the velocity and the density of stabilized soils a linear relationship is obtained for measuring after compaction of specimens similar to variation of velocity with water content. The study of Su (2012) observed a similar trend. According to (Su, 2012) increasing curing period enhances the wave velocity of lime stabilized soils due to pozzolanic reactions which make soils stiffer with increasing time. For clay-lime mixtures, a large increment occurs in the wave velocity from the 1$^{st}$ to 7$^{th}$ day of curing however cement stabilized soils has larger increments in same conditions. This can be explained by slow pozzolanic reactions in lime stabilization. It was also pronounced that the velocity of clay-lime mixtures decreases with increasing compaction water content (above optimum water content). When clay-lime mixtures are saturated, the wave velocity increases from about1200 m/sec to 1600 m/sec. It can be concluded that the wave velocity of water is 1600 m/sec.

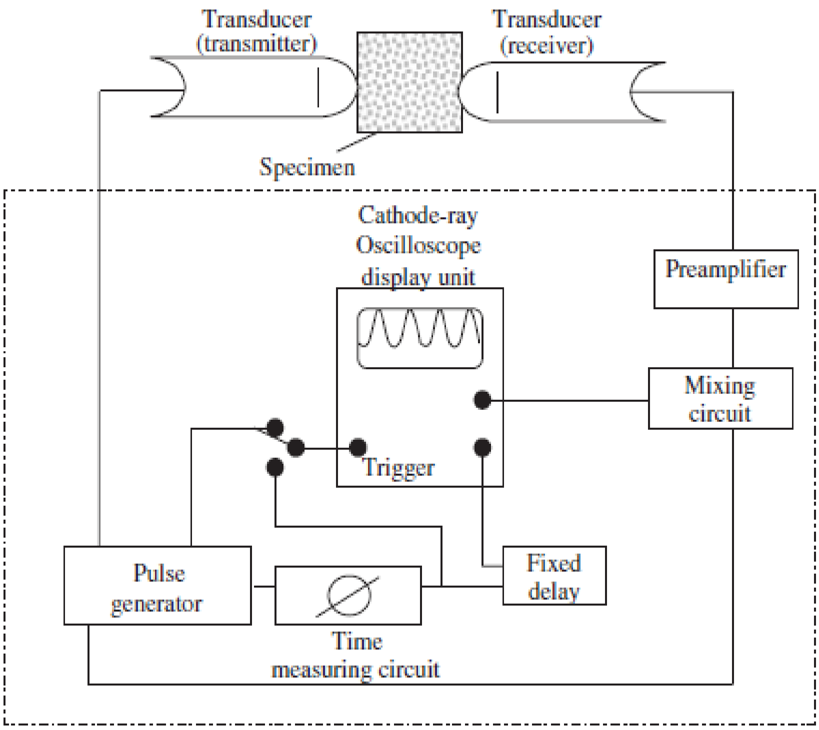


Figure 4.22. Schematic diagram of pulse velocity apparatus based on ASTM C586 (Kewalramani and Gupta, 2006)

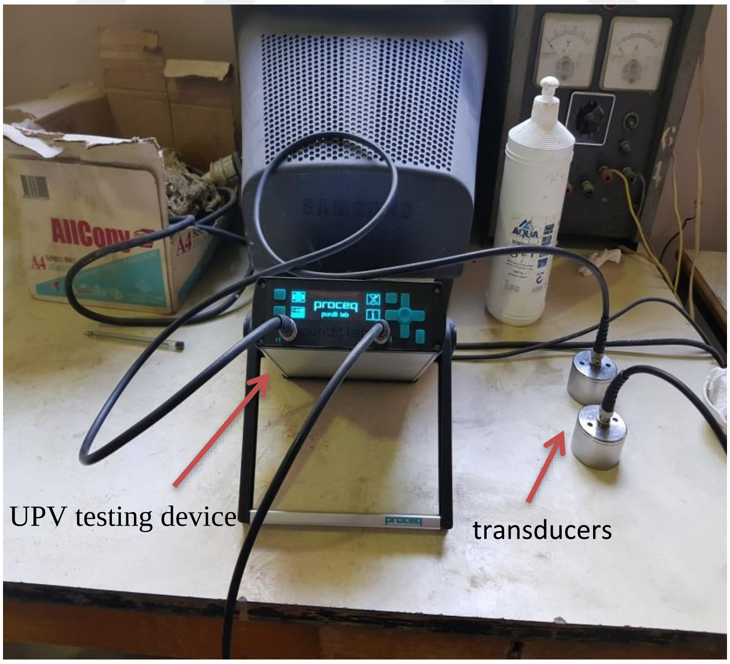


Figure 4.23. UPV testing device and transducers

In Figure 4.22 and Figure 4.23 schematic diagram of pulse velocity apparatus based on ASTM C586 and UPV testing device and transducers in Ege University are given, respectively. Implementing a speedy alteration of potential from a transmitter-driver to a piezoelectric transformation element generates ultrasonic pulse which results in it to vibrate at its basic frequency. The transducer contacts with the material to transfer the vibrations to the material. After travelling along the material, vibrations reach the receiver. The travel time of pulse among the transmitter and the receiver is utilized to calculate the wave velocity. The transducers are brought into contact with the surface of specimens firmly and the travel time of the ultrasonic wave is shown by the screen of UPV testing device. To calculate the pulse velocity, the following equation can be used (Kewalramani and Gupta, 2006):

$$V = L/t \tag{4}$$

V, L and t stand for pulse velocity (m/sec), path length (m) and travel time, respectively.

Figure 4.24. Application of ultrasound gel to the transducer

Generally, a binding agent (a viscous material such as a jelly or grease) is used to enable the vibrational energy to enter the test device and be picked up by the receiving transducer (Pundit, 1990; Panzera et al., 2011). In this thesis, before UPV testing ultrasound gel was used on the surface of transducers (as is shown in Figure 4.24) which contacted with specimens for each specimen and calibration provided using a calibration specimen. Then UPV tests were carried out longitudinally and transversely as is shown in Figure 4.25. Similar UPV values were obtained for both types of measuring. However, the data which was obtained by longitudional measurements were used in this study to avoid the possibility that the ultrasonic waves can select the path over where they contact.

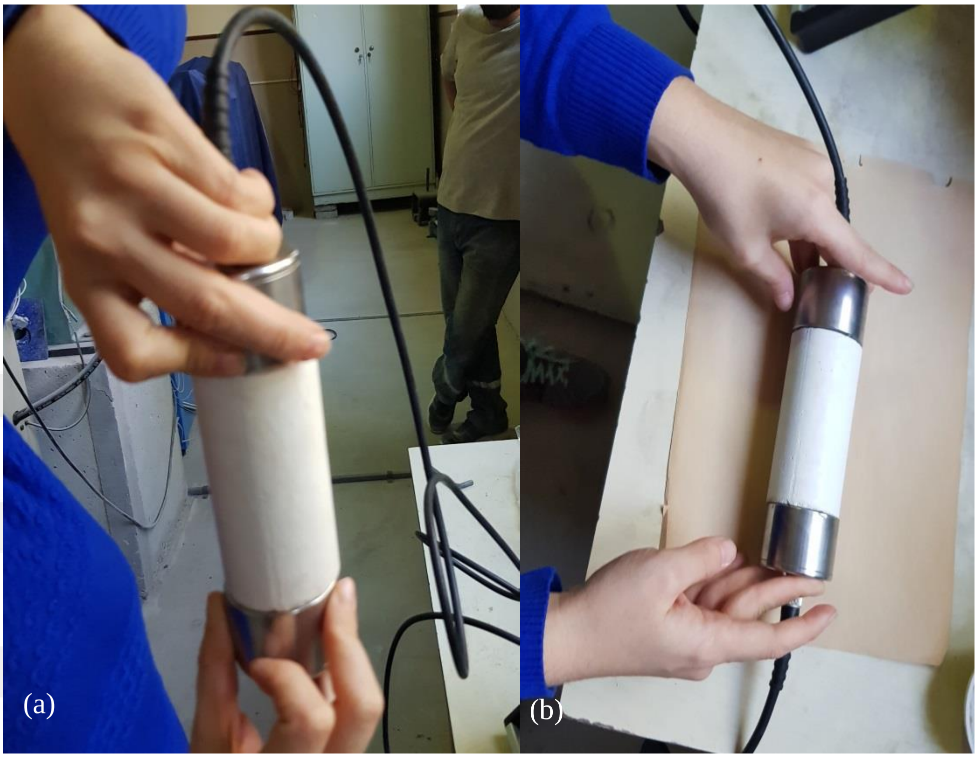


Figure 4.25. Application of UPV test on pure kaolin specimen subjected to a F-T cycle a) longitudinally, b) transversely

Figure 4.26 shows UPV values of specimens subjected to 0, 1, 3, 7 and 10 freeze-thaw cycles. As can be seen in Figure 4.26 increasing number of freeze-thaw (F-T) cycles reduced UPV of all specimens. In the literature it was explained that as F-T cycles increase, the volume of voids and micro cracks in the transition zone of the stabilized specimens increase. Thus, the capability of stabilized specimen to transfer ultrasonic pulses decrease. Applied F-T cycles alter the structures of the stabilized specimens, make these specimens less dense and enhance their voids (Eigenbrod, 1996; Viklander, 1998; Abo-Qudais, 2005; Yarbaşı et al., 2007). Lime is more effective on stiffness of specimens as compared to fiber reinforcement. As is known increasing stiffness enhances UPV. In Figure 4.26 it can be seen that before detrimental F-T effect, lime stabilized specimens had higher UPV values in comparison with specimen without lime. After a F-T cycle generally lime stabilized specimens had higher UPV. However, three or more F-T cycles affected lime stabilized specimens significantly and lime stabilized specimens performed similarly with the other specimens. As is known wave propagation continues through fastest path. After three F-T cycles randomly distributed fibers (BF or PF) offered an altenative path, distribution of fibers were more effective as compared with lime due to the fact that lime content (3% by weight of soil) was low and not adequate to higher UPV. It is clear that 3% lime stabilized 0.5% PF reinforced specimens performed best in terms of UPV. For PF, 0.5% fiber content was better in all conditions. 1% fiber content was better for BF reinforced specimens without lime whereas 0.5 fiber content was better for lime stabilized BF reinforced specimens. This means that void-fillling effect was more evident in PF reinforced specimens. Since basalt fiber surface has more interfacial adhesion and this property restricts the movement of basalt fiber.

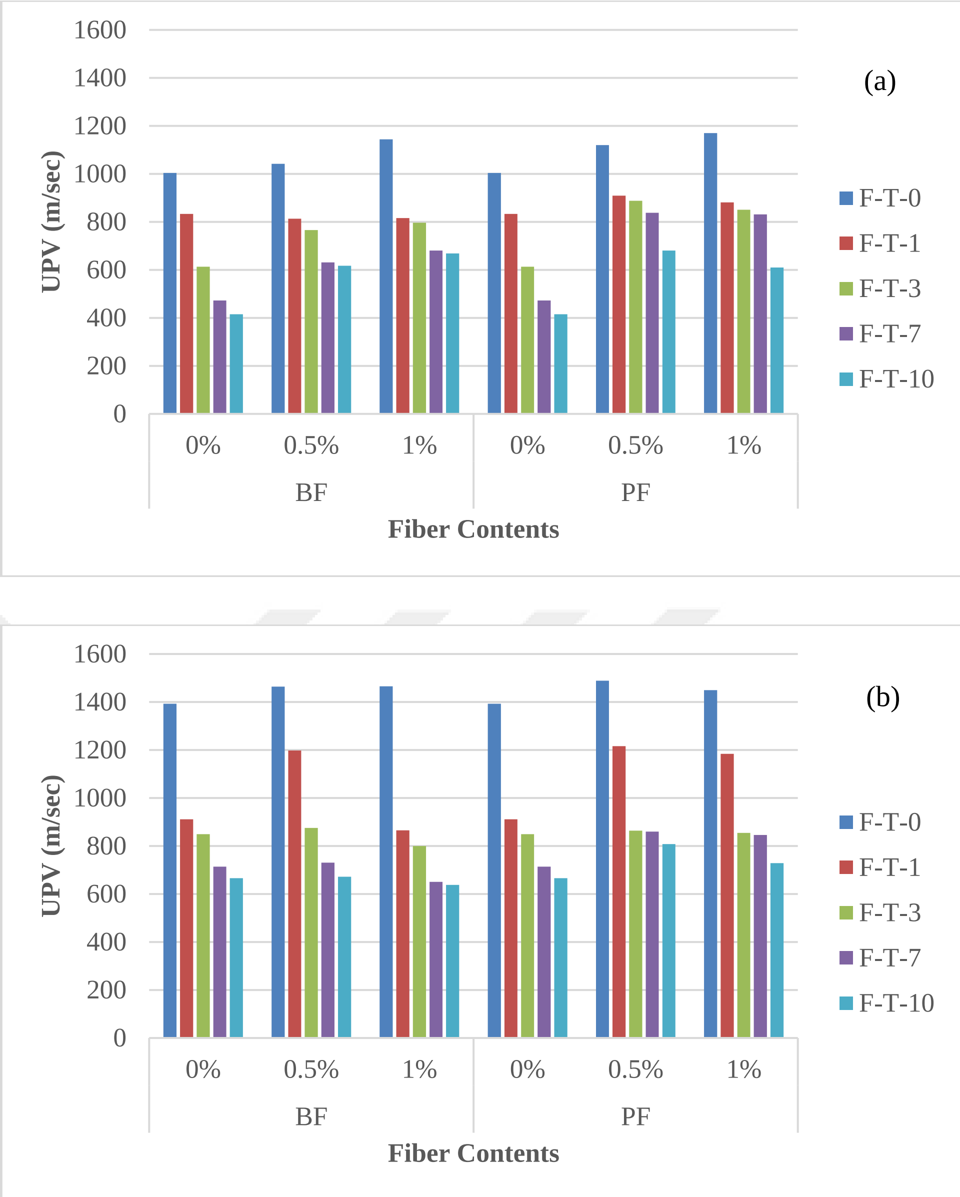


Figure 4.26. Ultrasonic pulse velocity values of a) specimens free of lime and b) 3% lime stabilized specimens subjected to 0, 1, 3, 7 and 10 freeze-thaw cycles

Variation of UPV of PF and BF reinforced specimens without lime inclusion and PF and BF reinforced 3% lime stabilized specimens with mass loss (ML) under 1, 3, 7 and 10 freeze-thaw cycles were drawn in Figure 4.27. An acceptable correlation among ML and UPV were obtained for specimens without lime whereas for lime stabilized specimens there were not remarkable correlation. For specimens without lime, UPV is proportional to mass loss. When specimens are exposed to F-T action, voids and pores causing a decrease in UPV values arise in their structure and greater weight losses are observed. However, lime stabilized specimens have more stiff structure which leads to higher UPV values. Besides, mass losses of lime stabilized specimens are low.

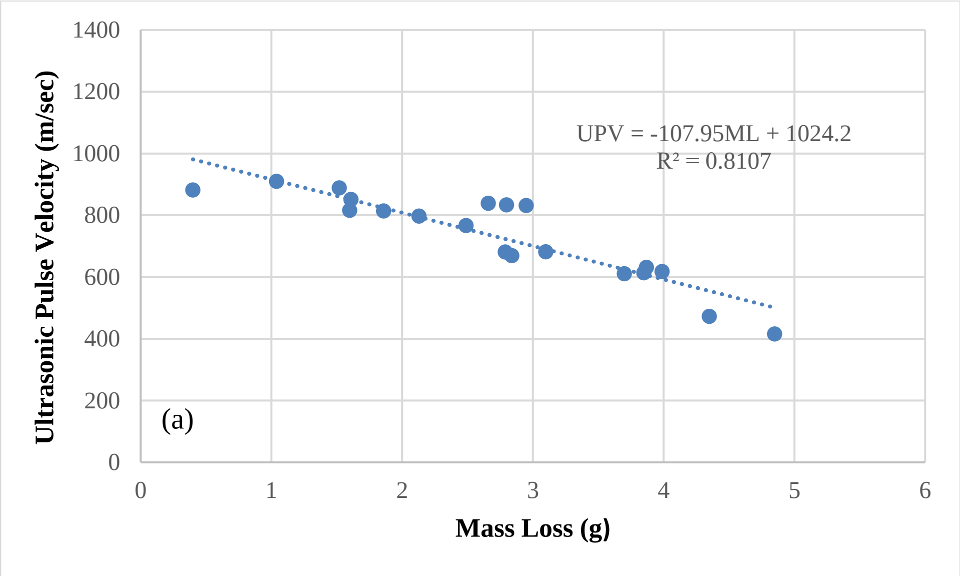


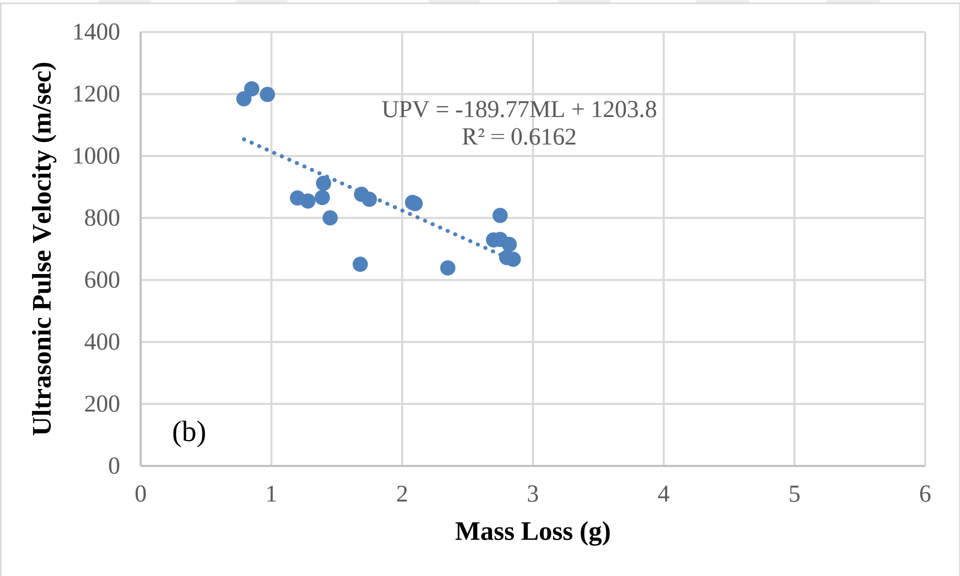


Figure 4.27. Variation of UPV of PF and BF reinforced a) specimens without lime inclusion b) 3% lime stabilized specimens with mass loss under 1, 3, 7 and 10 freeze-thaw cycles

Figure 4.28 shows UPV and UCS relationships obtained using linear curve fitting approximation for specimens including BF and PF and 3% lime stabilized BF and PF reinforced specimens, respectively. Analyzing Figure 4.28, for specimens without lime inclusion the correlation among UPV and UCS is at low level whereas for lime stabilized specimens the correlation is acceptable. If specimens were not subjected to detrimental F-T effect, correlations would be better.

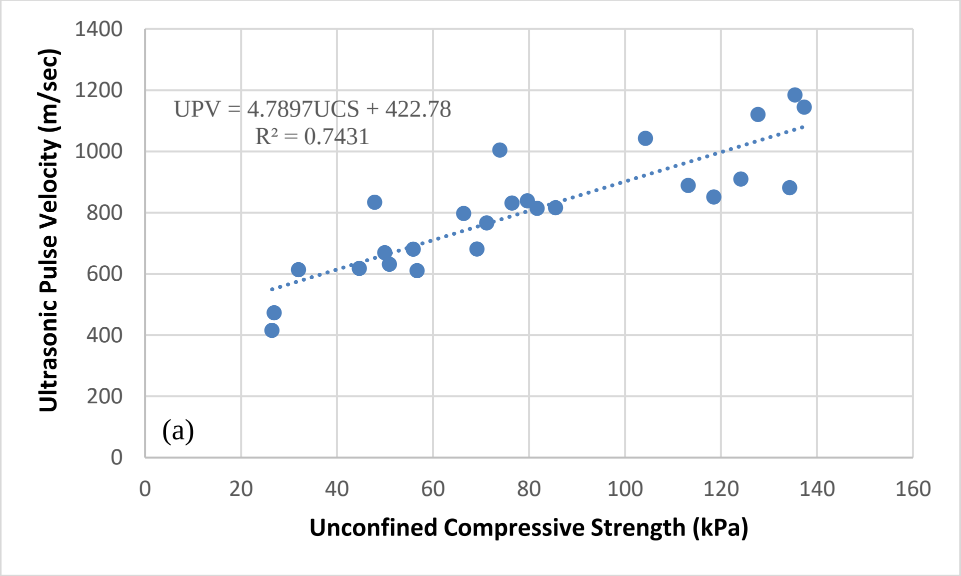


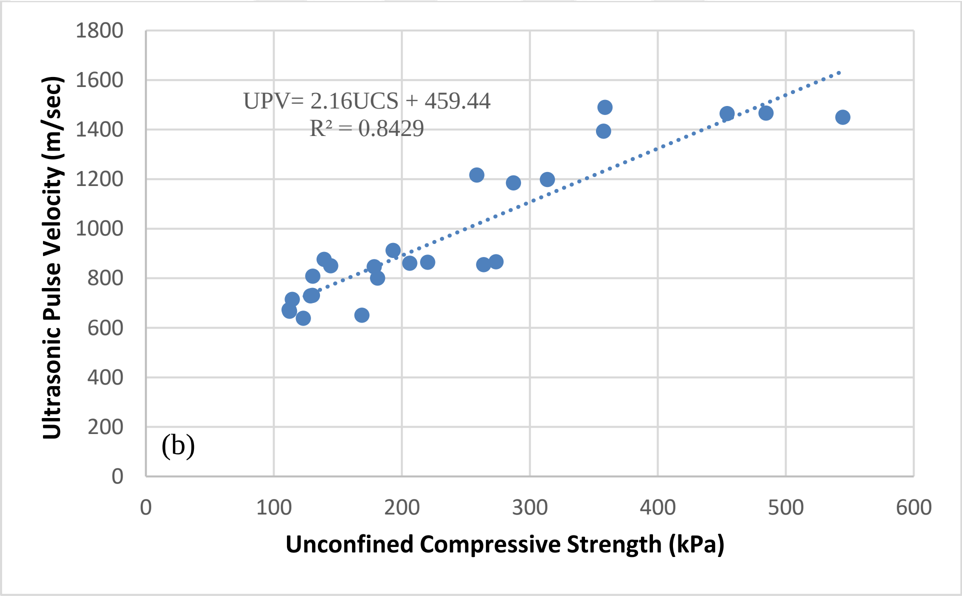


Figure 4.28. UPV and UCS relationships for a) specimens including BF and PF b) 3% lime stabilized BF and PF reinforced specimens

## 4.5. Modeling of Test Data

In this part of this thesis, empirical and statistical approaches are made to model the strength and freeze-thaw resistance of fiber reinforced lime stabilized clay.

### 4.5.1. Nonlinear Multiple Regression Models

The multivariate nonlinear regression method is used to model the behavior of a variant depending on two or more parameters. Unlike linear regression where the solution is a line, the solution can be a curved, planar, or more complex surface.

Mostly, in solutions using the least squares method, a model which has m numbers data and n numbers unknowns is calculated, iteratively. Let's think about a curvilinear model *y=f(x,α)* which is related to m data points and n numbers α parameters. Obtaining α values is possible by minimizing the sum of the squares of the residuals:

$$S = \sum_{i=1}^{m} r_i^2 \qquad (5)$$

where $r_i$ is the residual or error values, and is the difference between the predictions calculated from the obtained equation with real values:

$$r_i = y_i - f(x_i, a) \qquad (6)$$

is expressed as above.

Minimizing the sum of the squares of the errors would be possible if the gradient is equal to zero:

$$\frac{\partial S}{\partial \alpha_j} = 2\sum_i r_i \frac{\partial r_i}{\partial \alpha_j} \qquad (7)$$

For a nonlinear equation, it is an initial value problem, since the partial derivatives of the residuals are functions of both independent and dependent parameters, and the k values are determined from the following equation for the iteration:

$$\alpha_j^{k+1} = \alpha_j^k + \Delta\alpha \qquad (8)$$

In this equation, Δα is known as the increment vector. At each iteration, the residuals are recalculated by opening the Taylor series around $\alpha_j^k$, and n becomes a linear equation by placing these equations into the gradient equations. The matrix form of these equations is as follows:

$$J^T W J \ \Delta\alpha = J^T W \Delta y \qquad (9)$$

Where W is the weight matrix of the residuals, J is the matrix containing the partial derivatives of the residuals according to the α parameter. Equation (9) provides a solution to the problem of nonlinear least squares (Kelley, 1999; Strutz, 2010)

### 4.5.2. Empirical Equations for Verification of Unconfined Compressive Strength of Stabilized/Reinforced Specimens

Nonlinear regression analyses were employed to establish possible and plausible relationships among dependent parameters including fiber type, fiber content, fiber length and normalized unconfined compressive strength. The data was divided into four parts: a) Basalt fiber reinforced soil, b) Basalt fiber reinforced soil stabilized with lime c) Polypropylene fiber reinforced soil and d) Polypropylene fiber reinforced soil stabilized with lime. Scatter plots of the individual dependent parameters against normalized unconfined compressive strength revealed that, of all these parameters, fiber content (FC) and curing period (CP) are more effective to the changes in normalized unconfined compressive strength (n_UCS), which is defined as the ratio of the UCS of any specimen over the UCS of the reference specimen. n_UCS values are obtained by normalizing UCS values by UCS of 1-day cured pure clay. Unfortunately, meaningful relationships could not be obtained for fiber reinforced specimens free of lime.

In Table 4.1, the simple statistical analysis of data in hand for lime stabilized specimens was tabulated. Since the FC and CP parameters are predefined values, the deviation of fiber content is very low and, it is not surprising that deviation of CP values from their range is very high. Variance and skewness of fiber content are zero. Focusing on n_UCS values, it should be emphasized that the distribution of n_UCS values are right-skewed, and the standard deviation of the parameters are relatively high.

Table 4.1. Basic statistical analyses of the dependent and independent variables used in regression analyses of lime stabilized specimens reinforced with BF/PF

| Parameter/Property | FC | CP | n_UCS (BF) | n_UCS (PF) |
|---|---|---|---|---|
| Maximum | 0.0100 | 90 | 12.158 | 12.146 |
| Minimum | 0.0025 | 1 | 2.136 | 2.292 |
| Range | 0.0075 | 89 | 10.022 | 9.853 |
| Mean | 0.0063 | 31.5 | 5.264 | 5.771 |
| St. Deviation | 0.0028 | 35.604 | 2.637 | 2.654 |
| Variance | 0.0000 | 1267.66 | 6.952 | 7.045 |
| Skewness | 0.0000 | 0.927 | 1.053 | 0.784 |

In this regard, four relatively simple relationships are obtained to establish relationships among n_UCS, FC and CP parameters. Established relationships can be used for verification or completion of missing n_UCS parameter, by use of FC and CP parameters. It was aimed to select simpler models, for practical use. Two equations for each fiber type was given in Table 4.2 and scatter plots for calculated and experienced n_UCS values (Model 1 and Model 3) were shown in Table 4.2. SE, RA and $R^2$ stand for standard error, residual average and coefficient of determination, respectively. Equations are valid for ranges of independent parameters given in statistical analyses.

Table 4.2. Four relatively simple models for estimation using n_UCS, FC and CP

| **Model No.** | **Fiber type** | **Equation** | **SE** | **RA** | **$R^2$** |
|---|---|---|---|---|---|
| M1 | BF | $n\_UCS=8.0520-3137.874\times FC+570292.118\times FC^2-30476013.64\times FC^3+0.0634\times CP$ | 1.3828 | $2.39\times10^{-12}$ | 0.75 |
| M2 | BF | $n\_UCS=3.4066-0.0004/FC-0.9106\times \log(CP)+0.4744\times \log(CP)^2$ | 1.3781 | $-1.94\times10^{-16}$ | 0.74 |
| M3 | PF | $n\_UCS=0.5935+961.107\times FC-67293.127\times FC^2-0.5237\times \log(CP)+0.4104\times \log(CP)^2$ | 1.1109 | $4.33\times10^{-13}$ | 0.84 |
| M4 | PF | $n\_UCS=4.5386-0.04/FC+0.0654\times CP$ | 1.2101 | $-1.47\times10^{-15}$ | 0.80 |

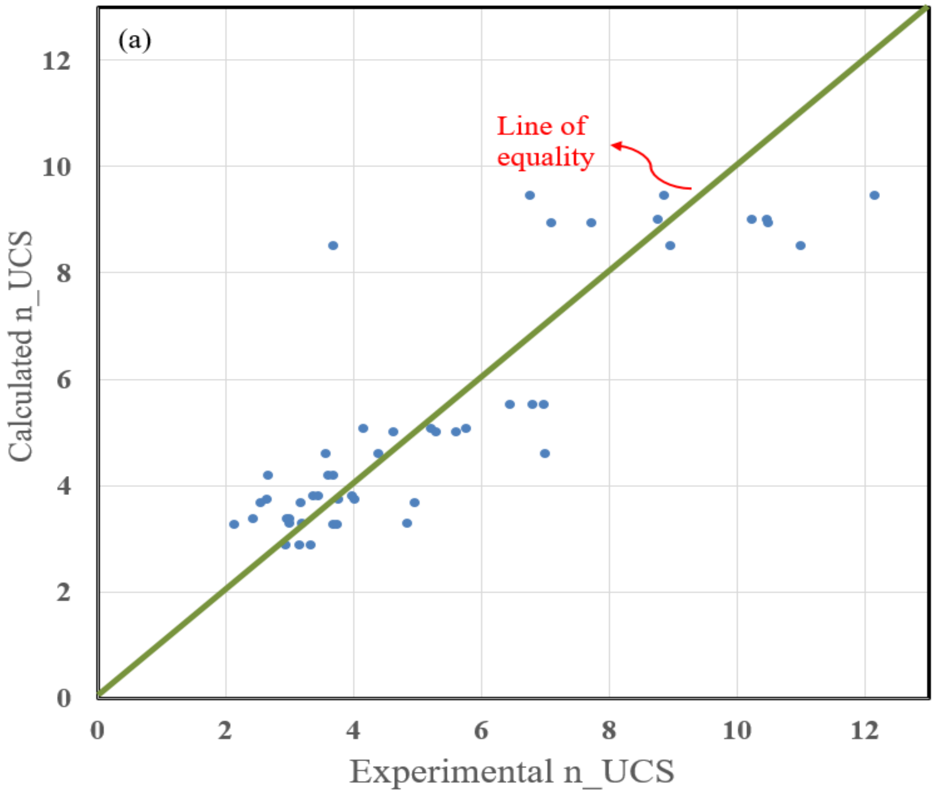


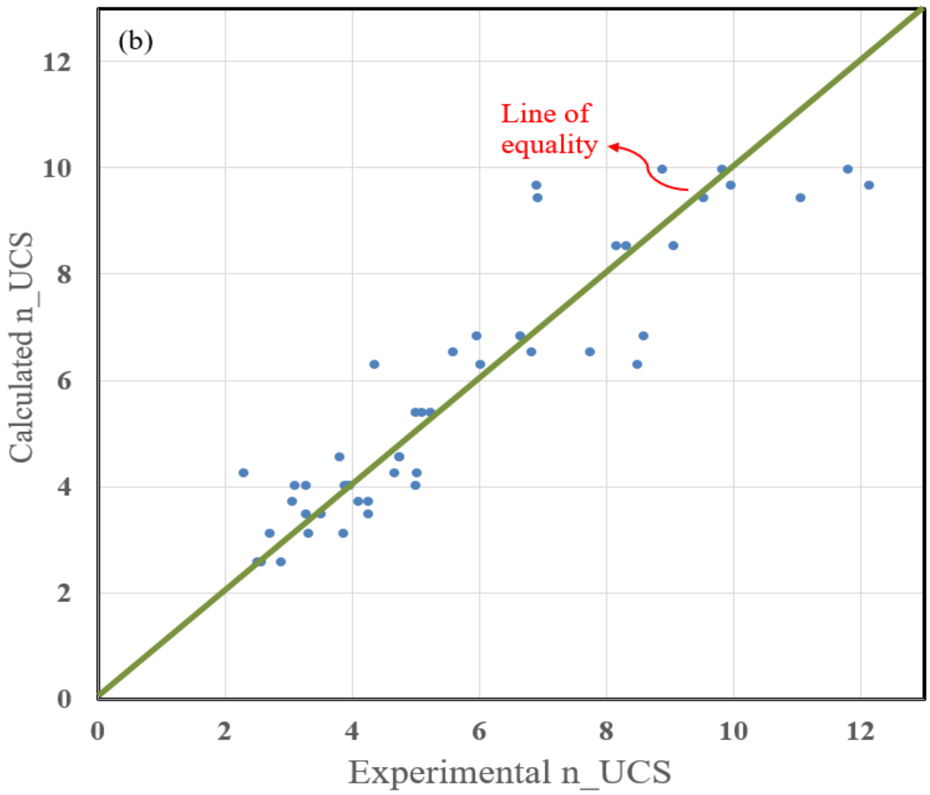


Figure 4.29. Scatter plots for calculated and experienced n_UCS values a) Model 1 b) Model 3

### 4.5.3. Empirical Equations for Prediction of Unconfined Compressive Strength of Specimens Subjected to Freeze-Thaw Actions

By carrying out regression analyses, it was aimed to find correlations among number of F-T cycles, mass loss of specimens, fiber content, lime content and ultrasonic pulse velocity measured. These analyses had two primary aims: first of all, it was aimed to obtain linear/nonlinear relationships among normalized UCS and UPV values of fiber reinforced lime stabilized specimens. UCS and UPV values were normalized using UCS and UPV values of pure clay exposed to one F-T action. The data was normalized in order to quantify the strength gain/loss using a reference value. In this regard, PF and BF reinforced soils were evaluated individually, and nonlinear regression analyses were employed to establish simple relationships among n_UPV (normalized ultrasonic pulse velocity)–n_UCS (normalized unconfined compressive strength) and n_UCS-PML (mass loss-in percent)-ncyc (number of freeze-thaw cycles). It was investigated whether changes in unconfined compressive strength could be explained in terms of results of ultrasonic pulse velocity tests, mass loss measurements and number of cycles as well.

A basic statistical analysis of data in hand was given in Table 4.3. Analyzing data in hand, for specimens reinforced with basalt fiber, it was understood that the decreases in n_UPV are not so drastic, as compared to that of n_UCS. Since the skewness parameters are similar for all parameters, right-tailed curves can be drawn for these distribution of data in hand. The standard deviation of these two parameters were considerably high compared to means. Since the standard deviation and variance of ML and ncyc is markedly high, it was considered to use these two parameters to explain the changes in n_UCS of specimens, as an alternative. Similar comments can be made for data obtained by testing PF-reinforced specimens. The changes in n_UCS are high in comparison with those in n_UPV. The variables are all right-skewed, following the same distribution. Variance of ML is higher for PF-reinforced specimens.

Table 4.3. Basic statistical analysis of four parameters used in nonlinear regression analyses for specimens reinforced with BF/PF subjected to F-T action

| **Parameter / Property** | **Specimens reinforced with Basalt fiber** | | | | **Specimens reinforced with Polypropylene fiber** | | | |
|---|---|---|---|---|---|---|---|---|
| | **n_UPV** | **n_UCS** | **PML** | **ncyc** | **n_UPV** | **n_UCS** | **PML** | **ncyc** |
| **Maximum** | 1.438 | 6.555 | 1.140 | 10.000 | 1.459 | 6.001 | 1.057 | 10.000 |
| **Minimum** | 0.741 | 0.933 | 0.277 | 1.000 | 0.732 | 1.184 | 0.114 | 1.000 |
| **Range** | 0.697 | 5.622 | 0.863 | 9.000 | 0.727 | 4.816 | 0.943 | 9.000 |
| **Mean** | 0.916 | 2.544 | 0.654 | 5.250 | 1.039 | 3.194 | 0.543 | 5.250 |
| **St. Deviation** | 0.173 | 1.664 | 0.246 | 3.606 | 0.184 | 1.546 | 0.278 | 3.606 |
| **Variance** | 0.030 | 2.768 | 0.061 | 13.000 | 0.034 | 2.389 | 0.077 | 13.000 |
| **Skewness** | 1.866 | 1.359 | 0.583 | 0.158 | 1.056 | 0.560 | 0.255 | 0.158 |

Above expressions somehow establish relationships among UPV, UCS and ML, however, further investigations were made to establish relationships among n_UPV and n_UCS; and PML, ncyc and n_UCS. The dependent parameters are selected after a trial and error approach, supported by a sensitivity analysis. Initially, more complex relationships were investigated between n_UPV and n_UCS. Over 70 relationships are obtained for both BF- and PF-reinforced specimens, surprisingly, very complex expressions which are far from practical use are able to quantify this relationship. Taking all models into consideration, maximum value of $R^2$ values ranges between 0.88 and 0.90, however these values are for tenth order polynomials. Three sample relationships for each fiber type, along with relevant statistical identifiers were given in Table 4.4. Equations are valid for ranges of independent parameters given in statistical analyses.

Table 4.4. Six relatively simple models for estimation of n_UCS using n_UPV (SE, RA and $R^2$ stand for standard error, residual average and coefficient of determination, respectively.)

| **Model No.** | **Fiber type** | **Equation** | **SE** | **RA** | **$R^2$** |
|---|---|---|---|---|---|
| M5 | BF | $n\_UCS=1/(2.7551-3.8334\times n\_UPV+1.4069\times n\_UPV^2)$ | 1.1898 | 0.0178 | 0.56 |
| M6 | BF | $n\_UCS=-10.1493+11.0521\times n\_UPV+1.9940/n\_UPV^2$ | 1.1993 | $6.38\times10^{-16}$ | 0.55 |
| M7 | BF | $n\_UCS= 2.9480\times n\_UPV^{2.2255}$ | 1.1617 | $3.3\times10^{-3}$ | 0.55 |
| M8 | PF | $n\_UCS=-2.2413+5.5847\times n\_UPV-0.3642/n\_UPV^2$ | 1.1218 | $2.78\times10^{-17}$ | 0.54 |
| M9 | PF | $n\_UCS= 6.2023\times n\_UPV-3.2485$ | 1.0821 | $1.39\times10^{-16}$ | 0.54 |
| M10 | PF | $n\_UCS= 6.2023\times(n\_UPV -0.5238)$ | 1.0821 | $1.47x10^{-15}$ | 0.54 |

Sample scatter-plots of calculated and experienced n_UCS values for models M5 and M8 were given in Figure 4.30. It is clear that, modeling ability these six models are thoroughly limited.

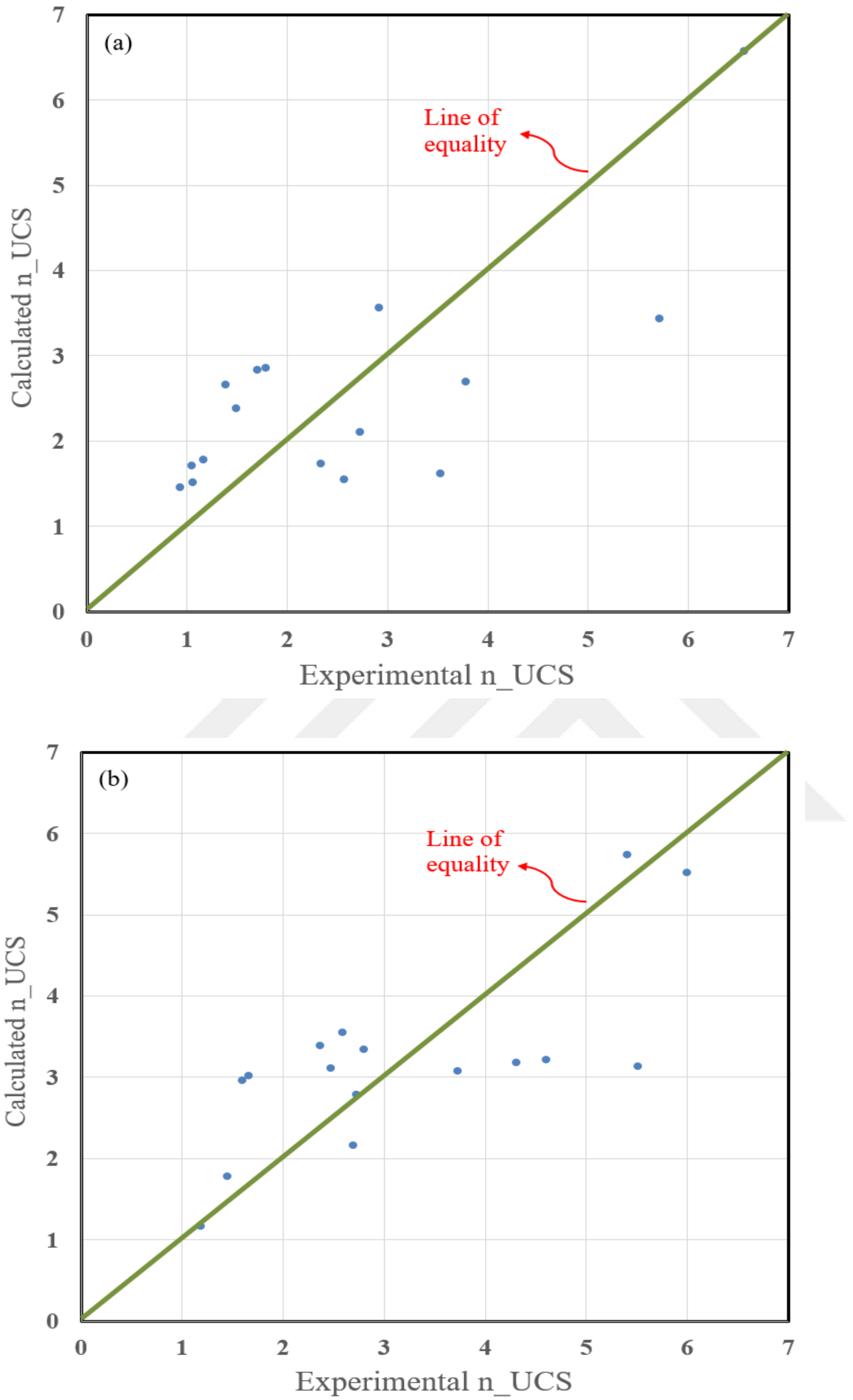


Figure 4.30. Scatter plots of experimentally obtained and calculated n_UCS values by a) Model 5 and b) Model 8.

After this unsuccessful attempt, it was considered to make a different approach, and it was tried to establish a model for prediction of n_UCS by use of n_UPV and ncyc parameters, but made no sense. Therefore, two final models for verification of test results was provided. It was aimed to model n_UCS values by use of PML and ncyc values. The results were interesting: these models, neglecting the effect of fiber length, type and content was successful as is shown in Table 4.5 and Figure 4.31.

Table 4.5. Four simple models for estimation of n_UCS using PML and ncyc (SE, RA and $R^2$ stand for standard error, residual average and coefficient of determination, respectively.)

| **Model No.** | **Fiber type** | **Equation** | **SE** | **RA** | **$R^2$** |
|---|---|---|---|---|---|
| M11 | BF | $n\_UCS=56.455-187.701/PML+232.721/PML^2-135.112/PML^3+37.045/PML^4-3.817/PML^5+0.653\times\log(ncyc)$ | 0.6855 | $1.07\times10^{-13}$ | 0.90 |
| M12 | BF | $n\_UCS=-22.584+58.277/PML-49.855/PML^2+17.938/PML^3-2.205/PML^4-0.978/ncyc$ | 0.7422 | $2.48\times10^{-14}$ | 0.87 |
| M13 | PF | $n\_UCS=-0.302+3.406/PML+0.356/PML^2-0.066/PML^3-21.005/ncyc+11.024/ncyc^2$ | 0.4866 | $3.19\times10^{-16}$ | 0.93 |
| M14 | PF | $n\_UCS=-11.843+6.178/PML-0.513/PML^2+3.214\times\log(ncyc)$ | 0.5558 | $-1.07\times10^{-15}$ | 0.90 |

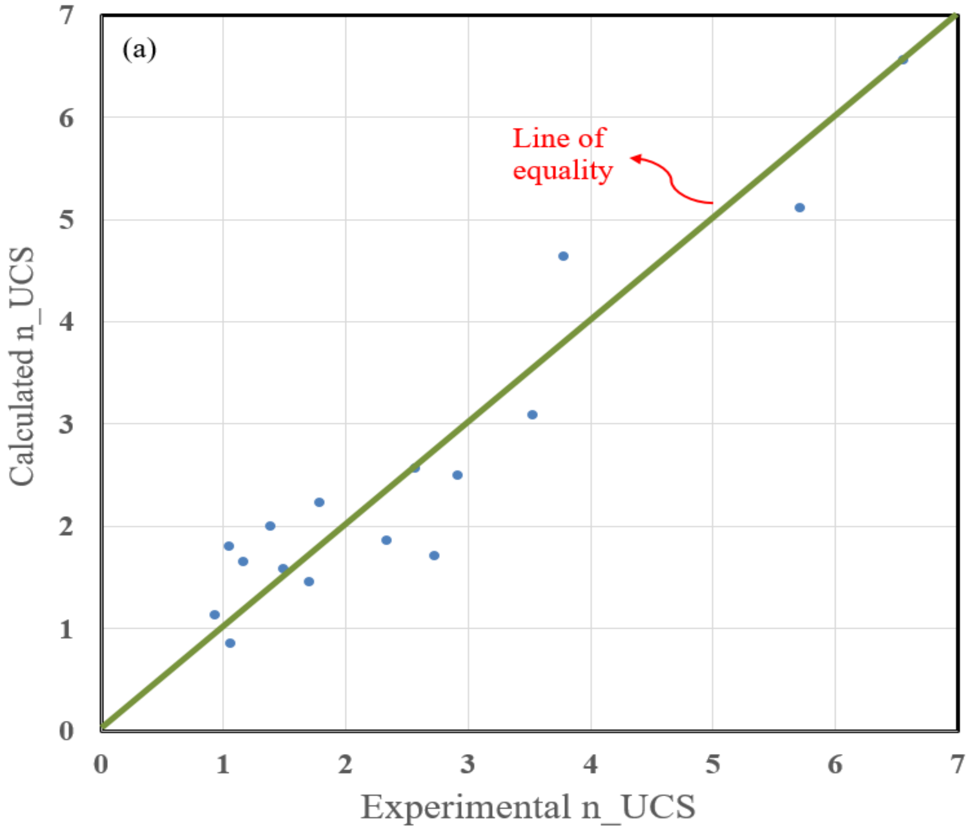


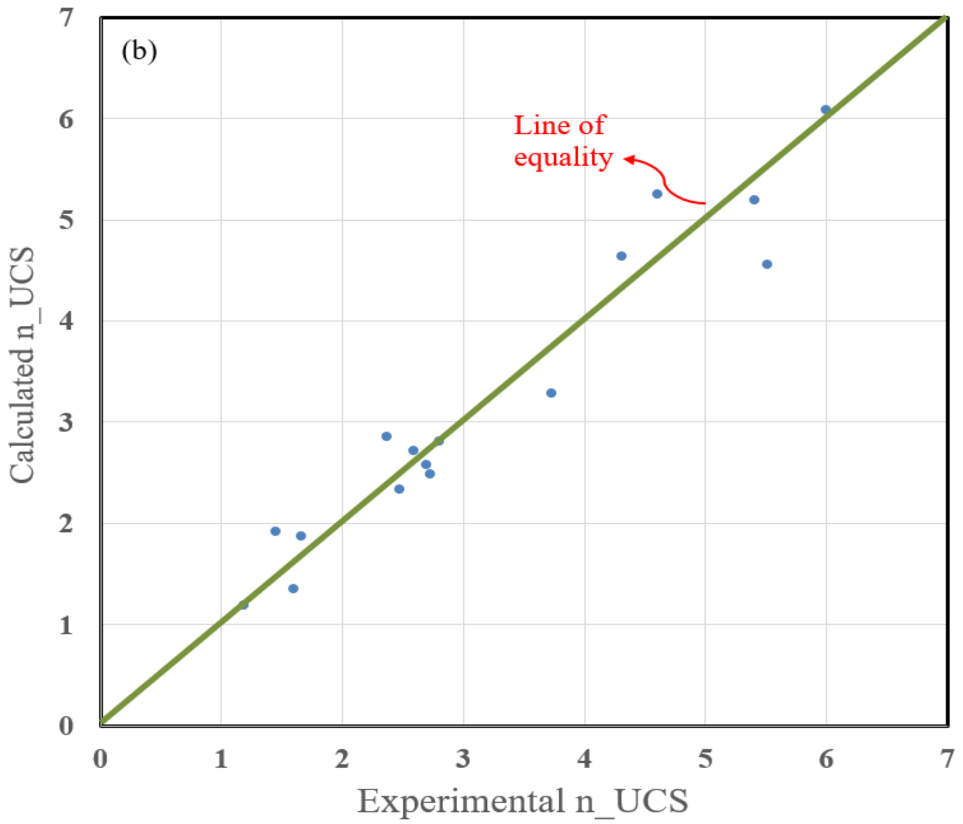


Figure 4.31. Scatter plots of experimentally obtained and calculated n_UCS values by a) Model 11 b) Model 13

# 5. CONCLUSIONS

In this thesis, an experimental study was undertaken to determine mechanical properties of fiber reinforced lime stabilized clay before and after freeze-thaw effect. In this scope, the effect of fiber material, fiber content and fiber length on strength of clay/lime stabilized clay was investigated. Following conclusions can be drawn from this thesis:

1. Lime stabilization increased the strength, and this increase was dependent on curing period. Increasing curing period improved the strength. Increasing lime content helped to an initial increase followed by a slight decrease in unconfined compressive strength of specimens. 6% lime content gave optimum gain in strength.
2. Specimens including both basalt fiber- and polypropylene fiber- mixture showed a more ductile fracture, in comparison with the others without fibers. In addition to that, lime made specimens stiffer. The specimens including lime exhibited more brittle behavior. The presence of fiber reduced this behavior.
3. Analyzing specimens without lime, reinforcement using both polypropylene and basalt fibre improved the strength positively. For basalt fiber the length of 6 mm and polypropylene fiber the length of 12 mm are the most effective in terms of strength. Analyzing specimens containing 9% lime, for basalt fiber the length of 6 mm (after 1, 7, 28-day curing) and for polypropylene fiber the length of 12 mm (after 1, 7, 28-day curing) had maximum strength in general. After 90-day curing for basalt fiber lengths of 12 mm and 19 mm were also effective. In addition, after 90-day curing for polypropylene fiber the length of 19 mm was effective too. The effective fiber length and content indicates how the fiber behaves like a composite with the ground as time increases.
4. Greatest strength improvement was obtained by use of 0.75% basalt fiber in 19 mm length with 9% lime after 90-day curing (1180 kPa). Analyzing specimens containing 3 and 6% lime and varying basalt fiber content in 12 mm length, it is concluded that 6% lime content gave more strength. For specimens including 3% lime, fiber content which gave maximum strength changed with curing period. Generally, for specimens including 6% lime, 0.75% BF content gave maximum strength.
5. Basalt fiber is an environmental friendly additive which can be used as alternative to polypropylene fiber in terms of strength. In many cases

specimens containing basalt and polypropylene fiber gave similar strengths.

6. Based on SEM/EDS images, basalt fiber surface has more interfacial adhesion to bond strength between the fiber and soil matrix than polypropylene fiber surface. Fiber roughness, soil grain size and orientation of the fiber in the soil relative to the failure plane seemed to have played a significant role in the stress transfer mechanism. Fiber reinforcement is a physical interaction among fiber and soil, it affects slightly of some engineering properties of soil whereas lime stabilization is a chemical reaction and alters some engineering properties of soil greatly.
7. Addition of lime enhanced the secant modulus ($E_{50}$) and reduced the correlation ($R^2$) between $E_{50}$ and unconfined compressive strength values for both basalt fiber-clay and polypropylene fiber-clay mixtures. Greatest secant modulus value was obtained by the use of 12 mm BF-lime-clay mixture with 0.5% fiber content after 90-day curing.
8. It is recommended to use 6 mm basalt fiber instead of 12 mm polypropylene fiber in stabilization, however this decision is also constrained in terms of market prices of fibers.
9. Increasing number of freeze-thaw cycles enhanced the mass loss. The addition of lime, basalt and polypropylene fiber reduced the mass loss. Mostly, 0.5% fiber content decreased the mass loss more and effective fiber type varied according to amount of fiber and number of cycles. In addition to that acceptable correlations among mass loss and unconfined compressive strength were obtained and particularly the correlation for lime stabilized specimens was better.
10. Freeze-thaw (F-T) cycles reduced the strength of all specimens. For lime stabilized specimens, first cycle decreased the strength significantly Generally, polypropylene fiber increased the strength more than basalt fiber and 1% fiber content was more effective to enhance the strength againist freeze-thaw cycles. Besides, acceptable correlations among mass loss and unconfined compressive strength (UCS) were obtained and particularly the correlation for lime stabilized specimens was better.
11. Increasing number of freeze-thaw cycles reduced ultrasonic pulse velocity (UPV) of all specimens. Before detrimental F-T effect, lime stabilized specimens had higher UPV values in comparison with specimen without lime. After a F-T cycle generally lime stabilized specimens had higher UPV. However, three or more F-T cycles affected lime stabilized specimens significantly and lime stabilized specimens performed similarly

with the other specimens. After three F-T cycles randomly distributed fibers (BF or PF) offered an altenative path, distribution of fibers was more effective as compared with lime. It is clear that 3% lime stabilized 0.5% polypropylene fiber reinforced specimens performed best in terms of UPV. For polypropylene fiber, 0.5% fiber content was better in all conditions. 1% fiber content was better for basalt fiber reinforced specimens without lime whereas 0.5% fiber content was better for lime stabilized BF reinforced specimens. Furthermore, an acceptable correlation among mass loss and UPV were obtained for specimens without lime whereas for lime stabilized specimens there were not remarkable correlation.

12. For specimens without lime inclusion the correlation among UPV and UCS is at low level whereas for lime stabilized specimens the correlation is acceptable. If specimens were not subjected to detrimental F-T effect, correlations would be better.
13. It is recommended to use polypropylene fiber instead of basalt fiber in cold regions.
14. Nonlinear regression analyses were employed to find out possible and plausible relationships for modeling unconfined compressive strength values in terms of dependent parameters. In this regard, for specimens that were not subjected to F-T action, relationships were obtained among normalized compressive strength, fiber content and curing period. For specimens subjected to F-T action, successful relationships among normalized unconfined compressive strength and normalized ultrasonic pulse velocity measurements could not be obtained. Later, better equations were obtained among normalized unconfined compressive strength values, number of F-T cycles and mass loss. These relationships can be used for verification of unconfined compressive strength values. The validity of relationships obtained within this study should be questioned by use of data obtained from experimental studies on different types of clays.

# REFERENCES

**Abdi, M.R., Parsapajouh, A. and Arjomand, M.A.**, 2008, Effects of random fiber inclusion on consolidation, hydraulic conductivity, swelling, shrinkage limit and desiccation cracking of clays, *International Journal of Civil Engineering*, 6(4):284–292 pp.

**Abo-Qudais, S.A.**, 2005, Effect of concrete mixing parameters on propagation of ultrasonic waves, *Construction and Building Materials*, 19:257–263 pp.

**Al Adili, A., Azzam, R., Spagnoli, G. and Schrader, J.**, 2012, Strength of soil reinforced with fiber materials (Papyrus), *Soil Mechanics and Foundation Engineering*, 48(6):241–247 pp.

**Alaimo, G., Valenza, A., Enea, D. and Fiore, V.**, 2016, The durability of basalt fibres reinforced polymer (BFRP) panels for cladding, *Materials and Structures*, 49(6):2053–2064 pp.

**Al-Mukhtar, M., Lasledj, A. and Alcover, J.F.**, 2014, Lime consumption of different clayey soils, *Applied Clay Science*, 95:133–145 pp.

**Al-Rawas, A.A., Hago, A.W. and Al-Sarmi, H.**, 2005, Effect of lime, cement and Sarooj (artificial pozzolan) on the swelling potential of an expansive soil from Oman, *Building and Environment*, 40(5):681–687 pp.

**Altun, S., Sezer, A. and Erol, A.**, 2009, The effects of additives and curing conditions on the mechanical behavior of a silty soil, *Cold Regions Science and Technology*, 56(2):135–140 pp.

**Atay, S.**, 2011, Maden İşletmelerinde Nakliye Yolları Tasarımı, Doktora Tezi, Dokuz Eylül Üniversitesi Fen Bilimleri Enstitüsü, 44–45s.

**ASTM C 586**, 1981, Test for pulse velocity through concrete, The American Society for Testing and Materials, West Conshohocken, PA.

**ASTM D 560**, 2016, Standard test methods for freezing and thawing compacted soil-cement mixtures, The American Society for Testing and Materials, West Conshohocken, PA.

## REFERENCES (continued)

**ASTM D 698**, 2012, Standard test methods for laboratory compaction characteristics of soil using standard effort (12,400 ft-lbf/ft$^3$ (600 kN-m/m$^3$)), The American Society for Testing and Materials, West Conshohocken, PA.

**ASTM D 854**, 2014, Standard test methods for specific gravity of soil solids by water pycnometer, The American Society for Testing and Materials, West Conshohocken, PA.

**ASTM D 2166**, 2016, Standard test method for unconfined compressive srength of cohesive soil, The American Society for Testing and Materials, West Conshohocken, PA.

**ASTM D 4318**, 2010, Standard test methods for liquid limit, plastic limit, and plasticity index of soils, The American Society for Testing and Materials, West Conshohocken, PA.

**ASTM D 4943-08**, 2008, Standard test method for shrinkage factors of soils by the wax method, The American Society for Testing and Materials, West Conshohocken, PA.

**Banibayat, P. and Patnaik, A.**, 2014, Variability of mechanical properties of basalt fiber reinforced polymer bars manufactured by wet-layup method, *Materials and Design*, 56, 898–906 pp.

**Basma, A. and Tuncer, E.R.**, 1991, Effect of lime on volume change and compressibility of expansive clays, *Transportation Research Record*, 1295: 52–61 pp.

**Bell, F.G. and Coulthard, J.M.**, 1990, Stabilization of clay soils with lime, *Municipal Engineer*, 7(3):125-140 pp.

**Bell, F.G.**, 1996, Lime stabilization of clay minerals and soils, *Engineering Geology*, 42(4):223–237 pp.

## REFERENCES (continued)


**Boardman, D.I., Glendinning, S. and Rogers, C.D.F.**, 2001, Development of stabilisation and solidification in lime-clay mixes, *Géotechnique*, 51(6):533-543 pp.

**Broderick, G.P. and Daniel, D.E.,** 1991, Stabilizing compacted clay againist chemical attack, *Journal of Geotechnical Engineering*, 116(10):1549–1567 pp.

**Cai, Y., Shi, B., Ng, C.W.W. and Tang, C.**, 2006, Effect of polypropylene fibre and lime admixture on engineering properties of clayey soil, *Engineering Geology*, 87(3):230–240 pp.

**Casagrande, M.D.T., Coop, M.R. and Consoli, N.C.**, 2006, Behavior of a fiber-reinforced bentonite at large shear displacements, *Journal of Geotechnical and Geoenvironmental Engineering*, 132(11):1505–1508 pp.

**Castro-Fresno, D., Movilla-Quesada, D., Vega-Zamanillo, Á. and Calzada-Pérez, M.A.**, 2011, Lime stabilization of bentonite sludge from tunnel boring, *Applied Clay Science*, 51(3):250–257 pp.

**Chamberlain, E. J., Iskandar, I. and Hunsickert, S.E.**, 1990, Effect of freeze–thaw on the permeability and macrostructure of soils, *Cold Region Research and Engineering Laboratory*, 90(1):145–155 pp.

**Cristelo, N., Cunha, V.M.C.F., Dias, M., Gomes, A.T., Miranda, T. and Araújo, N.**, 2015, Influence of discrete fibre reinforcement on the uniaxial compression response and seismic wave velocity of a cement-stabilised sandy-clay, *Geotextiles and Geomembranes*, 43(1):1–13 pp.

**Croft, J.B.**, 1967, The influence of soil mineralogical composition on cement stabilization, *Géotechnique*, 17(2):119-135 pp.

**Czigány, T., Vad, J. and Pölöskei, K.**, 2005, Basalt fiber as a reinforcement of polymer composites, *Periodica Polytechnica Ser. Mech. Eng.*, 49(1):3–14 pp.

## REFERENCES (continued)

**Dang, L. C., Fatahi, B. and Khabbaz, H.**, 2016, Behaviour of expansive soils stabilized with hydrated lime and bagasse fibres, *Procedia Engineering*, 143:658–665 pp.

**Deák, T. and Czigány, T.**, 2009, Chemical composition and mechanical properties of basalt and glass fibers: a comparison, *Textile Research Journal*, 79(7):645–651 pp.

**Dhand, V., Mittal, G., Rhee, K.Y., Park, S.J. and Hui, D.**, 2015, A short review on basalt fiber reinforced polymer composites, *Composites Part B: Engineering*, 73:166–180 pp.

**Di Ludovico, M.**, **Prota, A., Manfredi, G.**, 2010, Structural upgrade using basalt fibers for concrete confinement, *Journal of Composite for Construction*, 14(5):541-552 pp.

**Di Sante, M., Fratalocchi, E., Mazzieri, F. and Brianzoni, V.**, 2015, Influence of delayed compaction on the compressibility and hydraulic conductivity of soil-lime mixtures, *Engineering Geology*, 185:131–138 pp.

**Di Sante, M., Fratalocchi, E., Mazzieri, F. and Pasqualini, E.**, 2014, Time of reactions in a lime treated clayey soil and influence of curing conditions on its microstructure and behaviour, *Applied Clay Science*, 99:100–109 pp.

**Dias, D.P. and Thaumaturgo, C.**, 2005, Fracture toughness of geopolymeric concretes reinforced with basalt fibers, *Cement and Concrete Composites*, 27(1):49–54 pp.

**Eigenbrod, K.D.**, 1996, Effects of cyclic freezing and thawing on volume changes and permeabilities of soft fine-grained soils, *Canadian Geotechnical Journal*, 33(4):529–537 pp.

**Elgabbas, F., Ahmed, E.A. and Benmokrane, B.**, 2015, Physical and mechanical characteristics of new basalt-FRP bars for reinforcing concrete structures, *Construction and Building Materials*, 95:623–635 pp.

## REFERENCES (continued)

**Encyclopedia Britannica**, "Basalt", https://www.britannica.com/science/basalt (Date accessed: 5 November 2017)

**Encyclopedia Britannica**, "Kaolin", https://www.britannica.com/science/kaolin (Date accessed: 12 October 2017)

**Fiore, V., Scalici, T., Di Bella, G. and Valenza, A.**, 2015, A review on basalt fibre and its composites, *Composites Part B: Engineering*, 74:74–94 pp.

**Freilich, B., Li, C. and Zornberg, G.**, 2010, Effective shear strength of fiber-reinforced clays, 9th International Conference on Geosynthetics, Guarujá, Brazil, 4:1997–2000p.

**Freed, W.W.**, 1988, Fiber reinforced soil and method, U.S. Patent No. 4,790,691. Washington, DC: U.S. Patent and Trademark Office.

**Gao, L., Hu, G., Xu, N., Fu, J., Xiang, C. and Yang, C.**, 2015, Experimental study on unconfined compressive strength of basalt fiber reinforced clay soil, *Advances in Materials Science and Engineering*, 2015:1–8 pp.

**Garzón, E., Cano, M., O`Kelly, B.C. and Sánchez-Soto, P.J.**, 2016, Effect of lime on stabilization of phyllite clays, *Applied Clay Science*, 123:329–334 pp.

**Ghazavi, M. and Roustaie, M.**, 2010, The influence of freeze-thaw cycles on the unconfined compressive strength of fiber-reinforced clay, *Cold Regions Science and Technology*, 61(2):125–131 pp.

**Gholkar, A.P. and Jadhav, H.S.**, 2014, Experimental study of the flexural behaviour of damaged RC beams strengthened in bending moment region with basalt fiber reinforced polymer (BFRP) sheets, *International Journal of Engineering Research and Applications*, 4(7):142–145 pp.

**Greco, A., Maffezzoli, A., Casciaro, G. and Caretto, F.**, 2014, Mechanical properties of basalt fibers and their adhesion to polypropylene matrices, *Composites Part B: Engineering*, 67:233–238 pp.

## REFERENCES (continued)

**Han, C. and Cheng, P.**, 2015, Micropore variation and particle fractal representation of lime-stabilised subgrade soil under freeze–thaw cycles, *Road Materials and Pavement Design*, 16(1):19–30 pp.

**Hassini, S.**,1992, Some aspects of landfill design, Mediterranean Conf on Environmental Geotechnology, Cesme, Turkey,137–144p.

**Hausmann, M.R.**, 1990, Engineering Principles of Ground Modification, McGraw-Hil Book Co, Singapore, 656p.

**Hejazi, S. M., Sheikhzadeh, M., Abtahi, S. M. and Zadhoush, A.**, 2012, A simple review of soil reinforcement by using natural and synthetic fibers, *Construction and Building Materials*, 30:100–116 pp.

**Hirose, G. and Ito, Y.**, 2017, Experimental estimation of permeability of freeze-thawed soils in artificial ground freezing, *Procedia Engineering*, 189:332–337 pp.

**Hotineanu, A., Bouasker, M., Aldaood, A. and Al-Mukhtar, M.**, 2015, Effect of freeze-thaw cycling on the mechanical properties of lime-stabilized expansive clays, *Cold Regions Science and Technology*, 119:151–157 pp.

**Ingles, O.G., and Metcalf, J.B.**, 1972, Soil stabilization: principles and practise, Butterworths, Sydney, 374p.

**Jawad, I.T., Taha, M.R., Majeed, Z.H. and Khan, T.A.**, 2014, Research article soil stabilization using lime: advantages, disadvantages and proposing a potential alternative, *Research Journal of Applied Sciences, Engineering and Technology*, 8(4):510–520 pp.

**Jiang, H., Cai, Y. and Liu, J.**, 2010, Engineering properties of soils reinforced by short discrete polypropylene fiber, Journal of Materials in Civil Engineering, 22(12):1315–1322 pp.

**Kabay, N.**, 2014, Abrasion resistance and fracture energy of concretes with basalt fiber, *Construction and Building Materials*, 50:95–101 pp.

## REFERENCES (continued)

**Kamei, T., Ahmed, A. and Shibi, T.**, 2012, Effect of freeze-thaw cycles on durability and strength of very soft clay soil stabilised with recycled Bassanite, *Cold Regions Science and Technology*, 82:124–129 pp.

**Kassim, K.A. and Chern, K.K.**, 2004, Lime stabilized Malaysian cohesive soils, *Jurnal Kejuruteraan Awam*, 16(1):13–23 pp.

**Kavak, A., Güngör, A.G., Avşar, C. and Atbaş, B.**, 2008, Kireç ile zemin stabilizasyonu, Zemin Mekaniği ve Temel Mühendisliği Onikinci Ulusal Kongresi, Konya.

**Kelley, C.T.**, 1999, Iterative methods for optimization, Society for Industrial and Applied Mathematics.

**Kewalramani, M.A. and Gupta, R.**, 2006, Concrete compressive strength prediction using ultrasonic pulse velocity through artificial neural networks, *Automation in Construction*, 15(3):374–379 pp.

**Kızılçelik, M.M.**, 2010, Yüksek plastisiteli bir kilin kireç ile stabilizasyonu, Yüksek Lisans Tezi, Kocaeli Üniversitesi Fen Bilimleri Enstitüsü, 118s.

**Kizilkanat, A.B., Kabay, N., Akyüncü, V., Chowdhury, S. and Akça, A.H.**, 2015, Mechanical properties and fracture behavior of basalt and glass fiber reinforced concrete: An experimental study, *Construction and Building Materials*, 100:218–224 pp.

**Kværnø, S. H., and Øygarden, L.**, 2006, The influence of freeze-thaw cycles and soil moisture on aggregate stability of three soils in Norway, *Catena*, 67(3): 175–182 pp.

**Lambe, T. W.**, 1962, Chap. 4 of Foundation Engineering, Soil Stabilization, GA Leonards, G. A. (Eds.), McGraw Hill, New York, 88p.

**Li, J., Tang, C., Wang, D., Pei, X. and Shi, B.**, 2014, Effect of discrete fibre reinforcement on soil tensile strength, *Journal of Rock Mechanics and Geotechnical Engineering*, 6(2):133–137 pp.

## REFERENCES (continued)


**Li, W. and Xu, J.**, 2009, Mechanical properties of basalt fiber reinforced geopolymeric concrete under impact loading, *Materials Science and Engineering: A*, 505(1):178–186 pp.

**Lin, B., Zhang, F., Feng, D., Tang, K. and Feng, X.**, 2017, Accumulative plastic strain of saturated clay subjected to freeze- thaw cycles under long-term cyclic loading, *Engineering Geology*, (Accepted Manuscipt).

**Lipatov, Y.V., Gutnikov, S.I., Manylov, M.S., Zhukovskaya, E.S. and Lazoryak, B.I.**, 2015, High alkali-resistant basalt fiber for reinforcing concrete, *Materials and Design*, 73:60–66 pp.

**Little, D. N.**, 1987, Fundamentals of the stabilization of soil with lime, National Lime Association, Bulletin No. 332, Arlington, VA.

**Little, D. N.**, 1999a, Evaluation of structural properties of lime stabilized soils and aggregates, National Lime Association, Arlington, VA, 1:97p.

**Little, D.N., Males, E.H., Prusinski, J.R. and Stewart, B.**, 2000, Cementitious stabilization, 79th Millenium Rep. Series, Transportation Research Board, Washington, D.C, 1–7p.

**Liu, P.**, 2003, Test and study into strengthening technique of overwet and high liquid limit soil subbase (in Chinese), *Municipal Engineering Technology*, 21(2):97–102 pp.

**Liu, J., Wang, T. and Tian, Y.**, 2010, Experimental study of the dynamic properties of cement- and lime-modified clay soils subjected to freeze-thaw cycles, *Cold Regions Science and Technology*, 61(1):29–33 pp.

**Liu, W., Wu, Z., Li, Y., Song, Y., Ling, Z., Zhao, J. and Lv, Q.**, 2016, Experimental study on the gas phase permeability of methane hydrate-bearing clayey sediments, *Journal of Natural Gas Science and Engineering*, 36:378–384 pp.

## REFERENCES (continued)

**Lopresto, V., Leone, C. and De Iorio, I.**, 2011, Mechanical characterisation of basalt fibre reinforced plastic, *Composites Part B: Engineering*, 42(4):717–723 pp.

**Lu, Y., Liu, S., Weng, L., Wang, L., Li, Z. and Xu, L.**, 2016, Fractal analysis of cracking in a clayey soil under freeze-thaw cycles, *Engineering Geology*, 208:93–99 pp.

**Maher, M. H. and Ho, Y. C.**, 1994, Mechanical properties of kaolinite/fiber soil composite, *Journal of Geotechnical Engineering*, 120(8):1381–1393 pp.

**Mallela, J., Quintus, H. Von, and Smith, K.L.**, 2004, Consideration of lime-stabilized layers in mechanistic-empirical pavement design, The National Lime Association, Arlington, VA, June:1-36p.

**Mardani-Aghabaglou, A. Kalipcilar, I., Inan Sezer, G., Sezer, A., and Altun, S.**, 2015, Freeze-thaw resistance and chloride-ion penetration of cement-stabilized clay exposed to sulfate attack, Applied Clay Science, 115:179–188 pp.

**McCaustland, E.J.**, 1925, Lime dirt in roads, Proceedings of National Lime Association, Arlington, VA, 7:12-18p.

**Mehta, R.**, 2012, Interactions, imaging and spectra in SEM, Chapter 2, 17-29, Scanning Elecron Microscopy, Kazmiruk V. (Eds.), 842p.

**Miller, C.J. and Rifai, S.**, 2004, Fiber reinforcement for waste containment soil liners, *Journal of Environmental Engineering*, 130(8):891–895 pp.

**Minerals Education Coalition**, “Kaolinite”, https://mineralseducationcoalition.org/mineral-database/kaolinite (Date accessed: 30 December 2017)

## REFERENCES (continued)


**Mirzababaei, M., Miraftab, M., Mohamed, M. and McMahon, P.**, 2013, Unconfined compression strength of reinforced clays with carpet waste fibers, *Journal of Geotechnical and Geoenvironmental Engineering*, 139(3): 483–493 pp.

**Morova, N.**, 2013, Investigation of usability of basalt fibers in hot mix asphalt concrete, *Construction and Building Materials*, 47:175–180 pp.

**Nataraj, M.S. and McManis, K.L.**, 1997, Strength and deformation properties of soils reinforced with fibrillated fibers, *Geosynthetics International*, 4(1):65–79 pp.

**Nazarov, M. and Noh, D.Y.**, 2011, New Generation of Europium and Terbium Activated Phosphors from syntheses to applications, CRC Press, USA, 300p.

**Ndepete, C.P. and Sert, S.**, 2016, Use of basalt fibers for soil improvement, *Acta Physica Polonica A*, 130(1):355–356 pp.

**Olgun, M.**, 2013, Effects of polypropylene fiber inclusion on the strength and volume change characteristics of cement-fly ash stabilized clay soil, *Geosynthetics International*, 20(4):263-275 pp.

**Onyejekwe, S. and Ghataora, G.S.**, 2014, Effect of fiber inclusions on flexural strength of soils treated with nontraditional additives, *Journal of Materials in Civil Engineering*, 26(8):04014039-1.

**Orakoglu, M.E., Liu, J. and Niu, F.**, 2016, Experimental and modeling investigation of the thermal conductivity of fiber-reinforced soil subjected to freeze-thaw cycles, *Applied Thermal Engineering*, 108:824–832 pp.

**Orakoglu, M. E., Liu, J. and Niu, F.**, 2017, Dynamic behavior of fiber-reinforced soil under freeze-thaw cycles, *Soil Dynamics and Earthquake Engineering*, 101:269–284 pp.

**Oztas, T. and Fayetorbay, F.**, 2003, Effect of freezing and thawing processes on soil aggregate stability, *Catena*, 52:1–8 pp.

## REFERENCES (continued)

**Öztürk, S.**, 2007, Engineering properties of kaolinite clay reinforced with polypropylene fibers, MSc Thesis, Boğaziçi University, 121p.

**Pandian, A., Vairavan, M., Jebbas Thangaiah, W.J. and Uthayakumar, M.**, 2014, Effect of moisture absorption behavior on mechanical properties of basalt fibre reinforced polymer matrix composites, Journal of Composites, 2014:1–8 pp.

**Panzera, T.H., Christoforo, A.L., Cota, F.P., Borges, P.H.R. and Bowen, C. R.**, 2011, Ultrasonic pulse velocity evaluation of cementitious materials, 411-436, Advances in Composite Materials- Analysis of Natural and Man-Made Materials, Těšinova, P. (Eds.), 584p.

**Pearson, M., Donchev, T. and Salazar, J.** 2013, Long-term behaviour of prestressed basalt fibre reinforced polymer bars, *Procedia Engineering*, 54:261–269 pp.

**Plé, O., Lê, H. and Gotteland, P.**, 2009, A mechanical approach for fibre-reinforced clay in landfill caps cover application, *European Journal of Environmental and Civil Engineering*, 13(1):53–69 pp.

**Plé, O. and Lê, T.N.H.**, 2012, Effect of polypropylene fiber-reinforcement on the mechanical behavior of silty clay, *Geotextiles and Geomembranes*, 32:111–116 pp.

**Poltev, N.F.**, 1967, Effect of initial composition of melt rocks at its structure in the frozen state, Permafrost Research (VII) (in Russian), Kudryavtsev, V. A. (Eds.), Moscow University Press, Moscow, 89-97p.

**Polymer Solutions Group**, "About Scanning Electron Microscopy & Energy Dispersive Spectroscopy", https://www.polymersolutions.com/capabilities/scanning-electron-microscopy-with-energy-dispersive-spectroscopy/ (Date accessed: 9 November 2017)

## REFERENCES (continued)

**Pukánszky, B.**, 1995, Particulate filled polypropylene: structure and properties, Polypropylene structure, blends and composites, Springer Netherlands, 1-70p.

**Pundit**, 1993, Manual of Portable Ultrasonic Non Destructive Digital Indicating Tester, C. N. S. Instruments, London.

**Puppala, A. and Musenda, C.**, 2000, Effects of fiber reinforcement on strength and volume change in expansive soils, *Transportation Research Record: Journal of the Transportation Research Board*, 1736:134–140 pp.

**Qi, J., Vermeer, P.A. and Cheng, G.**, 2006, A review of the influence of freeze-thaw cycles on soil geotechnical properties, *Permafrost and Periglacial Processes*, 17(3):245–252 pp.

**Roustaei, M., Eslami, A. and Ghazavi, M.**, 2015, Effects of freeze-thaw cycles on a fiber reinforced fine grained soil in relation to geotechnical parameters, *Cold Regions Science and Technology*, 120:127–137 pp.

**Scalici, T., Pitarresi, G., Badagliacco, D., Fiore, V. and Valenza, A.**, 2016, Mechanical properties of basalt fiber reinforced composites manufactured with different vacuum assisted impregnation techniques, *Composites Part B: Engineering*, 104:35–43 pp.

**Senol, A., Ikizler, S.B., Etminan, E. and Demir, G.**, 2014, Improvement of low plasticity clayey soils using polypropylene fibers, *Pavement Performance Monitoring, Modeling, and Management*, ASCE, GSP 254:1–8 pp.

**Seydibeyoğlu, M.Ö., Mohanty, A.K. and Manjusri, M.**, 2017, Fiber technology for fiber-reinforced composites, Woodhead Publishing, 336p.

**Sepp, S.** "*Basalt*", www.sandatlas.org/basalt/ (Date accessed: 30 December 2017)

**Sherwood, P. T.**, 1993, Soil stabilisation with cement and lime, London: HMSO, 153p.

## REFERENCES (continued)

**Shi, J., Wang, X., Wu, Z. and Zhu, Z.**, 2017, Fatigue behavior of basalt fiber-reinforced polymer tendons under a marine environment, *Construction and Building Materials*, 137:46–54 pp.

**Shibi, T. and Kamei, T.**, 2014, Effect of freeze-thaw cycles on the strength and physical properties of cement-stabilised soil containing recycled bassanite and coal ash, *Cold Regions Science and Technology*, 106:36–45 pp.

**Sim, J., Park, C. and Moon, D. Y.**, 2005, Characteristics of basalt fiber as a strengthening material for concrete structures, *Composites Part B: Engineering*, 36(6):504–512 pp.

**Soğancı, A. S.**, 2015, The effect of polypropylene fiber in the stabilization of expansive soils, World Academy of Science, Engineering and Technology, *International Journal of Environmental, Chemical, Ecological and Geophysical Engineering*, 9(8):994–997 pp.

**Stephenson, R.W.**,1978, Ultrasonic Testing for Determining Dynamic Soil Moduli, Dynamic Geotechnical Testing, ASTM STP 654, American Society for Testing and Materials, 179-195p.

**Strutz, T.**, 2010, Data Fitting and Uncertainty: A Practical Introduction to Weighted Least Squares and Beyond, Wiesbaden, Germany: Vieweg, 244p.

**Su, Z.**, 2012, Durability performance of cementitiously stabilized layers, MSc Thesis, The University Of Wisconcin-Madison, 172p.

**Tang, C.S., Li, J., Wang, D.Y. and Shi, B.**, 2016, Investigation on the interfacial mechanical behavior of wave-shaped fiber reinforced soil by pullout test, *Geotextiles and Geomembranes*, 44(6):872–883 pp.

**Tang, C., Shi, B., Gao, W., Chen, F. and Cai, Y.**, 2007, Strength and mechanical behavior of short polypropylene fiber reinforced and cement stabilized clayey soil, *Geotextiles and Geomembranes*, 25(3):194–202 pp.

## REFERENCES (continued)

**Terrel, R.L., Epps, J.A., Barenberg, E.J., Mitchell, J.K. and Thompson, M. R.**, 1979, Soil stabilisation in pavement structures: a users manual, 1-2, Federal Highway Administration (FHWA), US Department of Transportation, Washington DC.

**The Columbia Encyclopedia, 6th ed.,** "Calcium Oxide", http://www.encyclopedia.com/science-and-technology/chemistry/compounds-and-elements/calcium-oxide (Date accessed: 6 November 2017)

**Tosun, K.**, 2007, Farklı çimento tiplerinin gecikmiş etrenjit oluşumu üzerindeki etkileri, Doktora Tezi, Dokuz Eylül Üniversitesi Fen Bilimleri Enstitüsü, 381s.

**Tonoz, M.C., Ulusay, R. and Gokceoglu, C.**, 2004, Effects of lime stabilization on engineering properties of expansive Ankara clay, *Engineering Geology for Infrastructure Planning in Europe*, Springer Berlin Heidelberg, 466-474 pp.

**TS EN 459-2**, 2012, Yapı kireci - Bölüm 2: Deney yöntemleri.

**Türköz, M.**, 2006, Şişen killerin kireç katkısı ile stabilizasyonı ve Eskişehir-Meşelik killerine uygulanması, *Eskişehir Osmangazi Üniversitesi Müh. Mim. Fak. Dergisi*, 19(2):76–87 s.

**Viklander, P.**, 1998, Laboratory study of stone heave in till exposed to freezing and thawing, *Cold Regions Science and Technology*, 27:141–152 pp.

**Wang, D., Abriak, N.E. and Zentar, R.**, 2013, Strength and deformation properties of Dunkirk marine sediments solidified with cement, lime and fly ash, *Engineering Geology*, 166:90–99 pp.

**Wang, D.Y,, Ma, W., Niu, Y.H,, Chang, X.X. and Wen, Z.**, 2007, Effects of cyclic freezing and thawing on mechanical properties of Qinghai-Tibet clay, Cold Regions Science and Technology, 48(1):34–43 pp.

## REFERENCES (continued)

**Wang, S., Yang, (Joey), Z. and Yang, P.**, 2017, Structural change and volumetric shrinkage of clay due to freeze-thaw by 3D X-ray computed tomography, *Cold Regions Science and Technology*, 138:108–116 pp.

**Wang, Z.**, **Zhao, X.L., Xian, G., Wu, G., Raman, R.K.S., Al-Saadi, S. and Haque, A.**, 2017, Long-term durability of basalt- and glass-fibre reinforced polymer (BFRP/GFRP) bars in seawater and sea sand concrete environment, *Construction and Building Materials*, 139:467-489 pp.

**Wang, X., Shi, J., Liu, J., Yang, L. and Wu, Z.**, 2014, Creep behavior of basalt fiber reinforced polymer tendons for prestressing application, *Materials and Design*, 59:558–564 pp.

**Wang, X., Shi, J., Wu, G., Yang, L. and Wu, Z.**, 2015, Effectiveness of basalt FRP tendons for strengthening of RC beams through the external prestressing technique, *Engineering Structures*, 101:34–44 pp.

**Wang, Z., Zhao, X.L., Xian, G., Wu, G., Singh Raman, R. K., Al-Saadi, S. and Haque, A.**, 2017b, Long-term durability of basalt- and glass-fibre reinforced polymer (BFRP/GFRP) bars in seawater and sea sand concrete environment, *Construction and Building Materials*, 139:467–489 pp.

**Yarbaşı, N., Kalkan, E. and Akbulut, S.**, 2007, Modification of the geotechnical properties, as influenced by freeze-thaw, of granular soils with waste additives, *Cold Regions Science and Technology*, 48(1):44–54 pp.

**Yesiller, N., Hanson, J.L., Rener, A.T. and Usmen, M.A.**, 2001, Ultrasonic testing for evaluation of stabilized mixtures, *Transportation Research Record: Journal of the Transportation Research Board*, 1757:32–42 pp.

**Yıldız, M., Soğancı, A.S., Demiröz, A. and Albayrak, V.**, 2004, Tekrarlı donma ve çözülmenin kireç ile stabilize edilmiş kil zeminlerin mukavemet ve permeabilitesine etkisi, Zemin Mekaniği ve Temel Mühendisliği Onuncu Ulusal Kongresi, İstanbul, 227-236s.

## REFERENCES (continued)


**Yıldız, M., and Soğancı, A. S.**, 2012, Effect of freezing and thawing on strength and permeability of lime-stabilized clays, *Scientia Iranica*, 19(4):1013–1017 pp.

**Yilmaz, Y.**, 2015, Compaction and strength characteristics of fly ash and fiber amended clayey soil, *Engineering Geology*, 188:168–177 pp.

**Yilmaz, Y. and Karatas, K.**, 2011, Effect of polypropylene fibre on the strength characteristics of lightly cemented clayey soil mixtures, *Geo-Frontiers 2011: Advances in Geotechnical Engineering*, ASCE, 707–716 pp.

**Zaimoglu, A.S.**, 2010, Freezing-thawing behavior of fine-grained soils reinforced with polypropylene fibers, *Cold Regions Science and Technology*, 60(1):63–65 pp.

**Zaimoğlu, A.S., Hattatoğlu, F. and Akbulut, R.K.**, 2013, Yüke maruz ince daneli zeminlerin donma-çözülme davranışı, *Pamukkale Üniversitesi Mühendislik Bilimleri Dergisi*, 19(3):117–120 s.

**Zaimoğlu, A.Ş., Hattatoğlu, F., Akbulut, R.K. and Yetimoğlu, T.**, 2012, Freeze-thaw behavior of fine grained soils subjected to surcharge loads, 3rd International Conference on New Developments in Soil Mechanics and Geotechnical Engineering, Nicosia, North Cyprus, 28–30p.

**Zhang, Z., Ma, W., Feng, W., Xiao, D. and Hou, X.**, 2016, Reconstruction of Soil Particle Composition During Freeze-Thaw Cycling: A Review, *Pedosphere*, 26(2):167–179 pp.

# CURRICULUM VITAE

Aslı Boz was born in Konak, İzmir. After graduating from Hayrettin Duran Intensive High School in 2007, she received her B.Sc. degree from Celal Bayar University Department of Civil Engineering in 2014. In 2017, she studied in Université de Lorraine / France. Currently, Aslı Boz is a M.Sc. student in Ege University, İzmir.